Rapid screening methods for superior trait selections in lentil and field pea breeding

Linda McDonald

ORCID ID: 0000-0002-0501-559X

Doctor of Philosophy

July 2020

Faculty of Veterinary and Agricultural Sciences School of Agriculture and Food

The University of Melbourne

Submitted in total fulfilment for the degree of Doctor of Philosophy

Abstract

Most of the lentil and field pea grown in Australia are exported to India and surrounding countries, to the Middle East, Turkey and North Africa. While each country may utilise pulses differently, common to all, is that quality is based on the visual characteristics of the whole-grain and split-pulse, and its cooking quality.

One of the objectives of pulse-breeding programs is to ensure that the quality traits of new varieties align with the preferences defined by the export markets. Pulse-quality traits were historically determined using empirical tests to quantify seed size, colour, contamination and defects. Since many of these tests are time-consuming to perform, comprehensive quality evaluation is reserved for advanced germplasm. Therefore, adoption of rapid and objective methods would improve efficiency and consistency of quality evaluation and enable comprehensive assessment of early generation lines.

Technological advances in digital imaging and machine learning has seen a broad application of machine vision to assess agricultural products. While there is extensive research in this field, there are still relatively few machine vision methods which have been developed for the quality-assessment of lentil and field pea grains.

Within this study, rapid and objective methods were developed to assess three grain-traits, which related to visual characteristics of lentil and field pea and were identified to be important within breeding programs. The targeted applications were the classification of broad market classes of field pea, quantitation of bleaching discoloration within the 'green pea' market class and classification of split and dehulled fractions of lentil and field pea post milling. Machine vision algorithms were developed based on the analysis of multispectral images.

Linear discriminant analysis, based on image-derived colour, shape and size features, was used for the classification of field pea market classes. The model was applied to sound and defective grain samples, achieving perfect classification of sound grain and distinguishing sound from defective grain with 97% accuracy.

The extent of bleaching in green field pea samples was quantified through an objective model which was developed on visible reflectance spectra (spectrophotometric analysis) and

subsequently adapted for image-based analysis of grain colour. The image-derived colour scores closely matched the spectrophotometric analysis and additionally enabled the distribution or uniformity of bleaching to be objectively quantified within each sample. Furthermore, through the image analysis scoring system, the relative susceptibility to bleaching, of each genotype, was also quantified.

Milled fractions of lentil and field pea were classified through the application of artificial neural networks, where network architectures and inputs were compared. A convolutional neural network, trained on image-derived feature distributions, was found to be the most accurate and computationally efficient model.

Machine vision is an expanding field of research which offers the potential for consistent, accurate and rapid product-quality evaluation. The results of this study demonstrate the efficacy of machine vision applications throughout the pulse value chain and particularly within germplasm enhancement programs. Adoption of machine vision systems can increase the capacity for comprehensive screening at all stages of breeding which is currently not practicable through standard assessment methods.

Declaration

1. This thesis comprises only my original work toward the Doctor of Philosophy award except where indicated in the preface.

2. Due acknowledgement has been made in the text to all other material used.

3. This thesis is fewer than the maximum word limit in length, exclusive of tables, maps, bibliographies and appendices.

Preface

Chapter 1

Unpublished material not submitted for publication.

McDonald, L: Conceptualisation, Investigation, Visualisation, Writing original draft, Review and editing.

Panozzo, J: Conceptualisation, Supervision, Funding acquisition, Project administration, Review and editing.

Howell, K: Supervision, Review and editing.

Chapter 2

Published by PLoS One on May 13th, 2016.

MCDONALD, L. S., PANOZZO, J. F., SALISBURY, P. A. & FORD, R. 2016. Discriminant Analysis of Defective and Non-Defective Field Pea (Pisum sativum L.) into Broad Market Grades Based on Digital Image Features. PLoS ONE, 11, e0155523.

McDonald, L: Conceptualisation, Data curation, Formal analysis, Investigation, Methodology, Validation, Visualisation, Writing original draft, Review and editing.

Panozzo, J: Conceptualisation, Formal analysis, Review and editing, Supervision, Funding acquisition, Project administration, Review and editing.

Salisbury, P: Supervision, Review and editing.

Ford, R: Supervision, Review and editing.

Chapter 3

Published by PLoS One on August 23rd, 2019.

MCDONALD, L., SALISBURY, P., FORD, R. & PANOZZO, J. 2019. Quantifying the colour loss of green field pea (Pisum sativum L.) due to bleaching. PLoS ONE, 14, e0221523.

McDonald, L: Conceptualisation, Data curation, Formal analysis, Investigation, Methodology, Validation, Visualisation, Writing original draft, Review and editing.

Panozzo, J: Conceptualisation, Methodology, Supervision, Funding acquisition, Project administration, Review and editing.

Salisbury, P: Supervision, Review and editing.

Ford, R: Supervision, Review and editing.

Chapter 4

Published by Legume Science on September 30th, 2020

MCDONALD, L., MAHARJAN, P., PORTMAN, D. & PANOZZO, J. 2020. Bleaching color-loss of green field pea: An investigation on inference of genotypic-resistance based on chlorophyll and phenolic acid content. Legume Science. 2020;e63. https://doi.org/10.1002/leg3.63.

McDonald, L: Conceptualisation, Data curation, Formal analysis, Investigation, Methodology, Validation, Visualisation, Writing original draft, Review and editing.

Panozzo, J: Conceptualisation, Methodology, Supervision, Funding acquisition, Project administration, Review and editing.

Maharjan, P: Methodology, Data curation, Validation, Review and editing.

Portman, D: Data curation

Chapter 5

Submitted for publication to Computers and Electronics in Agriculture on July 8th, 2020.

MCDONALD, L., ASSADZADEH, S. & PANOZZO, J.
Images, features, or feature distributions? A comparison of inputs for training convolutional neural networks to classify lentil and field pea milling fractions

McDonald, L: Conceptualisation, Data curation, Formal analysis, Investigation, Methodology, Validation, Visualisation, Writing original draft, Review and editing.

Panozzo, J: Conceptualisation, Methodology, Supervision, Funding acquisition, Project administration, Review and editing.

Assadzadeh, S: Methodology, Review and editing.

Chapter 6

Unpublished material not submitted for publication.

McDonald, L: Conceptualisation, Investigation, Writing original draft, Review and editing.

Panozzo, J: Supervision, Review and editing.

Funding

All research presented within this thesis was jointly funded by Agriculture Victoria and the Grains Research and Development Corporation (DAV00132 and DAV00158)

Acknowledgements

I am grateful to be surrounded by so many family, friends and colleagues who have encouraged, challenged, prayed and cared for me throughout my PhD candidature; who have taken an interest in my work and in my wellbeing and who now celebrate with me in the completion of this thesis. Thank you all!

To my supervisors Dr. Joe Panozzo, Dr. Kate Howell, Prof. Rebecca Ford and A/Prof. Phillip Salisbury: thank you for your guidance, support and feedback throughout the course of my PhD. I am fortunate to have had such an encouraging supervisory panel.

A special thanks to Dr. Joe Panozzo for mentoring me as a research scientist, it is a privilege and honour to be counted among your students. Thank you for your example of selfless leadership, for the many hours that you continue to dedicate to the success and development of others. I hope I can imitate your generosity throughout my career.

To my husband and best friend, Tim, I am so thankful to you and for you. You have shared in every high and low moment of this venture and have remained a constant strength for me. If not for your steadfast support I would not have completed this. Thank you for keeping me grounded and for bringing so much laughter into our home. And thank you for the beautiful desk you built for me to work at! I love you dearly and look forward to our life beyond this PhD.

To my parents, Doug and Glenis, and grandparents, Dorothy and Eric†, Graham† and Elsie†, I owe an enormous measure of gratitude. You have each invested so much into my personal and professional development over the years. I am truly blessed to have such a faithful and loving family-heritage. Thank you for being there to listen and share advice and thank you for the constant reminders of your love, thoughts and prayers and of God's faithfulness.

"For God has not given us a spirit of fear,
but of power and of love and of a sound mind."
2 Timothy 1:7

And to my siblings Jeanne, Soli, Annette and Cindy: I love you all dearly and give thanks for you. Thank you for checking in with me often and cheering me on.

Table of contents

FRONT MATTER

Abstract **1**

Declaration 3

Preface **4**

Acknowledgements **6**

Table of contents **7**

List of tables **10**

List of figures **12**

CHAPTER 1: GENERAL INTRODUCTION

Spectral-based technologies offer opportunities for high-throughput, non-destructive phenomic screening of lentil and field pea grains **16**

1.1 The pulse industry: production and consumption 16

1.2 Plant breeding objectives 17

1.3 Grain Quality 19

1.3.1 Industry assessment 19

1.3.2 Germplasm screening in breeding programs 19

1.3.3 Pulse quality screening: an opportunity for machine vision 19

1.4 Machine Vision (MV) 23

1.4.1 MV systems for agricultural products 23

1.4.2 MV developments and opportunities for lentil and field pea 25

1.5 Conclusions of the literature review 31

1.6 Thesis objectives 32

1.7 References 34

CHAPTER 2

Discriminant analysis of defective and non-defective field pea (*Pisum sativum L.*) into broad market grades based on digital image features **43**

Abstract 43

2.1 Introduction 44

2.2 Materials & Methods 45

2.2.1 Sample collection and classification 45

2.2.2 Model development 47

2.3 Results and discussion 50
2.3.1 Model 1 51
2.3.2 Model 2 53
2.3.3 Defect prediction Model 54
2.4 Conclusion 55
2.5 Acknowledgements 55
2.5 References 55

CHAPTER 3

Quantifying the colour loss of green field pea (*Pisum sativum L.*) due to bleaching 58
Abstract 58
3.1 Introduction 59
3.2 Materials and methods 61
3.2.1 Colour-sorted samples and data collection 61
3.2.2 Time-course samples and data collection 62
3.2.3 Development of the bleaching-score model 62
3.2.4 Image processing to obtain single seed colour spectra 63
3.2.5 Quantifying bleaching by image analysis 64
3.2.6 Quantifying bleaching in the time course samples 64
3.3 Results and discussions 65
3.3.1 Bleaching score model and image processing 65
3.3.2 Results of the bleaching model 67
3.3.3 Determining time-course bleaching response 69
3.4 Conclusion 71
3.5 Acknowledgments 71
3.6 References 71

CHAPTER 4

Concentrations of phenolic acids and chlorophylls are depleted in green pea (*Pisum Sativum L.*) during bleaching but are not directly related to known bleaching-resistance of a genotype 74
Abstract 74
4.1 Introduction 75
4.2 Materials and Methods 76
4.2.1 Samples 76
4.2.2 Bleaching green peas 77

4.2.3 Image Capture 77
4.2.4 Image processing and color analysis 78
4.2.5 Analysis of chlorophyll content 78
4.2.6 Analysis of phenolic profiles 79
4.2.7 Moisture Analysis 80
4.3 Results and discussion 80
4.3.1 Grain color 80
4.3.2 Chlorophyll content 83
4.3.3 Phenolic acid content 87
4.4 Conclusions 90
4.5 Acknowledgments 91
4.6 References 91

CHAPTER 5

Images, features, or feature distributions? A comparison of inputs for training convolutional neural networks to classify lentil and field pea milling fractions 94
Abstract 94
5.1 Introduction 95
5.2 Materials and methods 98
5.2.1 Grain samples and reference data acquisition 98
5.2.2 Image acquisition and processing 98
5.2.3 Neural network models 99
5.3 Results and discussion 102
5.3.1 Network performance: Comparison of architecture and inputs 103
5.3.2 Training dataset size 107
5.4 Conclusion 107
5.5 Acknowledgements 109
5.6 References 109

CHAPTER 6

General discussion 112
6.1 Field pea market-grade classification 113
6.2 Quantitation of bleaching-discoloration in green pea 114
6.3 Milling efficiency 116
6.4 Concluding remarks 117

List of tables

Chapter 1

Table 1.1. Summary of machine vision developments for evaluation of lentil and field pea quality

Chapter 2

Table 2.1. Descriptions of field pea market grades

Table 2.2. Field pea calibration and validation sets

Table 2.3. Seed characteristics extracted through image processing

Table 2.4. Linear discriminant analysis models and parameters

Table 2.5. Classification Rates of Models

Chapter 3

Table 3.1. Modelling the spectrophotometer output. MLR input model variables for transforming pixel intensity values to the reflectance units of the spectrophotometer.

Table 3.2. Performance of pixel intensity transformation models. Correlation coefficients and Lin's concordance test statistics for the MLR models developed to transform pixel intensity values to reflect reflectance units of the spectrophotometer.

Table 3.3. Critical value computation. Constant coefficient values for calculating critical values (Equations 1a and 1b)

Table 3.4. Performance of bleaching score prediction models based on image analysis. Correlation coefficients, Lin's concordance test statistics and Root Mean Square Error (RMSE) values for image predictions of bleaching scores compared with spectrophotometer-derived bleaching scores.

Table 3.5. Rate of bleaching. Regression analysis on mean of single-seed bleaching scores

Table 3.6. Uniformity of bleaching. Regression analysis on bleaching uniformity scores

Chapter 4

Table 4.1. Descriptive statistics of color scores for whole grain, cotyledon and hull.

Table 4.2. Descriptive statistics for the concentration (mg/100g DB) of chlorophyll in green pea cotyledon and hull samples.

Table 4.3. Concentration (mg/kg DB) of the main phenolic acids detected in the green pea cotyledon and hull samples.

Chapter 5

Table 5.1. Description of milling classes for lentil and field pea. Milled lentil and field pea samples were manually sorted to the five classes.

Table 5.2. Total number of lentil and field pea images within each of the milling classes

Table 5.3. Architecture of the two CNN models; ImgCNN (trained on multispectral image inputs) and DistCNN (trained on FDVs)

Table 5.4. Description of the features computed from multispectral images

Table 5.5. Neural network performance. Accuracy and computational cost of three network architectures trained on multispectral image (ImgCNN), FDV (DistCNN) and image-feature (SmpFCN) inputs.

List of figures

Chapter 1

Figure 1.1. Annual global yield of pulse grains since 1961 (FAOSTAT, 2020).

Figure 1.2. Major global producers and exporters of lentil and field pea (FAOSTAT, 2020).

Figure 1.3. Seed size evaluation of desi chickpea.

Chapter 2

Figure 2.1. Field pea market grades. a) White Pea, b) Blue Pea, c) Mottled Dun Pea, d) Kaspa Dun Pea, e) Green Dun Pea, f) Yellow Forage Pea, g) Marrowfat Pea, h) Kaspa-Type Pea.

Figure 2.2. Model development flow chart.

Figure 2.3. Image pre-processing and processing flow chart

Figure 2.4. Colour factor variations between field pea market grades. Four representative samples from each market grade illustrate the variation in relative colour intensity factors. The violet, blue, green, orange, red and NIR colour factors for each sample are represented respectively by the violet diamonds, blue squares, green triangles, yellow squares, red squares and pink circles. These are the basis for predicting market grades through Model 1.

Figure 2.5. Performance of Model 2. (a) and (b) All samples that were correctly classified (red dots) fell along the one to one correlation line (green), i.e. the closest market grade mean was the correct market grade mean for that sample. All samples which did not lie on the green line (one to one correlation) were incorrectly classified (blue triangles). Plots (c) and (d) gave the same

Chapter 3

Figure 3.1. Spectral response of bleaching. Example spectra of five green pea genotypes at various stages of bleaching. Dark line (1) represented the least bleached and lightest grey line (5) represented the most bleached. (a) Original spectra measured by spectrophotometer; (b) Spectra in (a) sampled at 400,470,530,590 and 660nm; (c) Spectra at 400,470,530,590 and 660nm transformed according to the method outlined in the previous section.

Figure 3.2. Transformed spectral range. Transformed image spectra of single seeds (green lines, n = 11309) and whole samples (black lines, n = 145). The single seed values are more extreme than the whole sample values.

Figure 3.3. Bleaching score chart. Illustration of bleaching scores for the colour-sorted samples. The number above each square was the bleaching score assigned for that square.

Figure 3.4. Performance of image-based bleaching scores. Bleaching scores assessed by image analysis highly correlated with bleaching scores measured by colour spectrophotometer for (a) the colour sorted samples, R2 = 0.99, and (b) the time-course samples, R2 = 0.96. Blue lines represent the one-to-one relation.

Chapter 4

Figure 4.1. Illustration of the grain-sample presentation for images captured of (a) whole grain and (b) dehulled grain separated into cotyledon (left) and hull (right).

Figure 4.2. Individual value plots. Depiction of the range and distribution of color scores within each genotype for (a) Whole grain, (b) Cotyledon and (c) Hull samples.

Figure 4.3. Tukey simultaneous 95% confidence intervals. Differences in mean color scores between genotypes for (a) whole grain, (b) cotyledon and (c) hull.

Figure 4.4. Bleaching color extremities observed within each genotype. Images of cotyledon and hull for each of the five green pea genotypes from an initial subsample prior to storage (left) and a final subsample after 24-weeks of storage under light conditions (right).

Figure 4.5. Relationship between cotyledon chlorophyll content and (a) cotyledon color score, (b) whole grain color score and (c) whole grain color score grouped by genotypes with higher mean phenolic acid content, i.e. >100 mg/kg, (black dots) and with lower mean hull phenolic content, i.e. <100 mg/kg, (grey triangles).

Figure 4.6. Genotypic differences in the ratio of phenolic content in pea hulls to the chlorophyll content of pea cotyledon; (a) Interval plot of phenolic acid to chlorophyll ratio values grouped by genotype, (b) Relation between phenolic acid to chlorophyll ratio values and the genotypic bleaching susceptibility, (c) Interval plot of cotyledon chlorophyll A/B ratio grouped by genotype, (d) Relation between cotyledon chlorophyll A/B ratio and the genotypic bleaching susceptibility.

Figure 4.7 Chromatogram of phenolic extracts from hulls of OZB1309 (storage time = 0 weeks). (a) PDA chromatogram at 280 nm (b) QDa chromatogram at m/z of 278 and 308. Peak identity: 1 = o-coumaroyl malic acid; 2 = p-coumaroyl malic acid; 3a and 3b = cis trans and isomers of feruloyl malic acid.

Figure 4.8. Genotypic differences in phenolic acid content. Interval plots, grouped by genotype, for phenolic acid content of (a) cotyledon and (b) hull samples. Changes in phenolic acid concentration in (c) cotyledon and (d) hull for each genotype as whole grain color scores (i.e. bleaching scores) increased.

Chapter 5

Figure 5.1. Image pre-processing stages prior to training the three neural networks: ImgCNN, DistCNN and SmpFCN.

Figure 5.2. Neural network architectures for classification of lentil and field pea milling fractions. (a) ImgCNN: a convolutional network with multispectral image inputs of size 150x150x7. (b) DistCNN: a convolutional network with image-feature distributions (size 1x360x1) as the inputs. (c) SmpFCN: a fully connected network with image-feature vectors of size 1x24x1 as the inputs. The network diagrams displayed in this image were images were created with open source software developed by LeNail (2019).

Figure 5.3. Example feature vectors of (a) a lentil wholegrain with hull, (b) a dehulled lentil-split and (c) a broken fragment of lentil. Alternating shaded regions correspond to the feature distributions described in Table 4.

Figure 5.4. Validation accuracy over 50 training epochs for the ImgCNN (solid line), DistCNN (dashed line) and SmpFCN (dotted line) network architectures. Plot traces display the average of three training replicates for each model.

Figure 5.5. Validation precision and recall of the ImgCNN, DistCNN and SmpFCN architectures. (Left) Confusion matrices given as a percentage of the number of validation images in each class. Elements along each matrix diagonal are equivalent to the class recall values. Red tones indicate correctly classified images, blue tones indicate misclassified images and darker colours correspond to higher values. (Right) Tables of mean (± s.e.) of class precision and recall values. All depicted values are the average of three training replicates. Class names beginning with “L” and “P” are lentil and field pea classes respectively.

Figure 5.6. Comparison of (a) Validation accuracy, (b) network training time, (c) average class precision and (d) average class recall between the ImgCNN model (black) and DistCNN model (grey) with varying input dataset sizes.

CHAPTER 1: GENERAL INTRODUCTION

Spectral-based technologies offer opportunities for high-throughput, non-destructive phenomic screening of lentil and field pea grains.

1.1 The pulse industry: production and consumption

Pulse crops including lentil and field pea have been cultivated for several thousand years in many regions of the world (FAO, 2016b, Caracuta et al., 2015, Erskine et al., 2016) and are an integral component of many diverse cultures and cuisines (Sozer et al., 2017). Pulses are typically consumed as a minimally processed product, cooked either as whole-grain or split-grain to be included in dishes such as curries, soups and salads or sometimes ground to produce flour. Because of their relatively high protein content pulses are an important staple food in many countries. Among Western nations dietary protein is more commonly sourced from meat products, dairy or egg (FAO, 2016b) and pulse production in countries such as Canada, Australia and North America is predominantly for export markets. Pulse consumption remains popular in regions with a strong history of traditional pulse dishes, such as the Indian subcontinent, the Middle East, North Africa and the Mediterranean (Singh et al., 2000), however pulses are increasingly utilised in new processed food products (Sozer et al., 2017, Portman et al., 2018, Boukid et al., 2019, Joshi et al., 2017).

Pulses are also an important component of sustainable farming systems and beneficial to food security and rural income (Kumar et al., 2018, GPC, FAO, 2016a). Pulse crops contribute greatly to soil health and fertility, through nitrogen fixation, reduction of soil runoff and reduction of erosion (Kumar et al., 2019, Venkatesh et al., 2019, Nath et al., 2019). Moreover, pulse crops provide a disease break when sown in rotation with other crops, particularly cereal and oilseed (Nleya et al., 2004, Michaels, 2004, Meena et al., 2019, Hazra et al., 2014, Döring, 2015). With increasing global population, there is increased pressure on decreasing agricultural land parcels to produce crops of high-quality and nutritious grains which has been achieved through plant breeding and optimised agronomy.

1.2 Plant breeding objectives

Plant breeding, coupled with agronomic management strategies, aim to increase productivity through increased yield and disease-resistance, and adaptation across agroclimatic regions. Since the early 1960s global yields of pulse crops has increased overall by nearly 60% (Figure 1.1) due to the establishment of crop improvement programs in countries such as Canada and Australia which can be attributed to increased plant breeding using germplasm from the International Centre for Agricultural Research in Dry Areas (ICARDA).

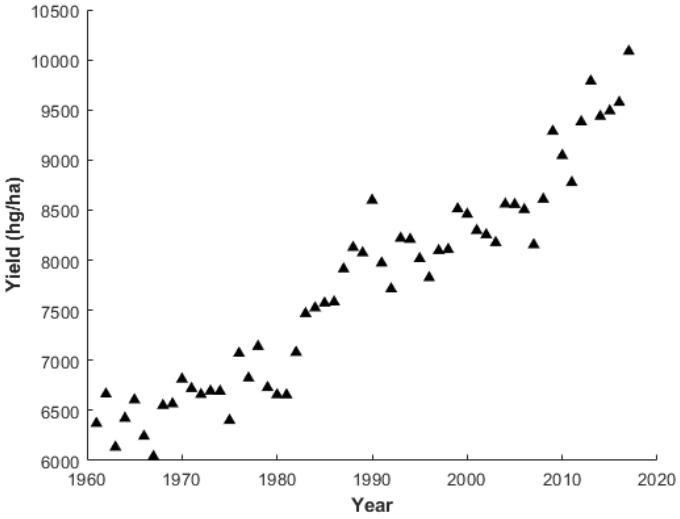

Figure 1.1. Annual global yield of pulse grains since 1961 (FAOSTAT, 2020).

Canada, Australia and North America are now consistently among the largest global producers and exporters of lentil and field pea (Figure 1.2). In Australia, lentil-breeding has concentrated on optimising phenology to develop varieties of increased plant-statue and adaptation for Mediterranean-type environments such as Victoria and South Australia. The production in Australia has concentrated on the medium-size lentil with grey seedcoat and red cotyledon. In the early years, Canada the largest producer and exporter of lentil produced predominantly the large green lentil known collectively as 'Lairds' and these breeding targets were later expanded to include red-lentils known as 'Crimsons'.

Field peas are phenotypically more diverse than lentil and vary widely in seed colour, shape and size and when used for human consumption, field peas are always dehulled and split. There are five main classes of field pea: Yellow (spherical seed with yellow cotyledon and translucent hull), Green (spherical seed with green cotyledon and translucent hull), Dun (spherical or dimpled seed with yellow cotyledon and green or brown hull), Maple (spherical seed with yellow

cotyledon and mottled/marbled hull) and Marrowfat (large seed, slightly dimpled and flattened with similar colouring to the Green class) (Khan and Croser, 2004). The largest producer of peas is Canada of which the dominant type is the yellow pea which consists of a yellow cotyledon and clear seedcoat. In Australia, field peas are typically the Dun-type and are predominantly exported to India and the subcontinent.

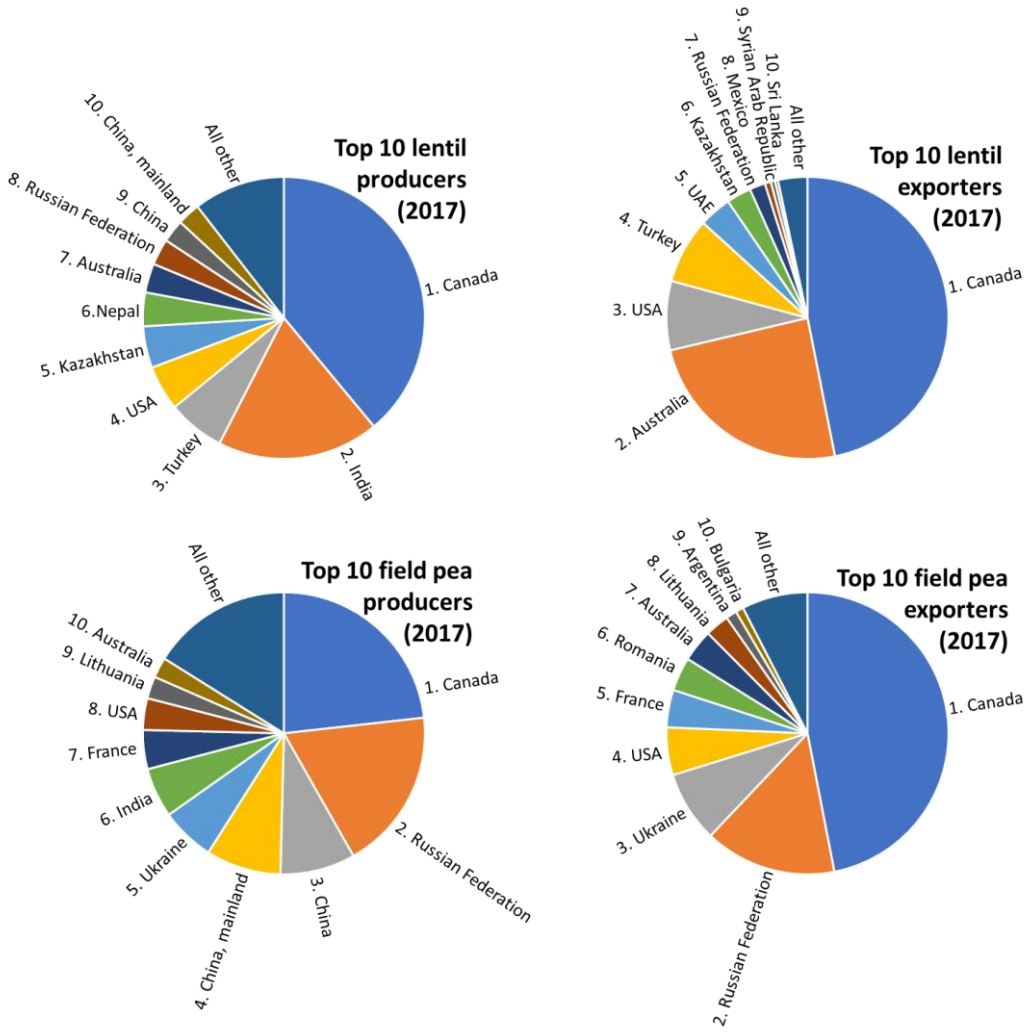

Figure 1.2. Major global producers and exporters of lentil and field pea (FAOSTAT, 2020).

Breeding objectives for quality traits are determined largely by export market specifications and form part of the overall strategy of breeding programs. Within the typical 10-year breeding cycle to produce a new pulse variety, germplasm is exhaustively evaluated for adaptation across diverse agro-ecological regions that are subjected to abiotic effects and ultimately impact on grain yield and quality. A range of agronomic practices such as time-of-sowing, plant row-spacing and fertiliser inputs are often superimposed on the evaluation of germplasm aimed to develop an optimised plant-management strategy to maximise production. Assessment for

grain quality traits occurs concomitantly with plant breeding and agronomy-research to ensure newly released cultivars align with end-use quality and the specifications of importing markets.

1.3 Grain Quality

1.3.1 Industry assessment

Assessment of quality-traits for lentil and field pea in the major-producer countries is largely determined using sieves to quantitate seed size, broken/split, mechanical damage, insect damaged grain. Visual inspection using colour reference charts is used to determine colour defects due to disease, mould, frost or heat stress (CGC, 2018; GTA, 2018 however, the interpretation of these standards by grain inspectors can be highly subjective and can result in misclassification of the market grade. Complicating this, is that these grading standards with definitions of acceptable limits of low-grade material or contaminant differ between countries (Gupta et al., 2011) often leading to disputes between the exporter and importer. Unlike the cereals industry which uses NIR to measure protein and moisture at the point of receival, there is no standardised in-field testing-equipment which can be used to quantify pulse-quality traits. Sensor-based technologies such as RGB scanners are now becoming more common and are finding applications in the food industry. For the grains industry, the technology is predominantly laboratory based but ultimately these instruments and the quantitation algorithms will be transferred to in field, either, on-farm, at the point of grain receival from growers or used by exporters.

1.3.2 Germplasm screening in breeding programs

The development time to produce new grain cultivars is a minimum of 10 years from the initial inter-cross in the glasshouse through to extensive in-field and multi-location testing to determine each germplasm's optimal adaptation. To minimise risk and ensure a successful outcome, breeding programs sow and harvest thousands of plots each of which is assessed for optimal phenotypic characteristics, resistance to disease and pathogens, grain yield, and quality traits. The period between harvest and sowing in the following season is between 12 and 16 weeks and during this period, grain quality traits are measured on the germplasm. An accurate assessment is crucial to avoid sub-optimal germplasm to be sown in the following planting season.

Testing for quality-traits is based on the grains-industry standard methodology with the emphasis on quantifying the characteristics of the seed, such as size, colour and defects.

Although these tests are not difficult, they are laborious, and protocols are often implemented such as delaying testing to later generations of the program when the germplasm numbers derived from each inter-cross have been reduced due to other selection strategies such as grain yields or disease susceptibility.

Seed Size

A common method to determine seed size of pulse grains is to mechanically pass the seed through a vibrating stack of sieves in order of decreasing aperture size (Figure 1.3). This process of mechanical sieving is susceptible to errors (LeMasurier et al., 2014). The irregular shape of some grains cause inconsistency in their sieving behaviour and the sample size can also contribute to misclassifications i.e. a sieve can be blocked by the volume of seed in the majority size fraction preventing smaller seed from falling through. LeMasurier, Panozzo, and Walker (2014) reported a misclassification rate of up to 10% in sieving lentils by this method. Through mechanical sieving, the seed size data which can be collected is limited since seed size units and increments are restricted to those of the sieves (Symons & Shahin, 2000). There is also an undesirable weighting of SSD and SSI toward the larger seed because the method itself uses mass rather than the seed count in each size fraction. Moreover, for some pulse types the size increments for SSD are not uniform across the distribution, skewing the visual representation and intuitive understanding of the data. For example, lentil sieve aperture sizes are typically given as 3.0, 3.5, 4.0, 4.5, 5.0, 6.0 and 7.0mm. As pulse-breeding applications and industrial pulse processing advances with the development of genomic selection (GS) models, there will be a greater emphasis on obtaining more accurate phenotypic data to increase the precision of GS.

Photograph: C. Walker

Figure 1.3. Seed size evaluation of desi chickpea.

Seed Colour

As with most agricultural products, colour is the primary determinant of quality and this equally applies to pulse breeding programs and grain-trading. Within grain laboratories, standard assessments of colour are commonly based on the Commission Internationale de l'Éclairage (CIE) based on L*a*b* space. This is a globally recognised and device-independent system and as such it is extremely useful for objective description and comparisons of colour. However, the CIE L*a*b* colour coordinates are under-utilised in the pulse industry and within breeding programs because they are largely unintuitive in this context due to the difficulty in interpreting three components within a three-dimensional space. Furthermore, colorimeters do not have the capability to assess colour variation or distribution within a sample (de Oliveira et al., 2016). This is undesirable in the pulse industry, where uniformity of grain colour is often an important quality for market acceptance and therefore also a breeding priority.

Seed Processing

Unlike cereals, pulse grains undergo minimal grain processing prior to cooking apart from dehulling of the seedcoat and splitting the cotyledons (Singh et al., 2000). The aim of the milling process is to obtain a product with minimal broken cotyledon. Traditionally, milling was carried out on a small scale where the process could be managed to optimise the outcome. With the recent development of large processing facilities in India, there is now a greater reliance on raw material with defined quality-specifications, however these specifications are still based on rudimentary parameters defined by market grades, and seed size which does not consider the composition of the grain. Seasonal effects due to abiotic factors arising from ambient temperatures, available soil moisture, frosts will affect seed size and shape and therefore impact on milling quality.

Within the laboratory, milling quality is assessed using small-scale equipment which is modelled on industrial-scale mills. The aim is to replicate the milling outcome and identify germplasm with inherently unacceptable milling behaviour. The process involves passing grain between two carborundum disks which results in five fractions (split-dehulled, split with hull, whole-grain dehulled, whole grain with hull and broken grain). Erskine et al. (1991) reported significant differences in milling quality between genotypes. Due to its economic impact for milling companies, breeding programs routinely undertake milling trials although the process is quite laborious as it involves manually sorting the five fractions. The ability to automate the

quantification of each milling fraction offers an opportunity to increase efficiencies with the laboratory and reduce costs.

Seed Defects

Pulses are highly susceptible to diseases and pests both during seed development and during storage. The effects are manifested by undesirable changes in the colour of the seed or through seed-damage. Ascochyta blight and Botrytis grey mould (Botrytis fabae and B. cinerea) are the two main diseases in lentil that infect the seed pod during seed development resulting in dark shrivelled seed of below marketable quality (Kaiser et al., 2000). These diseases can be controlled through the timely application of foliar sprays (Nleya et al., 2004) although breeding for resistance is also a major strategy (Erskine et al., 2016). Field peas are similarly affected by foliar diseases such as bacterial blight which will impact on the seed colour although insects which are most active after pod-flowering have a major effect on the quality of the seed. For example, the larvae of Etiella moth cause damage by chewing the seed within the pod, while the pea weevil feeds on the developing seed and later pupates within the seed rendering the seed unsuitable for processing.

In addition to pests and diseases, storage and handling practices can result in defective grain. On-farm storage is becoming more common as growers aim to minimise the effects of fluctuating grain prices, preferring to store grain on farm when grain prices are low and selling in a rising market. This strategy often presents challenges in grain-silo management in order to avoid a loss in marketable quality. Modern silos include the ability to aerate to either cool the grain or reduce moisture as these two factors are known to have the largest effect of stored grain (Mills, 1999) resulting in darkening of the lentil seed coat. It has been reported that darkening of the seed coat is due to changes in phenolic composition (Mirali et al., 2016, Nasar-Abbas et al., 2009). Similarly, sub-optimal storage conditions can cause a bleaching discoloration in dry green filed pea which subsequently detracts from the market grade (Phelps, 2015).

Resistance to the abiotic and biotic effects which result in defects, such as discoloration and insect damage, have become important germplasm selection criteria within lentil and field pea breeding programs (Erskine et al., 2016, Erskine and Sarker, 2004, Khan and Croser, 2004). However, assessments of grain defects are largely subjective deductions.

1.3.3 Pulse quality screening: an opportunity for machine vision

Within the international pulse industry there is general agreement about factors which impact on grain quality, such as the visible characteristics of the grains or defects due to insects, discoloration and mechanical damage. Even so, there are no common definitions of pulse quality (Gupta, Tiwari, & Singh Bawa, 2011). Quality assessment methods used within industry are largely subjective and the methods used within breeding programs are largely time-consuming and some which are destructive are reserved for screening only the advanced germplasm. With the technological advances in computing and digital imaging there is an increasing shift toward the use of machine vision systems for product-quality evaluation. Assessments based on image processing offer objective, time-efficient, non-destructive analyses (Aggarwal and Mohan, 2010) and would therefore benefit the pulse grain industry and breeding programs. Sensor-based screening of germplasm has also aided the development of genomic prediction models (Hayes et al., 2017). Furthermore, increasing genetic diversity within breeding programs enables greater potential for grain-quality gains and while there are many wild relatives for selection screening the volume of accessions for desired traits is inefficient (Coyne et al., 2020). So, development and adoption of rapid screening and objective measures for genebank accessions would enable more detailed profiling of each one and assist breeding selections (Nguyen and Norton, 2020).

1.4 Machine Vision (MV)

1.4.1 MV systems for agricultural products

Machine Vision (MV) systems integrate digital sensors (data acquisition) and computational infrastructure (data analysis) with the objective to automate tasks typically performed by the human vision system (Huang, 1996), such as the recognition or analysis of product-traits. MV systems enable objective and time-efficient analyses which has motivated the application of these systems across many industries to replace assessments that are inherently time-consuming or subjective. From very early generations of image processing algorithms, the potential was demonstrated for analyses which had greater consistency and better time-efficiency than human inspection (Churchill et al., 1992).

Sensor technologies incorporated into MV systems include conventional digital imaging, hyperspectral imaging, Near Infrared Reflectance (NIR), Mid Infrared Reflectance (MIR), X-ray, Magnetic Resonance Imaging (MRI) and ultrasound (Jha, 2016, Abasi et al., 2018), but the sensor technologies most commonly applied to agricultural products are NIR scanning, digital imaging

(in the visible region) and NIR-hyperspectral imaging. Some imaging systems have also been developed with three-dimensional viewing capabilities either with multiple-view cameras (Delwiche et al., 2013, Shahin et al., 2012) or the incorporation of a laser (LeMasurier et al., 2014). Selection between the various sensing technologies is determined by the desired application, for example NIR-based systems are useful for analysing compositional traits (e.g. protein or moisture content) and conventional digital imaging systems are useful for analysing physical and visual traits (Mahajan et al., 2015, Ratish et al., 2017, Fox and Manley, 2014). In this review we focus on the applications of visible digital imaging and NIR-hyperspectral imaging.

As well as the variation in the data acquisition properties (e.g. sensor types, resolution, light source), MV systems also vary in sample presentation (e.g. manual placement or automated conveyor system) and image processing software and algorithms, which also determine the level of automation of the system (e.g. automation or manual input requirements for image segmentation). Modelling techniques, from feature extraction to subsequent image analysis are also variable between systems and optimised for each application. Image processing and analysis algorithms, within MV systems determine how well the systems will recognise or analyse traits of interest within the images. Image analysis often involves image pre-processing to enhance the image (e.g. remove noise or detect edges), segmentation to identify the regions of interest and remove background pixel variations, feature extraction (explicitly for further model training or implicitly within neural networks) to obtain data which are in some way related to the desired learning objective and finally the use of machine learning models, typically supervised learning, to deduce the trait outputs. For analysis of hyperspectral images, generally image dimensionality is first reduced using Principal Component Analysis (PCA) prior to further data processing (Williams et al., 2009).

Modelling methods can be grouped as classification or quantification. Quantification is typically to describe characteristics of product colour, such as through regression analysis with pixel colour intensity values, or shape and size; in which case the trait values are often derived through geometric models. Quantification can also be used as an extension of classification models to determine the proportions of product classified into various categories (e.g. proportion of seed graded as defective). For classification models, the complexity of the task determines the suitability of various model types. Discriminant analysis and support vector machine methods are popular for classifying categories which are separable through a set of representative, image-derived features. With recent developments in computational capacity,

for big data processing, and Artificial Neural Network (ANN) architectures for deep learning, ANNs have become increasingly popular for both classification and quantification tasks, particularly for traits which are more difficult to model (LeCun et al., 2015).

Spectral-sensor technologies and computational systems have continued to evolve and become more powerful and cost effective. Some sensor-based systems are already internationally approved and adopted for product quality evaluation, for example NIR spectroscopy methods applied to wheat to determine ash content of flour, protein content of grain and flour and hardness of grain (AACC, 2020). Within the wider food and agriculture industries, product evaluation by MV is continually expanding (Rehman et al., 2019, Bhargava and Bansal, 2018, Nturambirwe and Opara, 2020, Mahendran et al., 2016, Brosnan and Sun, 2002, Brosnan and Sun, 2004, Davies, 2009, Dell' Aquila, 2009).

1.4.2 MV developments and opportunities for lentil and field pea

While the number of MV applications for the assessment of food-grain products is increasing (Vithu and Moses, 2016), there are still relatively few methods developed specifically for the assessment of lentil and field pea (Table 1.1). Image acquisition and processing techniques are largely transferrable across applications and so developments for one agricultural commodity could be adapted for another. In the following sections we review the developments in image-analysis methods for lentil and field pea assessment and identify further opportunities based on the requirements for rapid and objective assessment of industry-defined quality traits and the potential for adaption of MV methods which have been developed for other grain products.

Table 1.1. Summary of machine vision developments for evaluation of lentil and field pea quality

Seed Type	*Description of MV application*	*Type of image*	*Reference*
Lentil	Classification of lentil into three commercial grades (as defined by CGC)	RGB image	(Shahin and Symons, 2001)
	Quantification of a colour score to indicate seed browning	RGB image	(Dell'Aquila, 2006)
	Classification of seed type to distinguish between corn, lentil, barley and oats	RGB image	(Adjemout et al., 2007)
	Classification of lentil types based on seed size, shape and colour of individual seeds	RGB image	(Venora et al., 2007b)
	Geometrical properties of a red and a green lentil variety	RGB image	(Fıratlıgil-Durmuş et al., 2008)
	Size properties of seeds	RGB image	(Fıratlıgil-Durmuş et al., 2010)
	Determine seed size and shape characteristics for predicting dehulling efficiency of red lentils	RGB image	(Shahin et al., 2012)
	Quantification of seed dimension, shape and seed size distribution	Visible-multispectral image	(LeMasurier et al., 2014)
Lentil and field pea	Detection of fungal infection in five different pulses	NIR-hyperspectral image	(Karuppiah et al., 2016)
Field pea	Colour scoring system	RGB image	(Coles, 1997)
	Seed size distribution from images of non-singulated grain samples	RGB image	(Shahin and Symons, 2005)
	Size, shape and volume of various peas and beans	RGB image	(Kumar et al., 2013)
	Classification of seed with and without internal defects caused by weevil infestation	Visible-hyperspectral image	(Nansen et al., 2014)
	Classification of market grade for eight field pea types. Classification of defective grain.	Visible-multispectral image	(McDonald et al., 2016)
	Quantification of discoloration and uniformity in green pea	Visible-multispectral image	(McDonald et al., 2019)

Seed Size

Fundamental size and shape traits, such as grain length, width and volume, were among the first developments for image analyses in food-grain assessment. These traits are still some of the most commonly extracted image features because they relate directly to visual qualities of the grains (Mandal et al., 2012, Fıratlıgil-Durmuş et al., 2010, Mabille and Abecassis, 2003, Sankaran et al., 2016, Fıratlıgil-Durmuş et al., 2008, Costa et al., 2011, Aggarwal and Mohan, 2010). The majority of early applications used flatbed scanners for image acquisition and either required grain kernels to be non-touching (manually separated) to assist image segmentation (van Dalen, 2004, Igathinathane et al., 2009, Amaral et al., 2009) or required segmentation algorithms to identify and separate touching kernels (Mebatsion and Paliwal, 2011, Shahin and Symons, 2005). Grain dimensions and 2D shape features are extracted after image segmentation and boundary detection, therefore these pre-processing steps are critical to the accuracy of grain size analyses. Recent advances in image acquisition systems have incorporated mechanised grain dispersion onto conveyor systems so that kernels can be non-touching without the requirement for tedious sample placement (LeMasurier et al., 2014).

For image analysis to simulate the standard seed size assessment as described in Section 3.2.1, the method should be able to determine seed dimensions accurately, model the mass of seed and classify the seed into size groups according to size and mass. Accurate measurement techniques of seed length and width have been established through Image Analysis studies. Although some assessments from 2-dimesional image data have resulted in relatively large errors compared with the size of the seed (van Dalen, 2004, Mandal et al., 2012), it has been shown in other studies that with careful image segmentation and selection of regression models, seed dimensions can be accurately predicted (Walker and Panozzo, 2012, Igathinathane et al., 2009, LeMasurier et al., 2014).

Initial MV developments for Seed Size Distribution (SSD) of lentil can be credited to Shahin and Symons (2001). Similarly van Dalen (2004) proposed a prediction of size distribution of rice using a flatbed scanner. These studies demonstrated the potential of rapid seed size analysis however it is difficult to establish their accuracy as the image predictions were not compared to seed-sieving. Shahin and Symons (2005) built on previous work developing image analysis methods for assessment SSD of four pulse types: yellow pea, green pea, soybean and chickpea. The study reported that there were no significant differences between sieve and DIA output for chickpea and soybean, but there were significant differences between the two methods for green and

yellow pea SSD. The shape of chickpeas is non-uniform which causes a greater misclassification of size fractions through mechanical sieving than for field pea. It is likely that statistical interpretation reflects larger errors and variance for chickpea and soybean, compared to yellow and green peas, making significant differences difficult to establish between the two sizing methods. Nevertheless, an important finding of this study was that the image analysis method was robust and repeatable even for irregular shaped grains such as chickpea. The authors later followed with a similar study highlighting the application of DIA to classification of soybeans according to size uniformity of a sample (Shahin et al., 2006). They found agreement in excess of 84% with visual assessment. LeMasurier et al. (2014) developed a DIA method for assessment of lentil SSD which was predicted through a statistical model replicating the behaviour of seeds through sieves. Output from the DIA method was shown to closely match that of the sieves with R2>0.99 and Lin's concordance statistic > 0.99. Through image-based 'sieving' seed size traits can be quantified with more detail and consistency than mechanical sieving methods.

Application of MV to determine size traits has been thoroughly investigated across the grains industry. Image-based methods are rapid, robust in relation to sample size, and give consistent and accurate results. These methods would therefore be a valuable inclusion within lentil and field pea germplasm enhancement programs, both for routine germplasm-quality assessment as well as studies on the impact of abiotic effects on grain attributes (Bourgault et al., 2018).

Seed Colour

Objective assessments of grain colour are commonly conducted using a colorimeter to capture data within the CIE L*a*b* space although there have been some studies using image analysis models to replicate this output. For example, Zapotoczny and Majewska (2010) assessed wheat colour, of both the endosperm and grain coat, by machine vision using a conversion from RGB to XYZ and then XYZ to CIE L*a*b* spaces and reported significant correlations for CIE L*, a* and b* (r = 0.90, 0.84 and 0.80 respectively) with corresponding values measured by spectrophotometer. Standardising the assessment of colour is difficult since it is dependent on the surface properties of the subject, the illuminant, measurement area and geometry of the instrument. Yagiz et al. (2009) recommend caution when reporting on colour values measured by any system, even when the reference standards are correctly measured. They conducted a comparison of DIA and colorimeter assessments of Atlantic salmon colour and discovered that the visual representation of colour values calculated through DIA was closer to the expected colour of salmon than the values given by a colorimeter. However, this perceived error in

colorimeter measurement may be a property of the digital display misrepresenting the colorimeter values. Perhaps the most accurate method to date, for colour assessment by DIA, was proposed by León et al. (2006); among four other models investigated, a neural network model was proposed for measurement of L*a*b* values from RGB images, achieving a prediction error of less than 1%. Applying a method with such prediction accuracy, to assessment of pulse-grain colour seed-by-seed, would enable colour uniformity of a grain sample to be quantified.

Colour is a diverse and complex trait of pulse grains and, within the marketplace, vibrancy and uniformity of pulse colour (of whole grain or split cotyledon) are key to the visual appeal. However, colour can also be indicative of the grain condition (Coste et al., 2005), or admixture and other defects. CIE L*a*b* coordinates are objective but can be unintuitive in relation to many colour-based aspects of pulse quality. There are a range of applications of machine vision for colour assessment of lentil and field pea, including classification of market grades (McDonald et al., 2016, Shahin and Symons, 2001), detection of darkened and deteriorated lentil grains (Shahin and Symons, 2002, Dell'Aquila, 2006) and quantifying the colour of bleaching-susceptible field pea varieties (Coles, 1997, McDonald et al., 2019). With careful standardisation of pixel intensity values, image analysis offers greater flexibility than colorimetric methods to determine variety-specific quality traits and quantify uniformity objectively within pulse grain samples.

Seed Processing

MV assessment of lentil and field pea milling quality has multiple facets relating to traits of the milled product (e.g. cotyledon colour and split yield) and the milling potential of whole-grain samples. Milling potential is known to be impacted by moisture content (Singh et al., 2000) and size and shape characteristics of the grain as well as pre-treatments, such as soaking (Vishwakarma et al., 2018, Wang, 2005, Black et al., 1998). A machine vision method was developed by Shahin et al. (2012) to predict the dehulling efficiency of red lentil samples from image-derived grain shape and size features. The predicted de-hulling efficiencies were highly correlated ($R2 = 0.9$ and RMSE < 2%) with the laboratory method. Application of models such as this, within the breeding selection process, would enable predictive assessments of processing quality on early generation germplasm. Furthermore, the combination of visible image analysis, for prediction of size and shape traits, and NIR-hyperspectral image analysis for prediction of

compositional traits, such as moisture content (Huang et al., 2014), could improve the versatility of models for predicting milling potential from whole grain.

To date no image processing methods have been developed specifically for assessing the split and de-hulled grain yields of milled lentil or field pea product. It is necessary to mill the grain and attain split product for subsequent assessment of visual appeal (brightness and uniformity of colour) of the splits as well as the hydration and cooking quality. Manual sorting of split fractions is time-consuming; typically, fewer than 15 milled 100g samples of lentil can be hand-sorted per day. This type of application is an ideal candidate for time-efficient machine vision systems, particularly those with an integrated sorting system (Pearson et al., 2012).

Seed Defects

Defective grains are those which do not fit the industry specifications for sound grain within each market class. There are a wide range of defect types which include disease, mechanical damage, dockage (small grain), discoloration, admixture and contaminants, among others. To identify and assess defects through image processing it is useful to first create the reference profiles for sound grain within each market class. Lentil and field pea market classes are defined by visual characteristics relating to size, shape and colour of the grain. Image features based on these characteristics are therefore useful for creating profiles and classifying grain into market classes (McDonald et al., 2016). Classification models for seed type or market class (Weng et al., 2020, Adjemout et al., 2007, Visen et al., 2004, Venora et al., 2007a, Mahesh et al., 2011, Choudhary et al., 2009) are directly applicable to the assessment of admixture levels for objects which do not fit the market class profile of a sample (Ramirez-Paredes and Hernandez-Belmonte, 2020).

Grain defects which relate to colour are typically assessed through analysis of visible digital images (Dell'Aquila, 2006, Kılıç et al., 2007, Delwiche et al., 2013, Liu et al., 2015) and NIR-based screening, (NIR scanning or NIR-hyperspectral imaging), is generally preferred for the assessment of defects and infestations which impact composition of a sample. The application of NIR spectroscopy in agricultural products is based on chemical bonds of major constituents in the grain (such as protein, starch or water) absorbing radiation at excitation frequencies within the NIR region. Reflectance spectra display the overall response of the object constituents to incident radiation. With careful consideration of techniques for data pre-processing and subsequent multivariate regression, NIR spectroscopy has been shown to perform well for

predictions of major cereal grain constituents and classification of grain and admixture (Barton et al., 2000, Black and Panozzo, 1999). NIR spectroscopy is underutilised with pulse grains compared to cereals. This is perhaps a reflection of the traditional use of the grains; wheat composition plays an import role in functionality of the grain to produce high-quality baked, sheeted or extruded products (Pawlinsky and Williams, 1998), but typically pulses have been cooked simply as a whole or split grain product.

NIR-hyperspectral images contain both NIR spectral information as well as spatial information (Amigo et al., 2015). Therefore, analysis of hyperspectral images can be used to detect smaller concentrations or distributions of compounds present in grains. For example, it may be useful for detecting early stages and the location of disease in grains; this detail would be lost in the spectral noise of conventional NIR scanning. Hyperspectral image analysis has been applied to the detection of insect infestation and fungal infection in chickpeas, green peas, lentils, pinto beans and kidney beans (Karuppiah et al., 2016, Nansen et al., 2014), but is otherwise underdeveloped for lentil and field pea assessments. However, developments for wheat in particular demonstrate the potential of hyperspectral image analysis for detecting admixture and contaminants (Mahesh et al., 2011, Ravikanth et al., 2016, Ravikanth et al., 2015), sprouting (Xing et al., 2010) and seed damage or other grading factors (Singh et al., 2009, Shahin and Symons, 2008, Shahin and Symons, 2011).

Non-uniformity of visual characteristics within lentil and field pea samples is generally undesirable. Standard sieving methods can determine non-uniformity of grain size (Williams and Singh, 1988) however distributions of other characteristics, such as shape and colour, are determined through subjective visual estimates. Within breeding germplasm, non-uniformities can be the result of genetic segregation as well as grain defects. So it would be useful to have objective and quantitative measures for studies of genetic influence. McDonald et al. (2019) presented an equation for quantifying uniformity of colour within green field pea genotypes. Models such as this, or equivalently statistical features (Harden and Wood, 2017), based on image-derived traits enable the assessment of more than just size distributions within samples.

1.5 Conclusions of the literature review

The majority of global production of lentil and field pea continues to sustain traditional markets where the visual grain-characteristics are paramount to perceived quality. Therefore, visual traits including grain size, shape, colour, defects and uniformity as well as processing quality,

particularly milling efficiency, remain important breeding targets for ensuring the market success of newly released varieties. Current standard methods for quality assessment within breeding programs are often applied only to advanced germplasm due to the time-consuming nature of the assessments and the requirement for adequate volumes of grain to conduct the tests. Breeding programs would therefore benefit from the adoption of rapid and objective machine vision methods for screening grain quality traits.

The number of machine vision methods developed to date specifically for assessment of lentil and field pea are few by comparison with other agricultural products, such as wheat. However, these contributions, for analysis of size, shape and specific colour traits as well as the modelling of milling performance (for lentil) would significantly improve the efficiency and capacity of germplasm screening. The range of MV applications currently developed for lentil and field pea do not yet encompass the range of grain-assessments which are essential within breeding programs and so there is an opportunity and necessity for this development. For some of these grain traits, development of altogether new methods is required, and for other traits, such as some diseases, there are equivalent or similar models that exist for other grain types and these can be adapted for lentil and field pea.

Machine vision systems, adopted within plant breeding programs, would enable more detailed, targeted and higher throughput germplasm-screening. Image processing methods have the capacity to screen for multiple traits simultaneously. The robustness of image analysis to evaluate samples of any size would permit comprehensive quality assessments earlier within the breeding cycle, ultimately reducing the number of years between the first inter-cross and resultant variety for commercial release. Parallel development of machine vision methods within breeding programs would result in more robust models accounting for a greater diversity in the expressions of traits. Further to germplasm screening, MV models have potential application along the whole pulse value chain from pre-breeding, such as rapid screening of potential breeding candidates or development of genomic prediction models, through to post-breeding applications, i.e. the assessment of grains and defects within industry settings.

1.6 Thesis objectives

The broad aim of this study was to develop rapid and objective methods, based on analysis of visible-multispectral images, for screening visual quality traits of lentil and field pea. Three quality traits, which are important within breeding programs, were identified for method

development; namely classification of market grades, quantification of discoloration and assessment of milling efficiency. Therefore, the specific research aims of this thesis were the following:

1. Development and application of an algorithm to classify field pea market grades through the analysis of visible-multispectral images;

2. Development of a model to score the extent and uniformity of bleaching discoloration in green pea based on visible-multispectral image processing;

3. Application of the image-based colour-scoring system to identify and compare genotypic differences in green pea resistance to bleaching; and

4. Development and application of an algorithm for classifying lentil and field pea milled fractions through the analysis of visible-multispectral images

Diverse lentil and field pea grain samples were sourced from plant breeding programs (Agriculture Victoria, Horsham) to capture the variations of grain traits between genotypes and between market classes. Multispectral images of the grains were captured through an EyeFoss™ (FOSS Analytical, Hoganas, Sweden) which simultaneously measured grain surface height at each pixel by laser. The EyeFoss was selected in preference to conventional digital cameras for two key reasons: (1) The greater number of colour channels (405, 470, 530, 590, 660 and 850nm) which spanned the visible spectral region enabling more accurate analysis of grain colour traits; and (2) the simplicity of sample presentation due to the conveyor system within the EyeFoss which enabled rapid and automated image acquisition of individual grains within pulse samples. Image processing algorithms were developed within the Matlab programming environment (The MathWorks Inc., Natick, Massachusetts).

The remainder of this thesis is dedicated to addressing each of these research objectives. Chapter 2 details a new method for classification of field pea market classes through linear discriminant analysis. The model was based on image-derived colour, shape and size features of a diverse range of field pea samples sourced from the field pea breeding program in Horsham, Victoria (Australia). Both defective and sound grains were assessed to test robustness.

Quantitation of bleaching discoloration is addressed in Chapters 3 and 4. Development of the objective, trait-specific scoring system, based on spectrophotometric data, is detailed first

followed by the implementation of this model through multispectral-image processing. The image analysis scoring system was utilised further to model consistency of bleaching throughout grain samples as well as to quantify the relative susceptibility, to bleaching, of several green pea genotypes. Chlorophyll and phenolic compounds are associated with grain colour, therefore these constituents were analysed in relation to image-based bleaching assessments to determine if any relationship exists between the compositional traits and genotypic susceptibility.

Milling efficiency was identified as an important quality trait of both lentil and field pea. The standard method for assessment is one of the most time-consuming processes of quality evaluation due to the requirement for manual sorting of milled grain fractions. Therefore, in Chapter 5 a machine vision approach, based on convolutional neural networks, is presented for classification of milling fractions through multispectral-image analysis with specific attention given to model accuracy and time-efficiency.

1.7 References

AACC. 2020. Approved Methods of Analysis [Online]. St. Paul, MN, U.S.A.: Cereals & Grains Association. Available: http://methods.aaccnet.org/ [Accessed 19/7/2020].

ABASI, S., MINAEI, S., JAMSHIDI, B. & FATHI, D. 2018. Dedicated non-destructive devices for food quality measurement: A review. Trends in Food Science & Technology, 78, 197-205.

ADJEMOUT, O., HAMMOUCHE, K. & DIAF, M. Automatic seeds recognition by size, form and texture features. Signal Processing and Its Applications, 2007. ISSPA 2007. 9th International Symposium on, 12-15 Feb. 2007. 1-4.

AGGARWAL, A. K. & MOHAN, R. 2010. Aspect ratio analysis using image processing for rice grain quality. International Journal of Food Engineering, 6, Article 8.

AMARAL, A. L., ROCHA, O., GONÇALVES, C., FERREIRA, A. A. & FERREIRA, E. C. 2009. Application of image analysis to the prediction of EBC barley kernel weight distribution. Industrial Crops and Products, 30, 366-371.

AMIGO, J. M., BABAMORADI, H. & ELCOROARISTIZABAL, S. 2015. Tutorial: Hyperspectral image analysis. A tutorial. Analytica Chimica Acta, 896, 34-51.

BARTON, F. E., II, SHENK, J. S., WESTERHAUS, M. O. & FUNK, D. B. 2000. The development of near infrared wheat quality models by locally weighted regressions. Journal of Near Infrared Spectroscopy, 8, 201-208.

BHARGAVA, A. & BANSAL, A. 2018. Fruits and vegetables quality evaluation using computer vision: A review. Journal of King Saud University - Computer and Information Sciences.

BLACK, C. K. & PANOZZO, J. F. 1999. Whole grain quality evaluation in wheat based on near infrared spectroscopy. In: PANOZZO, J. F., RATCLIFFE, M., WOOTTON, M. & WRIGLEY, C. W.

(eds.) Proceedings of the 49th Australian Cereal Chemistry Conference. Cereals 99. Melbourne, Victoria: Royal Australian Chemical Institute, Cereal Chemistry Division.

BLACK, R. G., SINGH, U. & MEARES, C. 1998. Effect of genotype and pretreatment of field peas (Pisum sativum) on their dehulling and cooking quality. Journal of the Science of Food and Agriculture, 77, 251-258.

BOUKID, F., ZANNINI, E., CARINI, E. & VITTADINI, E. 2019. Pulses for bread fortification: A necessity or a choice? Trends in Food Science & Technology, 88, 416-428.

BOURGAULT, M., LÖW, M., TAUSZ-POSCH, S., NUTTALL, J. G., DELAHUNTY, A. J., BRAND, J., PANOZZO, J. F., MCDONALD, L., O'LEARY, G. J., ARMSTRONG, R. D., FITZGERALD, G. J. & TAUSZ, M. 2018. Effect of a Heat Wave on Lentil Grown under Free-Air CO2 Enrichment (FACE) in a Semi-Arid Environment. Crop Science, 58, 803-812.

BROSNAN, T. & SUN, D.-W. 2002. Inspection and grading of agricultural and food products by computer vision systems--a review. Computers and Electronics in Agriculture, 36, 193-213.

BROSNAN, T. & SUN, D.-W. 2004. Improving quality inspection of food products by computer vision--a review. Journal of Food Engineering, 61, 3-16.

CARACUTA, V., BARZILAI, O., KHALAILY, H., MILEVSKI, I., PAZ, Y., VARDI, J., REGEV, L. & BOARETTO, E. 2015. The onset of faba bean farming in the Southern Levant. Scientific Reports, 5, 14370.

CHOUDHARY, R., MAHESH, S., PALIWAL, J. & JAYAS, D. S. 2009. Identification of wheat classes using wavelet features from near infrared hyperspectral images of bulk samples. Biosystems Engineering, 102, 115-127.

CHURCHILL, D. B., BILSLAND, D. M. & COOPER, T. M. 1992. Comparison of Machine Vision With Human Measurement of Seed Dimensions. Transactions of the ASAE, 35, 61-64.

COLES, G. D. 1997. An Objective Dry Pea 'Colour' Scoring System for Commercial and Plant Breeding Applications. Journal of the Science of Food and Agriculture, 74, 435-440.

COSTA, C., ANTONUCCI, F., PALLOTTINO, F., AGUZZI, J., SUN, D. W. & MENESATTI, P. 2011. Shape Analysis of Agricultural Products: A Review of Recent Research Advances and Potential Application to Computer Vision. Food and Bioprocess Technology, 4, 673-692.

COSTE, F., RAVENEAU, M. P. & CROZAT, Y. 2005. Spectrophotometrical pod colour measurement: a non-destructive method for monitoring seed drying? The Journal of Agricultural Science, 143, 183-192.

COYNE, C. J., KUMAR, S., VON WETTBERG, E. J. B., MARQUES, E., BERGER, J. D., REDDEN, R. J., ELLIS, T. H. N., BRUS, J., ZABLATZKÁ, L. & SMÝKAL, P. 2020. Potential and limits of exploitation of crop wild relatives for pea, lentil, and chickpea improvement. Legume Science, 2, e36.

DAVIES, E. R. 2009. The application of machine vision to food and agriculture: A review. Imaging Science Journal, 57, 197-217.

DE OLIVEIRA, E. M., LEME, D. S., BARBOSA, B. H. G., RODARTE, M. P. & PEREIRA, R. G. F. A. 2016. A computer vision system for coffee beans classification based on computational intelligence techniques. Journal of Food Engineering, 171, 22-27.

DELL'AQUILA, A. 2006. Red-Green-Blue (RGB) colour density as a non-destructive marker in sorting deteriorated lentil (Lens culinaris Medik.) seeds. Seed Science and Technology, 34, 609-619.

DELL' AQUILA, A. 2009. Digital imaging information technology applied to seed germination testing. A review. Agronomy for Sustainable Development, 29, 213-221.

DELWICHE, S. R., YANG, I. C. & GRAYBOSCH, R. A. 2013. Multiple view image analysis of freefalling U.S. wheat grains for damage assessment. Computers and Electronics in Agriculture, 98, 62-73.

DÖRING, T. F. 2015. Grain Legume Cropping Systems in Temperate Climates. In: RON, A. M. D. (ed.) Grain Legumes New York: Springer, New York, NY.

ERSKINE, W. & SARKER, A. 2004. LENTIL | Breeding. In: WRIGLEY, C. (ed.) Encyclopedia of Grain Science. Oxford: Elsevier.

ERSKINE, W., SARKER, A. & KUMAR, S. 2016. Lentil Breeding. Reference Module in Food Science. Elsevier.

ERSKINE, W., WILLIAMS, P. C. & NAKKOUL, H. 1991. Splitting and dehulling lentil (Lens culinaris): Effects of genotype and location. Journal of the Science of Food and Agriculture, 57, 85-92.

FAO. 2016a. International Year of Pulses [Online]. Available: http://www.fao.org/pulses-2016/en/ [Accessed].

FAO. 2016b. Trends in worldwide production, consumption and trade of pulses [Online]. Available: http://www.fao.org/pulses-2016/news/news-detail/en/c/381491/ [Accessed 30/05/2019 2019].

FAOSTAT. 2020. Value of Agricultural Production [Online]. Available: http://www.fao.org [Accessed 19/7/2020 2019].

FıRATLıGIL-DURMUŞ, E., ŠARKA, E. & BUBNÍK, Z. 2008. Image vision technology for the characterisation of shape and geometrical properties of two varieties of lentil grown in Turkey. Czech Journal of Food Sciences, 26, 109-116.

FıRATLıGIL-DURMUŞ, E., ŠÁRKA, E., BUBNÍK, Z., SCHEJBAL, M. & KADLEC, P. 2010. Size properties of legume seeds of different varieties using image analysis. Journal of Food Engineering, 99, 445-451.

FOX, G. & MANLEY, M. 2014. Applications of single kernel conventional and hyperspectral imaging near infrared spectroscopy in cereals. Journal of the Science of Food and Agriculture, 94, 174-179.

GPC. Global Pulse Confederation [Online]. Available: http://globalpulses.com [Accessed 26/05/2019].

GUPTA, M., TIWARI, B. & SINGH BAWA, A. 2011. 15 - Quality standards and evaluation of pulses. In: TIWARI, B. K., GOWEN, A. & MCKENNA, B. (eds.) Pulse Foods. San Diego: Academic Press.

HARDEN, S. & WOOD, J. A. 2017. A Single Parameter for Within-Sample Uniformity of Seed Size in Grain, with an Emphasis on Pulses. Cereal Chemistry, 94, 430-436.

HAYES, B. J., PANOZZO, J., WALKER, C. K., CHOY, A. L., KANT, S., WONG, D., TIBBITS, J., DAETWYLER, H. D., ROCHFORT, S., HAYDEN, M. J. & SPANGENBERG, G. C. 2017. Accelerating wheat breeding for end-use quality with multi-trait genomic predictions incorporating near infrared and nuclear magnetic resonance-derived phenotypes. Theoretical and Applied Genetics, 130, 2505-2519.

HAZRA, K. K., VENKATESH, M. S., GHOSH, P. K., GANESHAMURTHY, A. N., KUMAR, N., NADARAJAN, N. & SINGH, A. B. 2014. Long-term effect of pulse crops inclusion on soil-plant nutrient dynamics in puddled rice (Oryza sativa L.)-wheat (Triticum aestivum L.) cropping system on an Inceptisol of Indo-Gangetic plain zone of India. Nutrient Cycling in Agroecosystems, 100, 95-110.

HUANG, T.S. 1996. Computer Vision: Evolution and Promise. CERN School of Computing, no. 19: 21-25, http://cds.cern.ch/record/400313/files/ p21.pdf.

HUANG, M., WANG, Q., ZHANG, M. & ZHU, Q. 2014. Prediction of color and moisture content for vegetable soybean during drying using hyperspectral imaging technology. Journal of Food Engineering, 128, 24-30.

IGATHINATHANE, C., PORDESIMO, L. O. & BATCHELOR, W. D. 2009. Major orthogonal dimensions measurement of food grains by machine vision using ImageJ. Food Research International, 42, 76-84.

JHA, S. N. 2016. Chapter 7 - Imaging Methods. In: JHA, S. N. (ed.) Rapid Detection of Food Adulterants and Contaminants. San Diego: Academic Press.

JOSHI, M., TIMILSENA, Y. & ADHIKARI, B. 2017. Global production, processing and utilization of lentil: A review. Journal of Integrative Agriculture, 16, 2898-2913.

KAISER, W. J., RAMSEY, M. D., MAKKOUK, K. M., BRETAG, T. W., AÇIKGÖZ, N., KUMAR, J. & NUTTER, F. W. 2000. Foliar Diseases of Cool Season Food Legumes and Their Control. In: KNIGHT, R. (ed.) Linking Research and Marketing Opportunities for Pulses in the 21st Century: Proceedings of the Third International Food Legumes Research Conference. Dordrecht: Springer Netherlands.

KARUPPIAH, K., SENTHILKUMAR, T., JAYAS, D. S. & WHITE, N. D. G. 2016. Detection of fungal infection in five different pulses using near-infrared hyperspectral imaging. Journal of Stored Products Research, 65, 13-18.

KHAN, T. N. & CROSER, J. S. 2004. PEA | Overview. In: WRIGLEY, C. (ed.) Encyclopedia of Grain Science. Oxford: Elsevier.

KıLıÇ, K., BOYACı, İ. H., KÖKSEL, H. & KÜSMENOĞLU, İ. 2007. A classification system for beans using computer vision system and artificial neural networks. Journal of Food Engineering, 78, 897-904.

KUMAR, M., BORA, G. & LIN, D. 2013. Image processing technique to estimate geometric parameters and volume of selected dry beans. Journal of Food Measurement and Characterization, 7, 81-89.

KUMAR, N., HAZRA, K., NATH, C., PRAHARAJ, C. & SINGH, U. 2018. Grain Legumes for Resource Conservation and Agricultural Sustainability in South Asia. In: MEENA, R. S., DAS, A., YADAV, G. S. & LAL, R. (eds.) Legumes for Soil Health and Sustainable Management. Springer Singapore.

KUMAR, N., NATH, C. P., HAZRA, K. K., DAS, K., VENKATESH, M. S., SINGH, M. K., SINGH, S. S., PRAHARAJ, C. S. & SINGH, N. P. 2019. Impact of zero-till residue management and crop diversification with legumes on soil aggregation and carbon sequestration. Soil and Tillage Research, 189, 158-167.

LECUN, Y., BENGIO, Y. & HINTON, G. 2015. Deep learning. Nature, 521, 436-444.

LEMASURIER, L. S., PANOZZO, J. F. & WALKER, C. K. 2014. A digital image analysis method for assessment of lentil size traits. Journal of Food Engineering, 128, 72-78.

LEÓN, K., MERY, D., PEDRESCHI, F. & LEÓN, J. 2006. Color measurement in L*a*b* units from RGB digital images. Food Research International, 39, 1084-1091.

LIU, D., NING, X., LI, Z., YANG, D., LI, H. & GAO, L. 2015. Discriminating and elimination of damaged soybean seeds based on image characteristics. Journal of Stored Products Research, 60, 67-74.

MABILLE, F. & ABECASSIS, J. 2003. Parametric modelling of wheat grain morphology: A new perspective. Journal of Cereal Science, 37, 43-53.

MAHAJAN, S., DAS, A. & SARDANA, H. K. 2015. Image acquisition techniques for assessment of legume quality. Trends in Food Science & Technology, 42, 116-133.

MAHENDRAN, R., AJAY VINO, S. & ANANDAKUMAR, S. 2016. Fundamentals of Computer Vision System for Sorting and Grading of Food Products. Reference Module in Food Science. Elsevier.

MAHESH, S., JAYAS, D. S., PALIWAL, J. & WHITE, N. D. G. 2011. Identification of wheat classes at different moisture levels using near-infrared hyperspectral images of bulk samples. Sensing and Instrumentation for Food Quality and Safety, 5, 1-9.

MANDAL, S., ROY, S. & TANNA, H. 2012. A low-cost image analysis technique for seed size determination Current Science, 103, 1401-1403.

MCDONALD, L., SALISBURY, P., FORD, R. & PANOZZO, J. 2019. Quantifying the colour loss of green field pea (Pisum sativum L.) due to bleaching. PLOS ONE, 14, e0221523.

MCDONALD, L. S., PANOZZO, J. F., SALISBURY, P. A. & FORD, R. 2016. Discriminant Analysis of Defective and Non-Defective Field Pea (<italic>Pisum sativum L</italic>.) into Broad Market Grades Based on Digital Image Features. PLoS ONE, 11, e0155523.

MEBATSION, H. K. & PALIWAL, J. 2011. A Fourier analysis based algorithm to separate touching kernels in digital images. Biosystems Engineering, 108, 66-74.

MEENA, B. P., BISWAS, A. K., SINGH, M., CHAUDHARY, R. S., SINGH, A. B., DAS, H. & PATRA, A. K. 2019. Long-term sustaining crop productivity and soil health in maize–chickpea system through integrated nutrient management practices in Vertisols of central India. Field Crops Research, 232, 62-76.

MICHAELS, T. E. 2004. PULSES, OVERVIEW. In: WRIGLEY, C. (ed.) Encyclopedia of Grain Science. Oxford: Elsevier.

MILLS, J. T. W., S. M ; WATTS, B. M.; LAMARI, L.; WHITE, N. D. G. 1999. Comparison of techniques to measure seed color and its relationship to other quality parameters in stored lentil (Lens culinaris Medik.). Seed science and technology, 27, 1015-1028.

MIRALI, M., PURVES, R. W. & VANDENBERG, A. 2016. Phenolic profiling of green lentil (Lens culinaris Medic.) seeds subjected to long-term storage. European Food Research and Technology, 242, 2161-2170.

NANSEN, C., ZHANG, X., ARYAMANESH, N. & YAN, G. 2014. Use of variogram analysis to classify field peas with and without internal defects caused by weevil infestation. Journal of Food Engineering, 123, 17-22.

NASAR-ABBAS, S. M., SIDDIQUE, K. H. M., PLUMMER, J. A., WHITE, P. F., HARRIS, D., DODS, K. & D'ANTUONO, M. 2009. Faba bean (Vicia faba L.) seeds darken rapidly and phenolic content falls when stored at higher temperature, moisture and light intensity. LWT - Food Science and Technology, 42, 1703-1711.

NATH, C. P., HAZRA, K. K., KUMAR, N., PRAHARAJ, C. S., SINGH, S. S., SINGH, U. & SINGH, N. P. 2019. Including grain legume in rice–wheat cropping system improves soil organic carbon pools over time. Ecological Engineering, 129, 144-153.

NGUYEN, G. N. & NORTON, S. L. 2020. Genebank Phenomics: A Strategic Approach to Enhance Value and Utilization of Crop Germplasm. Plants, 9.

NLEYA, T., VANDENBERG, A. & WALLEY, F. L. 2004. LENTIL | Agronomy. In: EDITOR-IN-CHIEF: COLIN, W. (ed.) Encyclopedia of Grain Science. Oxford: Elsevier.

NTURAMBIRWE, J. F. I. & OPARA, U. L. 2020. Machine learning applications to non-destructive defect detection in horticultural products. Biosystems Engineering, 189, 60-83.

PAWLINSKY, T. & WILLIAMS, P. 1998. Prediction of wheat bread-baking functionality in whole wheat kernels, using near infrared reflectance spectroscopy. Journal of Near Infrared Spectroscopy, 6, 121-127.

PEARSON, T., MOORE, D. & PEARSON, J. 2012. A machine vision system for high speed sorting of small spots on grains. Journal of Food Measurement & Characterization, 6, 27-34.

PHELPS, S. 2015. Bleaching in Green Pea [Online]. Available: https://saskpulse.com/files/general/151027_Bleaching_in_Green_Pea.pdf [Accessed].

PORTMAN, D., BLANCHARD, C., MAHARJAN, P., MCDONALD, L. S., MAWSON, J., NAIKER, M. & PANOZZO, J. F. 2018. Blending studies using wheat and lentil cotyledon flour—Effects on rheology and bread quality. Cereal Chemistry, 95, 849-860.

RAMIREZ-PAREDES, J.-P. & HERNANDEZ-BELMONTE, U.-H. 2020. Visual quality assessment of malting barley using color, shape and texture descriptors. Computers and Electronics in Agriculture, 168, 105110.

RATISH, R. K., AJAY, V. S., MEETHA, N. J. & MAHENDRAN, R. 2017. Nondestructive Quality Evaluation Techniques. Reference Module in Food Science. Elsevier.

RAVIKANTH, L., SINGH, C. B., JAYAS, D. S. & WHITE, N. D. G. 2015. Classification of contaminants from wheat using near-infrared hyperspectral imaging. Biosystems Engineering, 135, 73-86.

RAVIKANTH, L., SINGH, C. B., JAYAS, D. S. & WHITE, N. D. G. 2016. Performance evaluation of a model for the classification of contaminants from wheat using near-infrared hyperspectral imaging. Biosystems Engineering, 147, 248-258.

REHMAN, T. U., MAHMUD, M. S., CHANG, Y. K., JIN, J. & SHIN, J. 2019. Current and future applications of statistical machine learning algorithms for agricultural machine vision systems. Computers and Electronics in Agriculture, 156, 585-605.

SANKARAN, S., WANG, M. & VANDEMARK, G. J. 2016. Image-based rapid phenotyping of chickpeas seed size. Engineering in Agriculture, Environment and Food, 9, 50-55.

SHAHIN, M. A. & SYMONS, S. J. 2001. A machine vision system for grading lentils. Canadian Biosystems Engineering / Le Genie des biosystems au Canada, 43, 77-714.

SHAHIN, M. A. & SYMONS, S. J. Instrumental Colour and Size Grading of Pulse Grains. Proceedings of the World Congress of Computers in Agriculture and Natural Resources (13-15, March 2002, Iguacu Falls, Brazil), 2002 St. Joseph, MI. ASABE, 107-113.

SHAHIN, M. A. & SYMONS, S. J. 2005. Seed sizing from images of non-singulated grain samples. Canadian Biosystems Engineering / Le Genie des biosystems au Canada, 47, 3.49-3.55.

SHAHIN, M. A. & SYMONS, S. J. 2008. Detection of hard vitreous and starchy kernels in amber durum wheat samples using hyperspectral imaging (GRL Number M306). NIR news, 19 16–18.

SHAHIN, M. A. & SYMONS, S. J. 2011. Detection of Fusarium damaged kernels in Canada Western Red Spring wheat using visible/near-infrared hyperspectral imaging and principal component analysis. Computers and Electronics in Agriculture, 75, 107-112.

SHAHIN, M. A., SYMONS, S. J. & POYSA, V. W. 2006. Determining Soya Bean Seed Size Uniformity with Image Analysis. Biosystems Engineering, 94, 191-198.

SHAHIN, M. A., SYMONS, S. J. & WANG, N. 2012. Predicting dehulling efficiency of lentils based on seed size and shape characteristics measured with image analysis. Quality Assurance and Safety of Crops & Foods, 4, 9-16.

SINGH, C. B., JAYAS, D. S., PALIWAL, J. & WHITE, N. D. G. 2009. Detection of insect-damaged wheat kernels using near-infrared hyperspectral imaging. Journal of Stored Products Research, 45, 151-158.

SINGH, U., WILLIAMS, P. C. & PETTERSON, D. S. 2000. Processing and Grain Quality To Meet Market Demands. In: KNIGHT, R. (ed.) Linking Research and Marketing Opportunities for Pulses in the 21st Century: Proceedings of the Third International Food Legumes Research Conference. Dordrecht: Springer Netherlands.

SOZER, N., HOLOPAINEN-MANTILA, U. & POUTANEN, K. 2017. Traditional and New Food Uses of Pulses. Cereal Chemistry, 94, 66-73.

VAN DALEN, G. 2004. Determination of the size distribution and percentage of broken kernels of rice using flatbed scanning and image analysis. Food Research International, 37, 51-58.

VENKATESH, M. S., HAZRA, K. K., GHOSH, P. K. & MISHRA, J. P. 2019. Integrated phosphorus management in maize-chickpea rotation in moderately-alkaline Inceptisol in Kanpur, India: An agronomic and economic evaluation. Field Crops Research, 233, 21-32.

VENORA, G., GRILLO, O., RAVALLI, C. & CREMONINI, R. 2007a. Tuscany beans landraces, on-line identification from seeds inspection by image analysis and Linear Discriminant Analysis. Agrochimica, 51, 254-268.

VENORA, G., GRILLO, O., SHAHIN, M. A. & SYMONS, S. J. 2007b. Identification of Sicilian landraces and Canadian cultivars of lentil using an image analysis system. Food Research International, 40, 161-166.

VISEN, N. S., PALIWAL, J., JAYAS, D. S. & WHITE, N. D. G. 2004. Image analysis of bulk grain samples using neural networks. Canadian Biosystems Engineering / Le Genie des biosystems au Canada, 46, 7.11-7.15.

VISHWAKARMA, R. K., SHIVHARE, U. S., GUPTA, R. K., YADAV, D. N., JAISWAL, A. & PRASAD, P. 2018. Status of pulse milling processes and technologies: A review. Critical Reviews in Food Science and Nutrition, 58, 1615-1628.

VITHU, P. & MOSES, J. A. 2016. Machine vision system for food grain quality evaluation: A review. Trends in Food Science & Technology, 56, 13-20.

WALKER, C. K. & PANOZZO, J. F. 2012. Measuring volume and density of a barley grain using ellipsoid approximation from a 2-D digital image. Journal of Cereal Science, 55, 61-68.

WANG, N. 2005. Optimization of a Laboratory Dehulling Process for Lentil (Lens culinaris). Cereal Chemistry, 82, 671-676.

WENG, S., TANG, P., YUAN, H., GUO, B., YU, S., HUANG, L. & XU, C. 2020. Hyperspectral imaging for accurate determination of rice variety using a deep learning network with multi-feature fusion. Spectrochimica Acta Part A: Molecular and Biomolecular Spectroscopy, 234, 118237.

WILLIAMS, P., GELADI, P., FOX, G. & MANLEY, M. 2009. Maize kernel hardness classification by near infrared (NIR) hyperspectral imaging and multivariate data analysis. Analytica Chimica Acta, 653, 121-130.

WILLIAMS, P. C. & SINGH, U. 1988. Quality screening and evaluation in pulse breeding. In: SUMMERFIELD, R. J. (ed.) World crops: Cool season food legumes: A global perspective of the problems and prospects for crop improvement in pea, lentil, faba bean and chickpea. Dordrecht: Springer Netherlands.

XING, J., SYMONS, S., SHAHIN, M. & HATCHER, D. 2010. Detection of sprout damage in Canada Western Red Spring wheat with multiple wavebands using visible/near-infrared hyperspectral imaging. Biosystems Engineering, 106, 188-194.

YAGIZ, Y., BALABAN, M. O., KRISTINSSON, H. G., WELT, B. A. & MARSHALL, M. R. 2009. Comparison of Minolta colorimeter and machine vision system in measuring colour of irradiated Atlantic salmon. Journal of the Science of Food and Agriculture, 89, 728-730.

ZAPOTOCZNY, P. & MAJEWSKA, K. 2010. A comparative analysis of colour measurements of the seed coat and endosperm of wheat kernels performed by various techniques. International Journal of Food Properties, 13, 75-89.

CHAPTER 2

Discriminant analysis of defective and non-defective field pea (*Pisum sativum L.*) into broad market grades based on digital image features

This chapter has been published as:

MCDONALD, L. S., PANOZZO, J. F., SALISBURY, P. A. & FORD, R. 2016. Discriminant Analysis of Defective and Non-Defective Field Pea (Pisum sativum L.) into Broad Market Grades Based on Digital Image Features. PLoS ONE, 11, e0155523.

Abstract

Field peas (Pisum sativum L.) are generally traded based on seed appearance, which subjectively defines broad market-grades. In this study, we developed an objective Linear Discriminant Analysis (LDA) model to classify market grades of field peas based on seed colour, shape and size traits extracted from digital images. Seeds were imaged in a high-throughput system consisting of a camera and laser positioned over a conveyor belt. Six colour intensity digital images were captured (under 405, 470, 530, 590, 660 and 850nm light) for each seed, and surface height was measured at each pixel by laser. Colour, shape and size traits were compiled across all seed in each sample to determine the median trait values. Defective and non-defective seed samples were used to calibrate and validate the model. Colour components were sufficient to correctly classify all non-defective seed samples into correct market grades. Defective samples required a combination of colour, shape and size traits to achieve 87% and 77% accuracy in market grade classification of calibration and validation sample-sets respectively. Following these results, we used the same colour, shape and size traits to develop an LDA model which correctly classified over 97% of all validation samples as defective or non-defective.

2.1 Introduction

Field pea (Pisum sativum L.) is generally traded based on broad quality grades, each of which has its own market niche. Grades are determined subjectively and often classified inconsistently between the grain sellers and buyers, leading to trading disputes. Khan and Croser (2004) identified five broad types of field pea (yellow, marrowfat, dun, green/blue and maple) and six quality traits which heavily influence their marketing; admixture levels, insect damage, seed colour, seed size, seed cleanliness and product uniformity. Historically, these traits are based on appearance and are assessed visually. As such, the trading value of field pea (like most pulse grains) is subjectively determined. There is an opportunity, therefore, for objective measurement of grain products using colour grading systems or machine vision to reduce the potential for inconsistent assessment.

Within the grains research field, several studies have been conducted on the application of machine vision systems to quantitatively determine characteristics related to grain quality. Zapotoczny and Majewska (2010) investigated the measurement of wheat colour, of both the endosperm and grain coat, by machine vision. Fundamental size traits, such as grain length, width and volume, have been modelled in various studies (Mandal et al., 2012, Fıratlıgil-Durmuş et al., 2010, Walker and Panozzo, 2012, Mabille and Abecassis, 2003), as well as shape of grains (Costa et al., 2011, Mebatsion et al., 2012, Aggarwal and Mohan, 2010). Further to grain size, shape and colour analysis, machine vision studies have also been applied to assess traits which impact on grain processing, such as chalkiness in rice (Sun et al., 2014, Yoshioka et al., 2007), performance of wheat samples through a dockage tester (Paliwal, Visen et al. 2003) and distribution of grain size (Shahin et al., 2006, LeMasurier et al., 2014), which impacts on milling efficiency.

Machine vision sytems have also been used in the grains industry for colour-based grading and identifying defects and seed damage. While 2-dimensional colour, size and shape traits are the most commonly used, more recent focus has been on expanding the range of image traits to include textural, morphological, and wavelet features, enabling a suite of measurments from each image and contributing to an increased efficency and justification of the capital expenditure in setting up digital image technology. Anami and Savakar (2011) provided a summary on some of the most common feature extraction methods used in the analysis of grains, fruits and flowers. Choudhary et al. (2008) developed a model to classify cereal grains into grain type (wheat, rye, barley and oats) and reported that the combination of

morphological, colour, textural as well as wavelet features gave the best results for classification. A number of studies have identified type and extent of cereal grain (Mirik et al., 2006, Delwiche et al., 2013) and legume grain defects (Dell'Aquila, 2006, Nansen et al., 2014, Liu et al., 2015, Kılıç et al., 2007, Wiwart et al., 2009) through digital image analysis (DIA). Key to all of these assessments were the extracted image features chosen to inform statistical and analytical models for measuring and classifying the grain quality traits. Zheng et al. (2006) provided an overview of textural features for assessing food quality by DIA and identified the two most commonly adopted classification methods as Statistical Learning (SL), for example discriminant analysis and Bayesian learning, and Artificial Neural Networks (ANN). Choice of image features and classification method is important for ensuring accuracy and efficiency of field pea broad market grade assessment by DIA.

Field-pea market grades are classified by key visual-characteristics of seed shape, size and colour of seed coat and cotyledon. However, all of these characteristics can be altered by various seed defects. For example, diseases and/or weather damage can cause discoloration, deformation and/or shrivelling of seed. Therefore, the development of a robust model to classify broad market grades, of defective as well as non-defective grain, should use image features which best represent these key visual characteristics. While two-dimensional images of grain can contribute a large number of helpful size, shape and colour classification features, grain surface height information is also useful for measuring traits such as dimpling and correcting variations in colour intensity readings due to variable surface height. In this study, we developed models to classify field pea into broad market grades and investigated the impact of grain defects on model performance. We extracted a number of colour, shape and size (including laser-measured seed height) features from images of field pea seed. These features were used to build Linear Discriminant Analysis (LDA) models to classify the seed into common Australian market grades; White Pea, Blue Pea, Mottled-Dun Pea, Kaspa-Dun Pea, Green-Dun Pea, Yellow-Forage Pea, Marrowfat Pea, and Kaspa-Type Pea.

2.2 Materials & Methods

2.2.1 Sample collection and classification

Field pea seed samples were sourced from the 2013/14 and 2014/15 harvests of the breeding and agronomy trials undertaken by the Department of Economic Development, Jobs, Transport and Resources based in Horsham, Victoria, Australia. Samples were considered as defective when at least 75% of the seed were either disease-stained, weather damaged, insect damaged

or broken. Samples were considered as non-defective if less than 5% of the seeds were impacted by defects. The distinction between defective and non-defective samples was intended to improve clarity in observing the impact of defects on classification models. There were 239 non-defective grain samples and 78 defective samples selected at random within these two categories. Each field pea sample was manually classified into one of eight market grades (Fig 2.1 and Table 2.1). Samples were then divided into calibration and validation sets (Table 2.2); a Calibration set of 175 samples (including 39 defective samples) and a Validation set of 142 samples (including 39 defective samples).

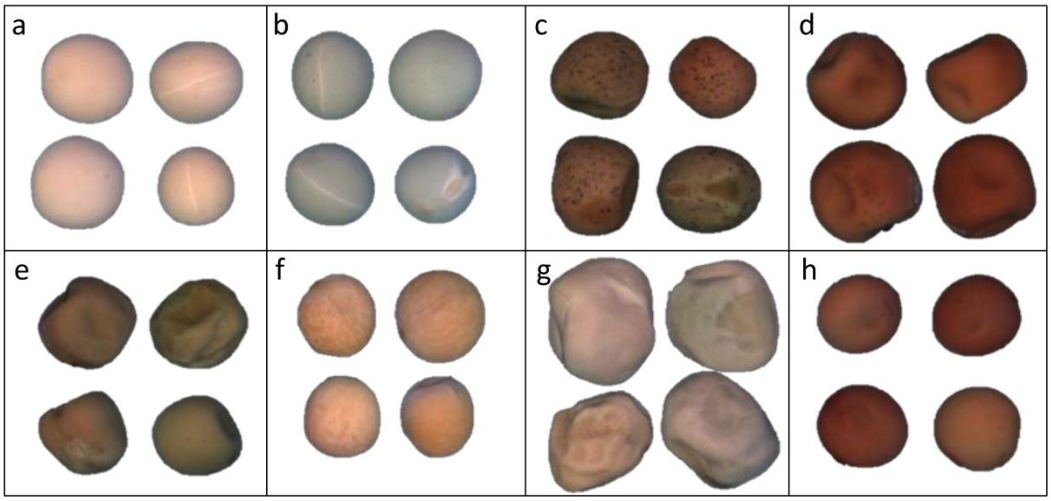

Figure 2.1. Field pea market grades. a) White Pea, b) Blue Pea, c) Mottled Dun Pea, d) Kaspa Dun Pea, e) Green Dun Pea, f) Yellow Forage Pea, g) Marrowfat Pea, h) Kaspa-Type Pea.

Table 2.1. Descriptions of field pea market grades

White Pea	***Blue Pea***	***Mottled Dun Pea***	***Kaspa Dun Pea***
Yellow cotyledon with white, opaque seed coat. Smooth spherical seed.	Green cotyledon with white-opaque seed coat. Smooth spherical seed.	Yellow cotyledon with a green/tan and speckled seed coat. Dimpled seed.	Yellow cotyledon with a tan coloured seed coat. Dimpled seed.
Green Dun Pea	***Yellow Forage Pea***	***Marrowfat Pea***	***Kaspa-Type Pea***
Yellow cotyledon with a tan and green coloured seed coat. Heavily dimpled seed.	Yellow cotyledon with opaque white seed coat. These look similar to white peas but are generally smaller in size and deeper yellow in colour.	Yellow cotyledon with white, opaque seed coat. Large, heavily dimpled seed	Yellow cotyledon with a tan coloured seed coat. Round seed with smooth seed coat (minimal dimples)

Table 2.2. Field pea calibration and validation sets

Market Grade	*All Calibration Samples*	*Defective Samples in Calibration Set*	*All Validation Samples*	*Defective Samples in Validation set*
White	50	4	45	4
Blue	31	0	44	0
Mottled Dun	7	4	5	4
Kaspa Dun	13	7	8	6
Green Dun	16	0	5	1
Yellow Forage	5	5	6	6
Marrowfat	6	0	2	0
Kaspa type	47	19	27	18
	175	**39**	**142**	**39**

2.2.2 Model development

Model development is depicted in Fig 2.2 and detailed below.

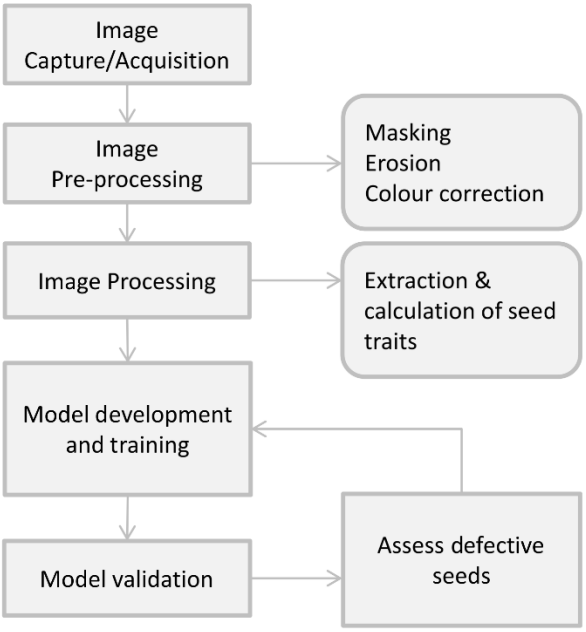

Figure 2.2. Model development flow chart.

Image Capture

Images were captured through an EyeFoss™ (FOSS Analytical, Hoganas, Sweden) as described by LeMasurier et al. (2014). For each individual field pea seed, the EyeFoss™ captured six colour intensity images (under LED light sources of 405, 470, 530, 590, 660 and 850nm) and simultaneously measured surface height, by laser, at each pixel location. Colour intensity and height images were stored as double precision, floating point number arrays.

Image Pre-processing

Each image was segmented, using the method described by LeMasurier et al. (2014), to create a binary image mask (M1), which was used to detect the seed boundary and to measure size and shape characteristics. A second binary mask image (M2) was created by setting a threshold of 20 units on the heights image. M2 was used in the calculation of colour and height traits to avoid interference from seed boundary values where height was near zero and colour intensity values were affected by shadowing.

Image Processing

Single-seed images were processed according to the flow chart in Fig 2.3. All single-seed features extracted from the images are outlined in Table 2.3. The median value, of each feature across all seeds in each sample, was taken as the feature value for that sample. Feature values were standardised to have zero mean and unit standard deviation across the Calibration Set of samples.

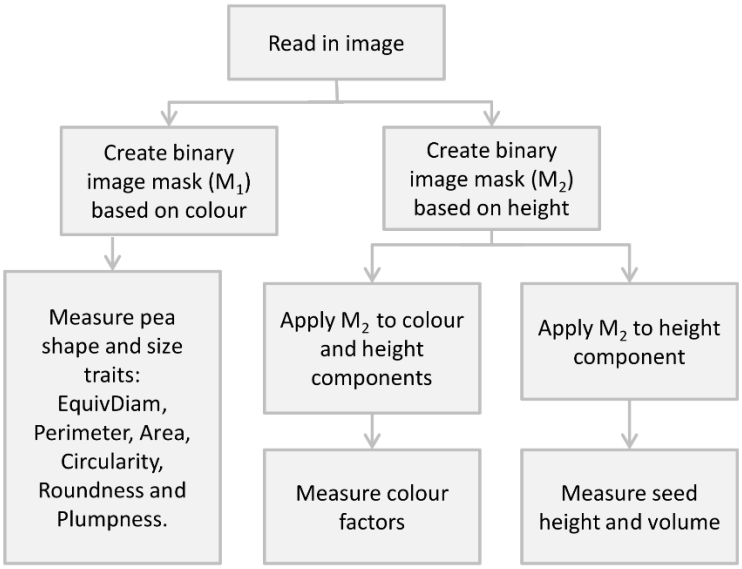

Figure 2.3. Image pre-processing and processing flow chart

Table 2.3. Seed characteristics extracted through image processing

Single Seed Features	*Measurement/Calculation*
Violet colour factor	Apply the mask $\mathbf{M_2}$ to both the height image and the violet (405nm) colour intensity image. Within the seed region, divide each pixel colour value by the corresponding height value[a].The violet factor was taken as the median of all corrected pixel colour values.
Blue colour factor, Green colour factor, Orange colour factor, Red colour factor and NIR colour factor	As for Violet colour factor but calculate on the blue (470nm), green (530nm), orange (590nm), red(660nm) and NIR (850nm) intensity images, respectively.
Seed height	Apply the mask $\mathbf{M_2}$ to the height image and take the median value within the seed region.
Equivalent diameter, Area and Plumpness	As detailed by LeMasurier et al. (2014)
Perimeter	Number of pixels in seed boundary
Volume	Sum of all values within seed region of heights image (after applying $\mathbf{M_1}$)
Circularity	(area x 4) / (Equivalent diameter x Perimeter)

Model development

Market grades of field pea are defined by visual traits (Table 2.1), therefore all image features (Table 2.3) were deliberately related directly to colour, size or shape of the seeds. Features were tested to ensure linear independence and then selected for model training based on prior knowledge of dominant discriminating traits of market grades. Therefore, preference was given first to colour, then size and then shape features. Features were added one at a time to the model and those which did not improve accuracy of classifications were discarded. Models were trained such that they would require the minimum number of features to achieve greatest possible accuracy and robustness in predictions. Since there was clear visual distinction between field pea market grades (Fig 2.1), it was assumed that, with the appropriate selection of image features, market grades would be linearly separable. LDA was therefore chosen as the classification method because of its relative simplicity and lower computational cost compared with other classification methods. The LDA models were constructed and analysed through Matlab (R2014b) with the Statistics Toolbox.

Model 1 and 2

The first LDA model (Model 1) was trained on the non-defective samples of the Calibration Set and validated on the non-defective samples of the Validation Set. This was done to observe the greatest potential accuracy of predicting field pea market grades, since the market grades are defined by appearance of non-defective grain. The performance of this model was then tested on the defective samples of the Validation Set to observe the impact of seed defects on market grade assessment. A second LDA model (Model 2) was subsequently calibrated and validated,

on the full Calibration Set and Validation Set respectively (including defective samples) to observe changes to classification robustness from Model 1. Features were chosen for Model 2 to give the simplest model with the most accurate predictions for both defective and non-defective field pea samples.

Predicting defects

A difference in classification accuracy between Model 1 and Model 2, in assessment of the defective samples, was assumed to indicate that a third LDA model could be constructed based on the same input variables to distinguish defective from non-defective field pea samples.

2.3 Results and discussion

The three LDA models which were developed are outlined in Table 2.4 with their respective calibration and validation sample sets, input variables and output classes. The performance of each model is outlined in Table 2.5.

Table 2.4. Linear discriminant analysis models and parameters

	Model 1	*Model 2*	*Defect prediction Model*
Calibration samples	Calibration Set excluding defective samples	Full Calibration Set	Full Calibration Set
Validation samples	Full Validation Set; Separately assessing non-defective then defective samples	Full Validation Set	Full Validation Set
Input variables	Blue, green, orange and red factors	As for Model 1 plus violet colour factor, equivalent diameter, circularity and plumpness	As for Model 2
Classification Groups	White, Blue, Mottled-Dun, Kaspa-Dun, Green-Dun, Marrowfat and Kaspa type	White, Blue, Mottled-Dun, Kaspa-Dun, Green-Dun, Yellow-Forage, Marrowfat and Kaspa type	Defective and non-defective

Table 2.5. Classification Rates of Models

Prediction Model	*% Accuracy in prediction of non-defective calibration samples (n=136)*	*% Accuracy in prediction of defective calibration samples (n=39)*	*% Accuracy in prediction of non-defective validation samples (n=103)*	*% Accuracy in prediction of defective validation samples (n=39)*
Model 1	100	NA	100	69[a]
Model 2	100	87	100	77
Defect prediction model	100	100	97	100

Feature Selection

A one-way Multivariate Analysis of Variance (MANOVA) was performed on all extracted image features (Table 2) for the full set of calibration samples. Since the choice of features was based on the definitions of market grades, it was not surprising that the F statistic of each feature was significant ($p < 0.001$), indicating that any of the features could in some way be useful for separating samples according to their market grade. All feature vectors were found to be linearly independent by Singular Value Decomposition (SVD). Prior knowledge of dominant visual traits in the definitions of field pea grades determined the order of feature selection. Preference was given first to colour, then size and then shape features.

2.3.1 Model 1

Image colour traits alone were sufficient inputs to classify all of the non-defective field pea samples (both calibration and validation sets) into correct market grades. Four of the six colour traits (red, orange, green and blue factors) gave the optimum combination of input variables. The NIR factor did not vary markedly between different field pea groups (Fig 2.4) and therefore did not impact on market grade predictions. Violet colour intensity varied substantially between different market grades but had little impact on the prediction of non-defective grain samples as there was sufficient information in the four mid-range wavelength colour factors. Model 1 excluded predictions of Yellow-Forage peas since all samples of forage peas were defective.

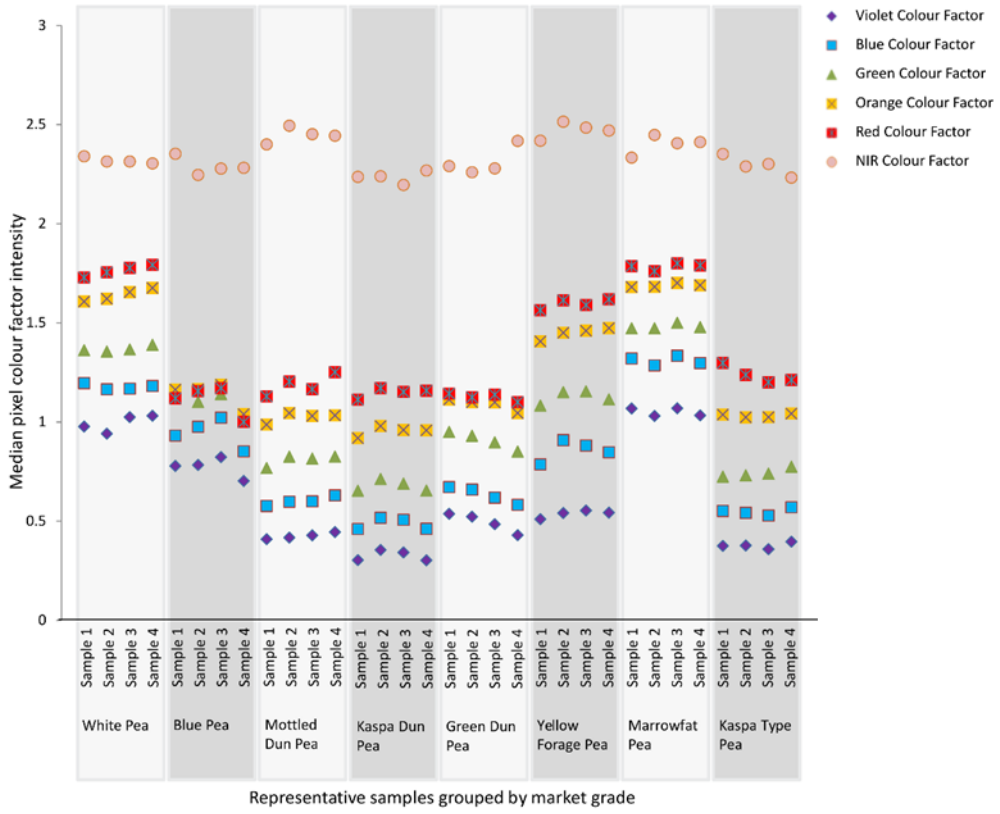

Figure 2.4. Colour factor variations between field pea market grades. Four representative samples from each market grade illustrate the variation in relative colour intensity factors. The violet, blue, green, orange, red and NIR colour factors for each sample are represented respectively by the violet diamonds, blue squares, green triangles, yellow squares, red squares and pink circles. These are the basis for predicting market grades through Model 1.

While non-defective peas were accurately classified into their appropriate market grade through Model 1, this was not the case for defective pea samples (Table 4). The majority of misclassified defective samples were from the Kaspa, Kaspa-Dun and Green-Dun groups, which were categorised as Mottled-Dun peas. This was not surprising, as disease staining, which can have similar dark toned patterns to seed coat speckling, was the most prevalent defect.

Defects other than disease staining also have impact on colour of the seeds. For example, harvest damage or insect damage can expose areas of the cotyledon. One white pea sample was misclassified as a marrowfat type because the seed surface colour was affected by areas of seed coat detaching from the cotyledon. Though white pea can be similar in colour to marrowfat pea, they are very different in size and shape (Table 2.2).

The results of Model 1 indicated that colour features were significantly impacted by defects in the field peas since the accuracy in prediction of defective validation samples was much lower than for non-defective validation samples. Therefore Model 2 was constructed to include inputs of seed size and shape traits (equivalent diameter, circularity and plumpness) additional to the violet colour factor and the inputs of Model 1 (Table 3).

2.3.2 Model 2

Model 2 maintained the accuracy of Model 1 in classifying market grades of non-defective samples and improved classification of defective sample sets (Table 4). Non-defective samples tended to lie closer, in terms of Mahalanobis distance, to their correct Market Grade mean than the defective samples (Fig 2.5c and d). In the Validation set, the mean Mahalanobis distance of defective and non-defective samples from their nearest class mean was 3.91±0.33 and 2.42±0.09 respectively. Therefore, the non-defective samples were more accurately predicted, and with greater confidence, than the defective samples.

Three defective samples that were correctly classified through Model 1, were then misclassified through Model 2. All three samples had both disease staining and insect damage. Two of the samples were white peas, misclassified as Yellow Forage peas, with seed smaller than the average size of White pea market grade. The third sample was a Mottled-Dun which was misclassified as a Kaspa-Dun type. In all three cases the exposed cotyledon appears to have affected model predictions by causing the average seed surface colour to be more yellow. Therefore, a method for identifying and removing areas of exposed cotyledon in seed images would be useful to improve market grade predictions based on seed coat appearance.

Of the defective samples that were initially misclassified through Model 1, more than 70% were subsequently classified correctly through Model 2. Most of these samples were defective due to disease staining, which did not appear to affect seed shape and size. This implied that the violet colour factor played a significant role in distinguishing disease staining apart from natural speckling. Nine of the defective samples, which had been misclassified through Model 1, remained misclassified through Model 2. These samples were predominantly disease stained Kaspa-Dun and Kaspa-Type samples, which were classified as Mottled-Dun pea by both models. So, while the violet colour factor had a significant role in distinguishing disease from speckling, it was not sufficient to discriminate the few samples that fell close to the classification border between their true class and the Mottled-Dun class. In a commercial setting this misclassification

rate is acceptable since samples would first be screened for defects and only the non-defective grain would then be classified further into market grades. A third LDA model was developed to classify grain as defective or non-defective.

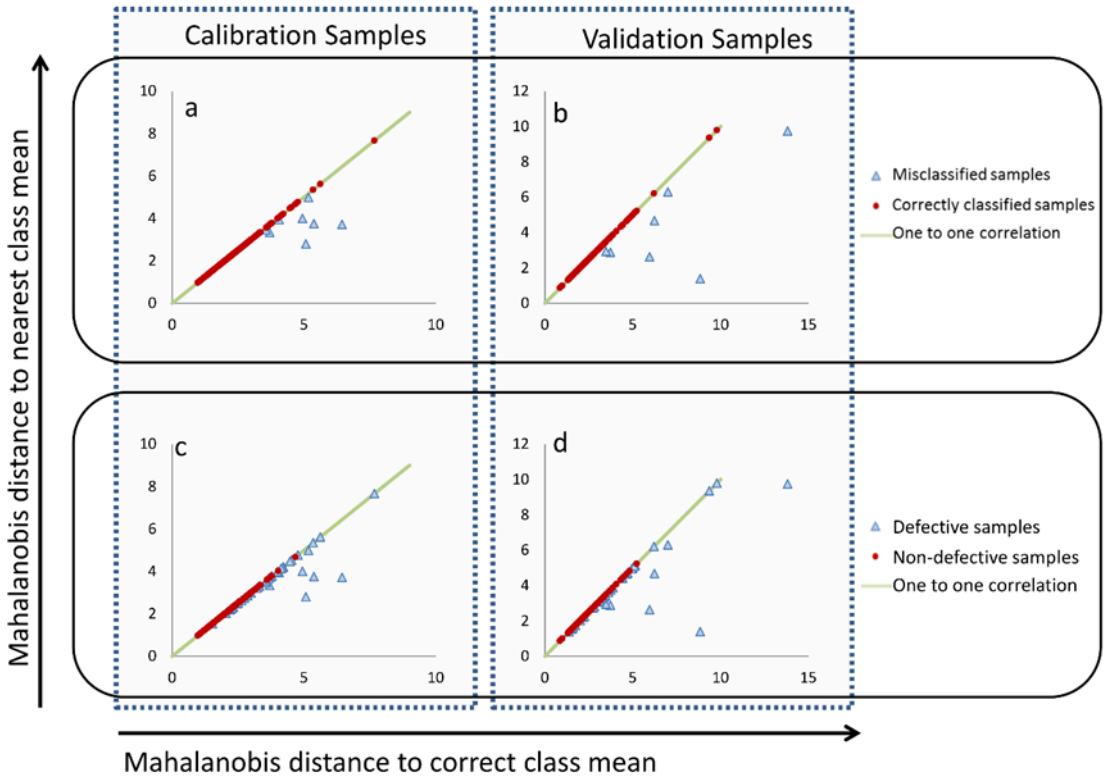

Figure 2.5. Performance of Model 2. (a) and (b) All samples that were correctly classified (red dots) fell along the one to one correlation line (green), i.e. the closest market grade mean was the correct market grade mean for that sample. All samples which did not lie on the green line (one to one correlation) were incorrectly classified (blue triangles). Plots (c) and (d) gave the same scatter plots as (a) and (b) but highlighted which samples were non-defective (red dots) and which were defective (blue triangles).

2.3.3 Defect prediction Model

Differences in results for classifying defective samples through Model 1 and Model 2 indicated that a LDA model based on the same inputs would be able to also predict which field pea samples were defective among various market grade types. This proved true, all defective samples (both calibration and validation) were correctly classified (Table 4). All non-defective seed calibration samples were correctly classified and all but three samples of the non-defective seed validation set were correctly classified. While this model is not extended in the present study, the results

indicate a modelling potential, to classify types of defects within grain samples, for example disease damage, insect damage and pre-harvest weather damage.

2.4 Conclusion

Digital image analysis combined with linear discriminant analysis provides an effective tool for classifying pea market grades. In this study market grades of non-defective and defective seed samples were classified at 100% and up to 87% correctly, respectively. The choice of input variables influenced the robustness of the models to predict the market grades of defective as well as non-defective seeds. The input variables were based on industry-standard marketing traits, related to visual grain qualities, removing subjectivity through the application of digital image analysis.

2.5 Acknowledgements

The authors gratefully acknowledge Dr. Jason Brand for providing the field pea samples used in this study and the technical input from Dr. Pankaj Maharjan and Slavica Laskovska.

2.5 References

AGGARWAL, A. K. & MOHAN, R. 2010. Aspect ratio analysis using image processing for rice grain quality. International Journal of Food Engineering, 6, Article 8.

ANAMI, B. S. & SAVAKAR, D. G. 2011. Suitability of feature extraction methods in recognition and classification of grains, fruits and flowers. International Journal of Food Engineering, 7, Article 9.

CHOUDHARY, R., PALIWAL, J. & JAYAS, D. S. 2008. Classification of cereal grains using wavelet, morphological, colour, and textural features of non-touching kernel images. Biosystems Engineering, 99, 330-337.

COSTA, C., ANTONUCCI, F., PALLOTTINO, F., AGUZZI, J., SUN, D. W. & MENESATTI, P. 2011. Shape Analysis of Agricultural Products: A Review of Recent Research Advances and Potential Application to Computer Vision. Food and Bioprocess Technology, 4, 673-692.

DELL'AQUILA, A. 2006. Red-Green-Blue (RGB) colour density as a non-destructive marker in sorting deteriorated lentil (Lens culinaris Medik.) seeds. Seed Science and Technology, 34, 609-619.

DELWICHE, S. R., YANG, I. C. & GRAYBOSCH, R. A. 2013. Multiple view image analysis of freefalling U.S. wheat grains for damage assessment. Computers and Electronics in Agriculture, 98, 62-73.

FıRATLıGIL-DURMUŞ, E., ŠÁRKA, E., BUBNÍK, Z., SCHEJBAL, M. & KADLEC, P. 2010. Size properties of legume seeds of different varieties using image analysis. Journal of Food Engineering, 99, 445-451.

KHAN, T. N. & CROSER, J. S. 2004. PEA | Overview. In: WRIGLEY, C. (ed.) Encyclopedia of Grain Science. Oxford: Elsevier.

KıLıÇ, K., BOYACı, İ. H., KÖKSEL, H. & KÜSMENOĞLU, İ. 2007. A classification system for beans using computer vision system and artificial neural networks. Journal of Food Engineering, 78, 897-904.

LEMASURIER, L. S., PANOZZO, J. F. & WALKER, C. K. 2014. A digital image analysis method for assessment of lentil size traits. Journal of Food Engineering, 128, 72-78.

LIU, D., NING, X., LI, Z., YANG, D., LI, H. & GAO, L. 2015. Discriminating and elimination of damaged soybean seeds based on image characteristics. Journal of Stored Products Research, 60, 67-74.

MABILLE, F. & ABECASSIS, J. 2003. Parametric modelling of wheat grain morphology: A new perspective. Journal of Cereal Science, 37, 43-53.

MANDAL, S., ROY, S. & TANNA, H. 2012. A low-cost image analysis technique for seed size determination Current Science, 103, 1401-1403.

MEBATSION, H. K., PALIWAL, J. & JAYAS, D. S. 2012. Evaluation of variations in the shape of grain types using principal components analysis of the elliptic Fourier descriptors. Computers and Electronics in Agriculture, 80, 63-70.

MIRIK, M., MICHELS JR, G. J., KASSYMZHANOVA-MIRIK, S., ELLIOTT, N. C., CATANA, V., JONES, D. B. & BOWLING, R. 2006. Using digital image analysis and spectral reflectance data to quantify damage by greenbug (Hemitera: Aphididae) in winter wheat. Computers and Electronics in Agriculture, 51, 86-98.

NANSEN, C., ZHANG, X., ARYAMANESH, N. & YAN, G. 2014. Use of variogram analysis to classify field peas with and without internal defects caused by weevil infestation. Journal of Food Engineering, 123, 17-22.

SHAHIN, M. A., SYMONS, S. J. & POYSA, V. W. 2006. Determining Soya Bean Seed Size Uniformity with Image Analysis. Biosystems Engineering, 94, 191-198.

SUN, C., LIU, T., JI, C., JIANG, M., TIAN, T., GUO, D., WANG, L., CHEN, Y. & LIANG, X. 2014. Evaluation and analysis the chalkiness of connected rice kernels based on image processing technology and support vector machine. Journal of Cereal Science, 60, 426-432.

WALKER, C. K. & PANOZZO, J. F. 2012. Measuring volume and density of a barley grain using ellipsoid approximation from a 2-D digital image. Journal of Cereal Science, 55, 61-68.

WIWART, M., FORDOŃSKI, G., ŻUK-GOŁASZEWSKA, K. & SUCHOWILSKA, E. 2009. Early diagnostics of macronutrient deficiencies in three legume species by color image analysis. Computers and Electronics in Agriculture, 65, 125-132.

YOSHIOKA, Y., IWATA, H., TABATA, M., NINOMIYA, S. & OHSAWA, R. 2007. Chalkiness in Rice: Potential for Evaluation with Image Analysis. Crop Science, 47, 2113-2120.

ZAPOTOCZNY, P. & MAJEWSKA, K. 2010. A comparative analysis of colour measurements of the seed coat and endosperm of wheat kernels performed by various techniques. International Journal of Food Properties, 13, 75-89.

ZHENG, C., SUN, D.-W. & ZHENG, L. 2006. Recent applications of image texture for evaluation of food qualities—a review. Trends in Food Science & Technology, 17, 113-128.

CHAPTER 3

Quantifying the colour loss of green field pea (*Pisum sativum L.*) due to bleaching

This chapter has been published as:

MCDONALD, L., SALISBURY, P., FORD, R. & PANOZZO, J. 2019. Quantifying the colour loss of green field pea (Pisum sativum L.) due to bleaching. PLOS ONE, 14, e0221523.

Abstract

Post-harvest change in the colour of green field pea (*Pisum sativum L.*) is undesirable as this impacts the visual quality and market value of the seed. To date, there is no standard, objective method to determine bleaching. Therefore, the aim of this study was to develop an objective method for scoring bleaching based on colour reflectance spectra, measured both by spectrophotometer and multispectral Image Analysis (IA). Green field pea seeds were sorted into samples of uniform colour and these were used to train the model. Spectra calculated from multispectral images (with colour bands at 405,470,530,590,660 and 850nm) were matched to the spectrophotometer output through multiple linear regression. All spectra were transformed to emphasize the wavelength regions most impacted during bleaching, following which two critical reflectance values were scaled to a single bleaching score.

The bleaching assessment method was tested in a time-course experiment comprising seeds from five green-pea genotypes stored for six months. Each sample was divided into two so that half of the seeds were stored in the dark and the remainder were exposed to controlled light to exaggerate bleaching. Throughout this period, the samples were imaged at six-weekly intervals. Assessment of bleaching by the IA method agreed well with spectrophotometer measurements, achieving a Lin's concordance statistic of 0.99 and 0.96 for the calibration and time-course samples respectively. The IA method proved more versatile because assessments could be made on individual seeds enabling the computation of bleaching uniformity within each sample. This method captured differences between genotypes in the extent, rate and uniformity of bleaching. All genotypes exhibited susceptibility to bleaching when stored under the controlled light conditions. Excell was observed to be the most susceptible genotype with the greatest bleaching-rate and OZB1308 displayed the most colour-stability.

3.1 Introduction

Green pea is one of the major market classes of the *Pisum sativum L*. pulse grain family (McDonald et al., 2016) and commonly used as a high-protein food source for human consumption as well as livestock feed. Canada is the largest producer and exporter of field pea globally (Statistica, 2017) and according to the Canadian Grain Standards Guide (CGC, 2018), field pea is classified as either 'green pea' or 'other than green pea' and then subsequently assessed for other quality traits. This classification emphasises the relative importance of the green pea type in comparison with the other field pea market classes.

Bleaching of green field pea adversely affects the visual quality of the grain and therefore also its market value. Bleaching is a discoloration of the pea seed as chlorophyll degrades, causing seed colour to fade toward lighter green and ultimately yellowish-cream (Ubayasena et al., 2013). The colour of agricultural food products is often closely related to compositional quality (Ornelas-Paz et al., 2008, Nasar-Abbas et al., 2008, Nasar-Abbas et al., 2009) and colour-uniformity is considered particularly important for marketability (Christiansen et al., 2012, Mendoza et al., 2006, Wu and Sun, 2013b). The industry standard maximum allowance (percent by weight) for bleached green pea varies between countries. Australian guidelines indicate a maximum of 1% off-colour seed for a field pea sample to achieve No. 1 grade (GTA, 2018) and in Canada the maximum allowance is 2% bleached seed (CGC, 2018). Bleaching is therefore undesirable as it can vary widely within a sample and this decreases colour uniformity and visual appeal of the seed (Ubayasena et al., 2013). It is generally thought that bleaching has no effect on the seed viability (Phelps, 2015), however Atak et al. (2008) conducted a study of three green pea genotypes and found that the darker seed had a higher vigour and germination rate than lighter seed.

Bleaching can occur pre-harvest once the seed has reached physiological maturity, particularly if the field pea plant is subjected to wet and dry soil-moisture cycles or the seed is exposed to light during the final desiccation phase (Gubbels and Ali-Khan, 1990, McCallum et al., 1997, Cheng et al., 2004). Therefore, delayed harvesting increases the risk of bleaching (French, 2016, Brand, 2015). Bleaching can also occur post-harvest due to sub-optimal storage conditions such as extended storage periods and exposure to high temperatures, high humidity or high light intensity (Jatoi et al., 2001, Ubayasena et al., 2010, Ubayasena et al., 2013).

While bleaching is a considerable marketing issue, the standard assessment technique is subjective and tedious. This involves a visual estimation of the extent of discoloration across individual seed lots and at times, manual dehulling of individual seeds to inspect cotyledon colour (CGC, 2018). Due to the impact that bleaching has on the market classification of field pea quality, it is the subject of ongoing plant breeding to develop cultivars which are resistant to bleaching. A machine-vision based scoring system would improve assessment efficiency and provide an objective measure of the distribution and extent of bleaching. A small number of studies which address the associated genetic inheritance and enzyme activity have quantified bleaching through various colour scales. However, there is a lack of consistency and formality among the methods. Gubbels and Ali-Khan (1990) used a visual comparison of the seed to colour-charts, giving each sample a number between 1, for bleached seed, and 9, for dark green. This method is intuitive but highly subjective and prone to human-error. McCallum et al. (1997) used video image analysis in the YUV colour space, Ubayasena et al. (2010) used the Hunter Lab "a" (red-green) colour component to assess the extent of bleaching and Steet and Tong (1996) used Commission Internationale de l'Eclairage (CIE) a* (red-green) to determine greenness and relate this to chlorophyll content in pureed green pea. The YUV colour space is objective but device-dependent and therefore not easily adopted as a repeatable standard method. The Hunter a and CIE a* scales are objective and device-independent; however, bleaching does not occur linearly with respect to either scale nor does a single component of each colour space fully capture the field pea colour change.

The CIE L*a*b* colour space is the most commonly used method for assessing pulse grains. It is intuitive and objective, designed to linearly align with human-perceived colour. For green pea, typically CIE L* values are between 50 and 66, CIE a* between -4 and -1 and CIE b* between 8 and 15 (NSDU, 2017). As green pea seeds bleach, their L* value increases, a* decreases in magnitude and b* increases; i.e. the seed becomes simultaneously lighter, less green and more yellow. The standard measure for assessing colour changes using the CIE L*a*b* space is ΔE; calculated as the Euclidean distance between two points in the colour space. However, since the changes in CIE L*, a* and b* are not linear and because different genotypes exhibit varying tones of green and yellow/cream as they bleach, an absolute ΔE value is not intuitive for scoring bleaching.

Digital image analysis has been explored for colour assessment of many agricultural food products (Wu and Sun, 2013a, Yan et al., 2010, Mendoza et al., 2006). The advantages of

assessing colour traits by IA are many; particularly, it is rapid, objective, repeatable and non-destructive and the high spatial resolution obtained enables detailed assessments (Wu and Sun, 2013b). Changes in image colour have been examined to indicate ripeness of fruits such as strawberries (2014) and apples (Garrido-Novell et al., 2012) and colour features have been used to identify types of green vegetables before and after heat treatment (Manninen et al., 2015). Furthermore digital images of lentils were analysed by Dell'Aquila (2006) to indicate seed viability based on browning of the seed-coat. Imaging analysis models based on digital colour features have also been applied to leaves and crop canopies to determine chlorophyll and biomass [28] and to indicate macronutrient deficiencies in plants (Wiwart et al., 2009).

The objective and consistent nature of image analysis and its usefulness in accurately and rapidly detecting and assessing colour changes in food products makes it an attractive method for assessing bleaching in field pea providing that image colour can be consistently calibrated. Therefore, the aims of this study were to: (1) Develop an objective model based on visible reflectance spectral analysis to determine bleaching scores for green field pea samples; (2) Develop an image analysis method, based on multispectral images, to replicate the spectral analysis bleaching scores and enable assessment of bleaching at a single seed level; and (3) Apply the image analysis method to quantify bleaching score, rate and uniformity of five green pea genotypes subjected to exaggerated bleaching conditions over a period of six months.

3.2 Materials and methods

All seed samples were sourced from a field trial grown in western Victoria (Australia) during the 2015 growing season. There were 12 field plots for each of five green pea genotypes (Excell, OZB1308, OZB1310, OZB1315 and OZB1324), totalling 60 samples. This study comprised two sets of sample-data referred to herein as the time-course data and the colour-sorted data. These data sets are detailed in the sections following.

3.2.1 Colour-sorted samples and data collection

Each of the 60 green pea samples was subsampled twice (approximately 150-200 seeds per subsample). One subsample was stored in the dark to avoid bleaching effects and the other was exposed to accelerated-bleaching conditions. These were stored in a single layer in a clear, 90mm diameter petri dish under fluorescent light with the mean intensity of 7500lx. The samples were stored for a period of 9 months beginning 58 days after harvest. The position of samples on the light shelf was re-randomised at fortnightly intervals. At the completion of the

nine month trial, each of the 120 green pea samples (60 stored in the dark and 60 stored in the light) was sorted by visual inspection into groups of like-colours. In total there were 145 colour-sorted samples. Multispectral images, with colour bands at 405, 470, 530, 590, 660 and 850nm, were collected for all samples using an EyeFoss™ (Foss Analytical, Hoganas, Sweden). Each sample was also measured for colour reflectance spectra by spectrophotometer (Minolta CM-5, Konica Minolta). Spectrophotometric measurements were taken through a glass petri dish (aperture 30mm, D65 illuminant, reflectance, spectral component excluded). Spectral data was collected as the mean of three sets of triplicate measurements and stored as discrete reflectance values recorded every 10nm from 360nm to 740nm. The data collected on the colour-sorted samples was used to develop and calibrate a model for objectively scoring bleaching based on colour reflectance spectra and to develop an image analysis method for scoring bleaching. Development of these methods is outlined in the following four sections.

3.2.2 Time-course samples and data collection

Seeds were collected from three plots of each of the five green pea genotypes in the source field trial. The 15 samples were then subsampled twice (approximately 150-200 seeds per subsample) and stored under the same light and dark conditions described for the colour-sorted samples. The time-course samples were stored for a period of six months and imaged every six weeks using an EyeFoss™. At these same time intervals, colour reflectance spectra were also measured for each sample by spectrophotometer with the same instrument settings as used for the colour-sorted samples.

3.2.3 Development of the bleaching-score model

The bleaching-score model was developed with the aim of producing a scale, ranging from 0 to 100, to quantify the extent of bleaching where 0 represented dark green seed and 100 represented completely bleached seed. Development of this model was based on spectrophotometric data of the colour-sorted green pea samples.

Discrete colour reflectance spectra were reduced to five reflectance values, measured at 400, 470, 530, 590 and 660nm (Fig 3.1b), corresponding to the colour bands of the multispectral images. On inspection of the spectra it was noted that there were two regions, centred around 470nm and 590nm, where the spectra distinctly changed shape in response to bleaching colour changes. The reduced spectra were subsequently transformed to enhance the detection of this response. This transformation comprised a linear slope adjustment, to create a zero-overall

gradient between 440 and 530nm, and a shift such that the transformed reflectance values at 530nm were all zero (Fig 3.1c). Two critical values, $C1$ and $C2$, were then calculated as a linear scaling of the transformed spectra at 470nm and 590nm, respectively (Equations 1a and 1b). The bleaching score, B, was then calculated as the average of the two critical values and scaled such that B was in the range [0,100]; $B = 50(C1 + C2)$.

$$C1 = \alpha_1 T(470nm) + \beta_1 \qquad (1a)$$

$$C2 = \alpha_2 T(590nm) + \beta_2 \qquad (1b)$$

Where $T(\lambda)$ is a transformed spectrum, in the form of the spectra depicted in Fig 3.1c , and $\alpha_1, \alpha_2, \beta_1$ and β_2 are constants to be determined such that $C1$ and $C2$ are in the range $[0,1]$.

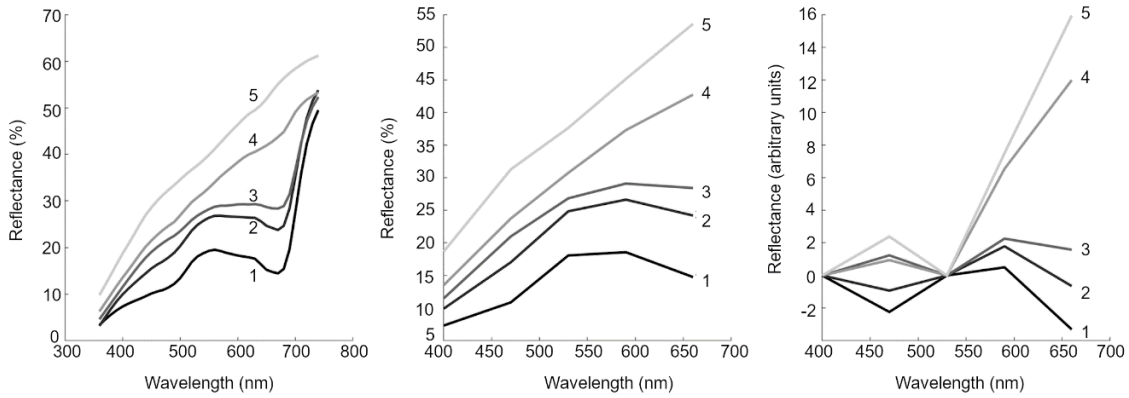

Figure 3.1. Spectral response of bleaching. Example spectra of five green pea genotypes at various stages of bleaching. Dark line (1) represented the least bleached and lightest grey line (5) represented the most bleached. (a) Original spectra measured by spectrophotometer; (b) Spectra in (a) sampled at 400,470,530,590 and 660nm; (c) Spectra at 400,470,530,590 and 660nm transformed according to the method outlined in the previous section.

3.2.4 Image processing to obtain single seed colour spectra

The EyeFoss™ is an instrument which captures multispectral images of individual seeds as they travel along a conveyor (LeMasurier et al., 2014). Therefore, for each green pea sample analysed through the EyeFoss there were as many multispectral images generated as there were seeds. Images were processed through Matlab and Image Processing Toolbox R2018b (The Mathworks Inc., Natick, Massachusetts, United States) software. Multispectral images were segmented to identify the seed region in each image and this region was then further eroded by five pixels around the boundary to circumvent interference of boundary-shadowing on the seed colour. For each seed, a discrete colour spectrum was computed; this comprised the 25th percentile

pixel intensity value of each of the six image colour bands within the seed region of the image. The 25th percentile value was used instead of the mean or median, to ensure that the representative colour of any given seed was not impacted by seed regions, such as the hilum or crease, which are naturally lighter in colour independent of bleaching. Discrete spectral values were then transformed through Multiple Linear Regression (MLR) models to match image intensity values to the reflectance units of the spectrophotometer output. The MLR models were constructed using the spectrophotometer output and the mean image-derived spectral values of the colour-sorted green pea samples. Dependent and independent variables of these MLR models are listed in Table 3.1. Through this transformation, only the first five transformed colour bands were retained as a part of the image-derived spectra, since the 6th colour band (850nm) was outside the range of the spectrophotometer measurements.

Table 3.1. **Modelling the spectrophotometer output.** MLR input model variables for transforming pixel intensity values to the reflectance units of the spectrophotometer.

Wavelength of modelled reflectance value	***Independent Variables ****	***Dependent Variable *****
400nm	405nm and 470nm	400nm
470nm	405nm, 470nm and 530nm	470nm
530nm	470nm, 530nm and 590nm	530nm
590nm	530nm, 590nm and 660nm	590nm
660nm	590nm, 660nm and 850nm	660nm

* Independent variables are the pixel intensity values of listed-wavelength image colour-band
** Dependent variables are the spectrophotometer-measured reflectance values at the listed wavelengths

3.2.5 Quantifying bleaching by image analysis

Discrete image spectra, calculated for each seed, were transformed in the same manner as the spectrophotometer spectra described earlier. Critical values $C1$ and $C2$ were then calculated according to Equations 1a and 1b and the bleaching score for each individual seed was subsequently calculated. The bleaching score for each sample was taken as the average of all the individual-seed bleaching scores within that sample.

3.2.6 Quantifying bleaching in the time course samples

Time course bleaching scores were predicted by image analysis for all the seeds in each sample. The rate of bleaching was measured by regression analysis for each genotype as the gradient of

the mean sample bleaching scores across all measurement dates. Uniformity, U_B, of bleaching was calculated for each genotype as $U_B = 1 - \frac{IPR_B}{100}$, where IPR_B is the inter-percentile range (calculated as the 90th percentile minus the 10th percentile) of bleaching scores. All statistical analyses were computed through the use of GenStat (18th Edition) software.

3.3 Results and discussions

3.3.1 Bleaching score model and image processing

Image processing results

Digital-image spectral-reflectance values calculated through MLR models highly correlated with the spectrophotometer output for both the colour-sorted sample set (which was used to calibrate the MLR models) and the time-course sample set (Table 3.2). The time-course samples were less uniform in colour than the colour-sorted samples and this had a small impact on the accuracy of reflectance predictions, resulting in a slightly lowered Lin's concordance statistic for each of the colour bands.

Table 3.2. Performance of pixel intensity transformation models. Correlation coefficients and Lin's concordance test statistics for the MLR models developed to transform pixel intensity values to reflect reflectance units of the spectrophotometer.

Colour-band wavelength	Sample Set	R^2	Lin's concordance statistic	Lin's concordance 95% C.I.
400nm	Colour-sorted	0.99	0.99	(0.98, 0.99)
470nm	Colour-sorted	0.99	0.99	(0.99,0.99)
530nm	Colour-sorted	0.99	0.99	(0.98, 0.99)
590nm	Colour-sorted	0.99	0.99	(0.99,0.99)
660nm	Colour-sorted	0.99	0.99	(0.99, 1.00)
400nm	Time-course	0.99	0.99	(0.98, 0.99)
470nm	Time-course	0.98	0.98	(0.98, 0.99)
530nm	Time-course	0.98	0.97	(0.96, 0.98)
590nm	Time-course	0.98	0.97	(0.96, 0.98)
660nm	Time-course	0.98	0.96	(0.95, 0.97)

Selection of critical value calculation constants

In order to calculate the bleaching scores for the colour-sorted and time-course samples, the critical value coefficients, ($\alpha_1, \alpha_2, \beta_1$ and $\beta_2$from Equations 1a and 1b) were determined using the maximum and minimum values of the single-seed, image-derived, spectral reflectance

values (Fig 3.2) at wavelengths of 470nm and 590nm, since these were more extreme than the whole-sample spectral values (which were an average of the single-seed values). The coefficients were calculated according to Equations 2a, 2b, 2c and 2d (Table 3.3).

$$\alpha 1 = \frac{1}{Max470 - Min470} \quad (2a)$$

$$\alpha 2 = \frac{1}{Max590 - Min590} \quad (2b)$$

$$\beta 1 = \frac{-Min470}{Max470 - Min470} \quad (2c)$$

$$\beta 2 = \frac{-Min590}{Max590 - Min590} \quad (2d)$$

Max470 and *Min470* are the maximum and minimum transformed spectral reflectance values of single seed observed at 470nm. Similarly, *Max590* and *Min590* are the maximum and minimum values at 590nm (Fig 3.2).

Table 3.3. Critical value computation.

Constant coefficient values for calculating critical values (Equations 1a and 1b)

Constant	***Value***
α_1	0.1204
α_2	0.0858
β_1	-0.5076
β_1	-0.1342

To apply this bleaching score model on images taken from another instrument, the coefficients in Table 3.3 would remain with the same values, however the MLR model transformations of pixel intensity values would have to be calculated specifically for each imaging instrument.

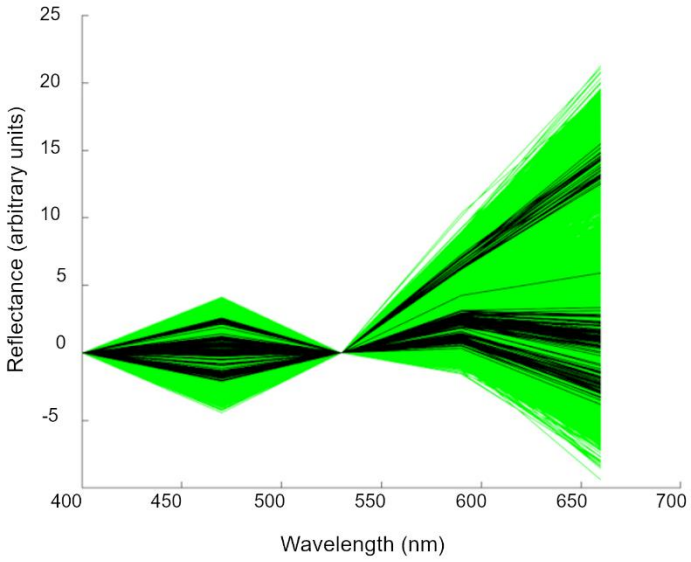

Figure 3.2. Transformed spectral range. Transformed image spectra of single seeds (green lines, n = 11309) and whole samples (black lines, n = 145). The single seed values are more extreme than the whole sample values.

3.3.2 Results of the bleaching model

The bleaching scores depicted in Fig 3.3, are linearly related to the transformed spectral values at 470nm and 590nm. Reflectance values at these wavelengths highly correlated between the spectrophotometer output and image predictions (Table 3.2). Therefore, it was expected that bleaching scores predicted through the image analysis method would be closely related to the bleaching scores calculated from the spectrophotometer output (Fig 3.4 and Table 3.4). Image analysis predictions of bleaching scores for the time-course samples had a greater RMS error than those for the colour-sorted samples (Table 3.4). This is likely due to the greater range of colours within each time-course sample and therefore more variability in the colour of the seed faces which were assessed by the spectrophotometer and those which were imaged.

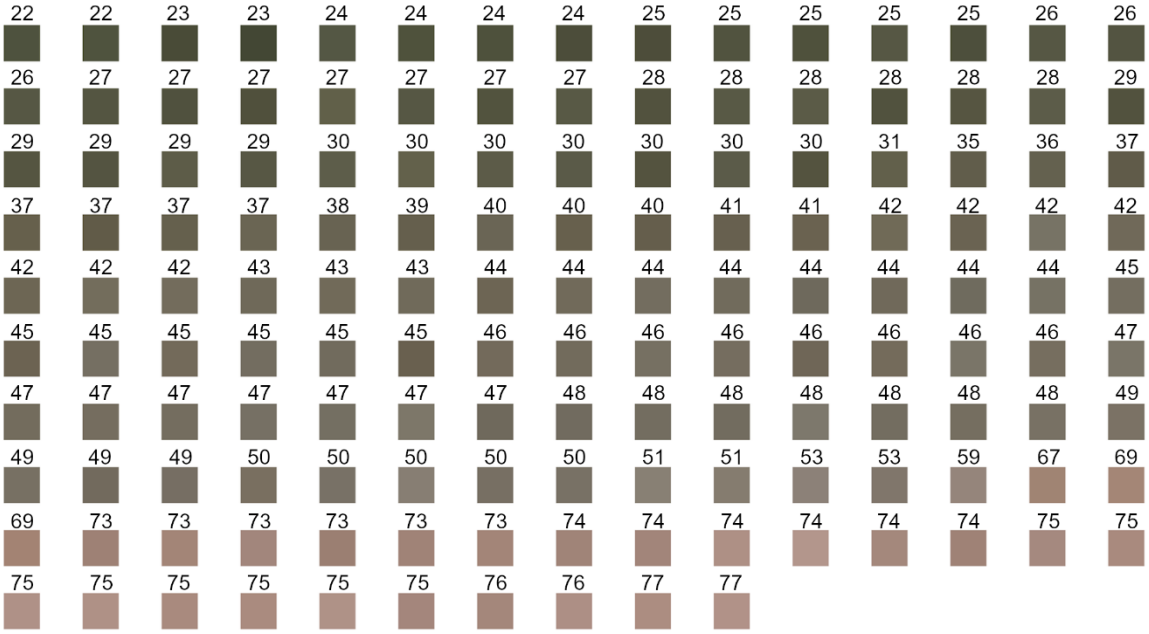

Figure 3.3. Bleaching score chart. Illustration of bleaching scores for the colour-sorted samples. The number above each square was the bleaching score assigned for that square.

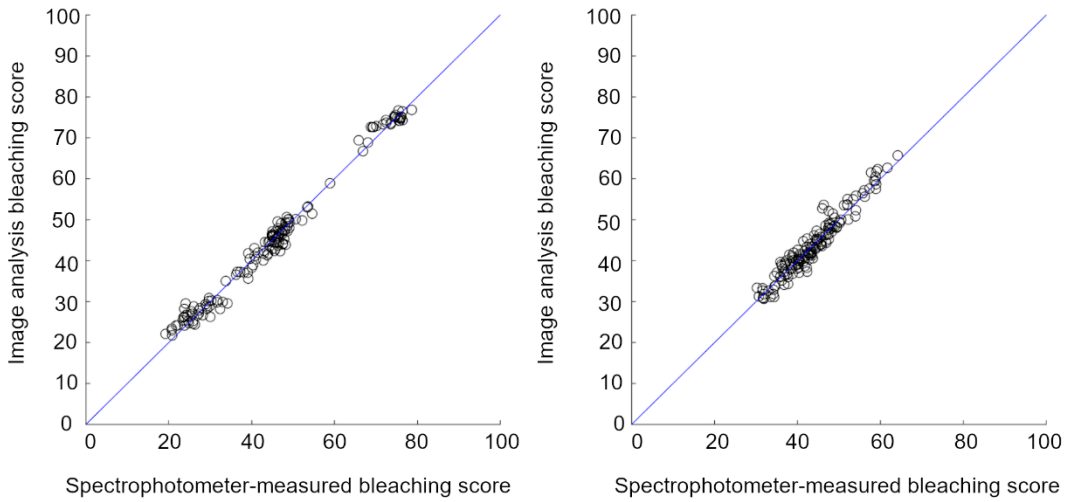

Figure 3.4. **Performance of image-based bleaching scores.** Bleaching scores assessed by image analysis highly correlated with bleaching scores measured by colour spectrophotometer for (a) the colour sorted samples, $R^2 = 0.99$, and (b) the time-course samples, $R^2 = 0.96$. Blue lines represent the one-to-one relation.

Table 3.4. Performance of bleaching score prediction models based on image analysis. Correlation coefficients, Lin's concordance test statistics and Root Mean Square Error (RMSE)values for image predictions of bleaching scores compared with spectrophotometer-derived bleaching scores.

Sample set	*Lin's Concordance statistic*	*Lin's Concordance 95% C.I.*	*RMSE*	*R^2*
Colour-sorted	0.99	(0.99, 1.00)	1.90	0.99
Time-course	0.96	(0.95, 0.97)	2.00	0.97

3.3.3 Determining time-course bleaching response

The time-course study was designed to assess bleaching scores at regular intervals throughout the storage period in order to quantify rates of bleaching and changes in bleaching uniformity within each genotype. Exposure of green pea to light is known to increase the rate of bleaching (Ubayasena et al., 2013) so storing samples under light would be expected to accelerate bleaching as compared to storing samples in the dark. Accordingly, genotypes with greater resistance to bleaching would be identified. The results of this experiment are outlined in Tables 3.5 and 3.6 for bleaching scores and bleaching uniformity assessments respectively.

Table 3.5. **Rate of bleaching.** Regression analysis on mean of single-seed bleaching scores

Genotype	*Storage*	*Mean bleaching score at T1*	*Rate of bleaching**	*Rate of bleaching 95% C.I.*	*p-value*
OZB1315	Dark	31.57± 0.67	0.63	(0.11, 1.15)	0.02
Excell	Dark	41.94 ± 0.47	0.32	(-0.10, 0.74)	0.13
OZB1310	Dark	38.84 ± 0.92	0.69	(0.12, 1.25)	0.02
OZB1308	Dark	37.75 ± 1.14	0.60	(0.12, 1.07)	0.02
OZB1324	Dark	45.52 ± 0.75	0.09	(-0.50, 0.68)	0.74
OZB1315	Light	32.24 ± 1.01	1.85	(1.17,2.54)	<0.001
Excell	Light	41.38 ± 0.54	5.49	(4.71, 6.256)	<0.001
OZB1310	Light	39.62 ± 0.84	3.46	(2.91, 4.00)	<0.001
OZB1308	Light	38.34 ± 0.81	2.82	(2.18, 3.48)	<0.001
OZB1324	Light	45.00 ± 0.83	3.65	(2.80, 4.50)	<0.001

***** Rate of bleaching was calculated as the average change in bleaching score over a 6-week period

Table 3.6. Uniformity of bleaching. Regression analysis on bleaching uniformity scores

Genotype	*Storage*	*Mean uniformity score at T1 ** *	*Uniformity gradient* (x10^{-3})*	*Uniformity gradient (x10^{-3}) 95% C.I.*	*p-value*
OZB1315	Dark	0.69 ± 0.01	-2.06	(-7.24, 3.12)	0.41
Excell	Dark	0.77±0.03	0.62	(-17.87, 9.10)	0.94
OZB1310	Dark	0.66 ± 0.01	0.86	(-4.06, 5.77)	0.71
OZB1308	Dark	0.71 ± 0.01	4.04	(-4.65, 12.73)	0.33
OZB1324	Dark	0.74 ± 0.01	-2.62	(-1.99, 4.60)	0.75
OZB1315	Light	0.67 ± 0.01	-42.79	(-53.31, -32.26)	<.001
Excell	Light	0.74 ± 0.02	-30.74	(-47.23, -14.25)	0.001
OZB1310	Light	0.66 ± 0.01	-47.04	(-54.16, -39.91)	<.001
OZB1308	Light	0.71 ± 0.01	-32.96	(-40.79, -25.12)	<.001
OZB1324	Light	0.76 ± 0.02	-35.54	(-49.70, -21.32)	<.001

***** Uniformity gradient was calculated as the average change in mean uniformity over a 6-week period

** Averaged across the three field-plot samples of the same genotype

The rate of bleaching for three of the genotypes (OZB1308, OZB1315 and OZB1310) indicated significant ($p<0.05$) bleaching of the seed over the storage period, i.e., the bleaching gradient was greater than zero (Table 3.5). However, since the magnitude of the gradients were small, this would likely be invisible to the human eye. By contrast, all samples stored under light showed a significantly high and visible shift toward bleaching over time. Therefore, each genotype exhibited some susceptibility to bleaching under these storage conditions. Excell had the steepest bleaching gradient and was the most heavily weighted toward the completely-bleached end of the scale at the completion of the storage period. Excell also had the least negative gradient for uniformity, suggesting that the colour, during bleaching, remained more uniform than for the other genotypes assessed. OZB1315 showed some resistance to bleaching overall (i.e. mean bleaching score did not shift far over the time-course study), however the uniformity of bleaching decreased at a greater rate than for all other genotypes, except OZB1310, demonstrating a tendency of OZB1315 to bleach unevenly. OZB1310 also bleached non-uniformly, maintaining a small proportion of dark green seed throughout the storage period. OZB1308 displayed the most colour stability. The rate of bleaching for OZB1308 was less than for OZB1324, OZB1310 and Excell and it generally maintained a far more uniform colour distribution than the other genotypes, making it the most bleaching-resistant of the five genotypes.

3.4 Conclusion

Currently, there is no standard objective measure of seed-bleaching and the grain industry often relies on visual classifications which are highly subjective. Bleaching of colour in green field pea impacts the perceived quality, therefore the ability to objectively measure the extent and uniformity of bleaching through image analysis provides a quantitative tool to investigate this phenomenon. This study presented objective methods for assessing bleaching based on visible reflectance spectra (spectrophotometer measurements) and digital image analysis. These methods were successfully applied to quantify the extent of bleaching in five green pea genotypes. The image analysis method was developed to score individual seeds which subsequently enabled the quantification of bleaching-uniformity throughout each sample. The methods presented in this study provide a mechanism to examine links between bleaching and other seed qualities (e.g. seed hardness and seed composition) and to study the impact of storage conditions and agronomic practices, such as timing of harvest, on bleaching responses. The application of a high-throughput, image-based method will allow for the quantification of genetic and environmental effects on colour and bleaching. This will lead to the development of germplasm with optimal market quality.

3.5 Acknowledgments

The authors gratefully acknowledge Dr. Jason Brand for providing the field pea samples used in this study and the technical input from Dr. Pankaj Maharjan and Slavica Laskovska.

3.6 References

ATAK, M., KAYA, M. D., KAYA, G., KAYA, M., KHALID, A. & KHAWAR, K. M. 2008. Dark green colored seeds increase the seed vigor and germination ability in dry green pea (Pisum Sativum L.). *Pakistan Journal of Botany,* 40**,** 2345-2354.

BRAND, J. 2015. Pulses in the Mallee 2015. *http://www.msfp.org.au/wp-content/uploads/Pulses-in-the-Mallee-2015-Jason-Brand-1.pdf,* Last accessed 10th October 2017.

CGC, C. G. C. 2018. Official Grain Grading Guide Winnipeg: Canadian Grain Commission.

CHENG, M., MCPHEE, K. E. & BAIK, B. K. 2004. Bleaching of Green Peas and Changes in Enzyme Activities of Seeds under Simulated Climatic Conditions. *Journal of Food Science,* 69**,** 511-518.

CHRISTIANSEN, A., CARSTENSEN, J., MØLLER, F. & NIELSEN, A. 2012. Monitoring the change in colour of meat: A comparison of traditional and kernel-based orthogonal transformations. *Journal of Spectral Imaging,* 3**,** a1.

DELL'AQUILA, A. 2006. Red-Green-Blue (RGB) colour density as a non-destructive marker in sorting deteriorated lentil (Lens culinaris Medik.) seeds. *Seed Science and Technology,* 34**,** 609-619.

FRENCH, R. J. 2016. Field Pea: Agronomy. *Reference Module in Food Science.* Elsevier.

GARRIDO-NOVELL, C., PÉREZ-MARIN, D., AMIGO, J. M., FERNÁNDEZ-NOVALES, J., GUERRERO, J. E. & GARRIDO-VARO, A. 2012. Grading and color evolution of apples using RGB and hyperspectral imaging vision cameras. *Journal of Food Engineering,* 113**,** 281-288.

GTA. 2018. *Australian Pulse Standards* [Online]. Grain Trade Australia. Available: http://www.graintrade.org.au/commodity_standards [Accessed].

GUBBELS, G. H. & ALI-KHAN, S. T. 1990. Screening green field pea genotypes for resistance to color loss. *Canadian Journal of Plant Science,* 70**,** 45-49.

JATOI, S., MUHAMMAD, A., SHAHZAD, N. & RASHID, A. 2001. Seed Deterioration Study in Pea, Using Accelerated Ageing Techniques. *Pakistan Journal of Biological Sciences,* 4**,** 1490-1494.

LEMASURIER, L. S., PANOZZO, J. F. & WALKER, C. K. 2014. A digital image analysis method for assessment of lentil size traits. *Journal of Food Engineering,* 128**,** 72-78.

LIU, C., LIU, W., LU, X., MA, F., CHEN, W., YANG, J. & ZHENG, L. 2014. Application of Multispectral Imaging to Determine Quality Attributes and Ripeness Stage in Strawberry Fruit. *PLOS ONE,* 9**,** e87818.

MANNINEN, H., PAAKKI, M., HOPIA, A. & FRANZÉN, R. 2015. Measuring the green color of vegetables from digital images using image analysis. *LWT - Food Science and Technology,* 63**,** 1184-1190.

MCCALLUM, J., TIMMERMAN-VAUGHAN, G., FREW, T. & RUSSELL, A. 1997. Biochemical and Genetic Linkage Analysis of Green Seed Color in Field Pea. *Journal of the American Society for Horticultural Science,* 122**,** 218-225.

MCDONALD, L. S., PANOZZO, J. F., SALISBURY, P. A. & FORD, R. 2016. Discriminant Analysis of Defective and Non-Defective Field Pea (*Pisum sativum*.) into Broad Market Grades Based on Digital Image Features. *PLoS ONE,* 11**,** e0155523.

MENDOZA, F., DEJMEK, P. & AGUILERA, J. M. 2006. Calibrated color measurements of agricultural foods using image analysis. *Postharvest Biology and Technology,* 41**,** 285-295.

NASAR-ABBAS, S. M., PLUMMER, J. A., SIDDIQUE, K. H. M., WHITE, P. F., HARRIS, D. & DODS, K. 2008. Nitrogen retards and oxygen accelerates colour darkening in faba bean (Vicia faba L.) during storage. *Postharvest Biology and Technology,* 47**,** 113-118.

NASAR-ABBAS, S. M., SIDDIQUE, K. H. M., PLUMMER, J. A., WHITE, P. F., HARRIS, D., DODS, K. & D'ANTUONO, M. 2009. Faba bean (Vicia faba L.) seeds darken rapidly and phenolic content falls when stored at higher temperature, moisture and light intensity. *LWT - Food Science and Technology,* 42**,** 1703-1711.

NSDU 2017. U.S. Pulse Quality Survey.

ORNELAS-PAZ, J. D. J., YAHIA, E. M. & GARDEA, A. A. 2008. Changes in external and internal color during postharvest ripening of 'Manila' and 'Ataulfo' mango fruit and relationship with

carotenoid content determined by liquid chromatography–APcI+-time-of-flight mass spectrometry. *Postharvest Biology and Technology,* 50**,** 145-152.

PHELPS, S. 2015. *Bleaching in Green Pea* [Online]. Available: https://saskpulse.com/files/general/151027_Bleaching_in_Green_Pea.pdf [Accessed].

STATISTICA. 2017. *Production volume of field peas worldwide from 2013 to 2017, by country* [Online]. Available: https://www.statista.com/statistics/722160/field-peas-production-volume-by-country-worldwide/ [Accessed 10th October 2018].

STEET, J. A. & TONG, C. H. 1996. Degradation Kinetics of Green Color and Chlorophylls in Peas by Colorimetry and HPLC. *Journal of Food Science,* 61**,** 924-928.

UBAYASENA, L., BETT, K., TAR'AN, B., VIJAYAN, P. & WARKENTIN, T. 2010. Genetic control and QTL analysis of cotyledon bleaching resistance in green field pea (Pisum sativum L.). *Genome,* 53**,** 346-359.

UBAYASENA, L., VIJAYAN, P., BETT, K. E., GRAY, G. R., KÜSTER, H. & WARKENTIN, T. D. 2013. Gene expression profiles of seed coats and biochemical properties of seed coats and cotyledons of two field pea (Pisum sativum) cultivars contrasting in green cotyledon bleaching resistance. *Euphytica,* 193**,** 49-65.

WIWART, M., FORDOŃSKI, G., ŻUK-GOŁASZEWSKA, K. & SUCHOWILSKA, E. 2009. Early diagnostics of macronutrient deficiencies in three legume species by color image analysis. *Computers and Electronics in Agriculture,* 65**,** 125-132.

WU, D. & SUN, D.-W. 2013a. Colour measurements by computer vision for food quality control – A review. *Trends in Food Science & Technology,* 29**,** 5-20.

WU, D. & SUN, D. W. 2013b. 6 - Food colour measurement using computer vision. *Instrumental Assessment of Food Sensory Quality.* Woodhead Publishing.

YAN, X., WANG, J., LIU, S. & ZHANG, C. Purity Identification of Maize Seed Based on Color Characteristics. 2010 Berlin, Heidelberg. Springer Berlin Heidelberg, 620-628.

CHAPTER 4

Concentrations of phenolic acids and chlorophylls are depleted in green pea (*Pisum Sativum L.*) during bleaching but are not directly related to known bleaching-resistance of a genotype

This chapter has been published as:

MCDONALD, L., MAHARJAN, P., PORTMAN, D. & PANOZZO, J. 2020. Bleaching color-loss of green field pea: An investigation on inference of genotypic-resistance based on chlorophyll and phenolic acid content. Legume Science. 2020;e63. https://doi.org/10.1002/leg3.63.

Abstract

Discoloration in green field pea due to bleaching is thought to be the result of chlorophyll depletion in the cotyledon, however the mechanisms of bleaching-resistance, exhibited within some genotypes, are not well understood. The antioxidant activity of phenolic compounds can inhibit chlorophyll degradation and therefore the presence of phenolic compounds may improve bleaching-resistance in the grain.

In this study five green pea genotypes, differing in resistance to bleaching, were assessed for grain-color as well as concentrations of chlorophyll and major phenolic acids, in both the hull and cotyledon. For each genotype, resistance to bleaching was inferred by the range of color scores observed. Chlorophyll and phenolic acid content both decreased overall as the whole-grain color became lighter (bleached) however there was no direct relation found between these compounds and the known resistance of each genotype. Chlorophyll content in the cotyledon was correlated (r=-0.73) with cotyledon color but not with whole-grain color (r=-0.21). Furthermore, the ratio of cotyledon chlorophyll A/B and the ratio of phenolic acid content (hulls) to total chlorophyll content (cotyledon) were not directly correlated with resistance.

Although the total chlorophyll and phenolic acid content were both depleted as the extent of bleaching increased, neither could fully explain differences in bleaching-resistance between genotypes. Furthermore, the green color of whole-grain samples, and the degradation of color, could not be fully attributed to the concentration of chlorophyll pigments. Therefore, it is likely

that other phenolic compounds contribute to both the grain color and the resistance to bleaching.

4.1 Introduction

Dry field pea (*Pisum sativum L.*) is an important agricultural commodity, cultivated globally both for human and stock consumption. It is a good source of plant-based protein, carbohydrates, minerals and phenolic compounds (Khan and Croser, 2004, Dahl et al., 2012, Singh and Pratap, 2016, Singh et al., 2017). Green pea is one of the most significant broad classes of dry field pea and is largely marketed based on visual appeal (McDonald et al., 2016, Khan and Croser, 2004, Ubayasena et al., 2013). Generally, green field pea have green cotyledons and opaque hulls (McDonald et al., 2016), although some genotypes have green hulls. Color uniformity is an important marketable trait for green pea and is regulated independently between countries (McCallum et al., 1997, Khan and Croser, 2004, Williams and Singh, 1988, Cheng et al., 2004, McDonald et al., 2019). Globally Canada is the largest producer of green pea and the Canadian Grain Commission specify a maximum allowance of 1%, 2% and 3% of pea grains of "other color" to qualify for the market grades of "No. 1 Canada", "No. 2 Canada" and "No. 3 Canada" respectively (Khan and Croser, 2004, Canadian Grain Commission, 2018). Similarly, Australian Pulse Standards allow a maximum of 1% (by weight) off-color hull or kernel to qualify for the market class of "No. 1 grade" (Grain Trade Australia, 2018). Higher graded field peas are marketed for human consumption and attract premium prices compared with the lower grades, which are used as livestock feed.

Chlorophyll is the main pigment contributing to the color of green field pea and it is reported to be depleted during cooking and processing of the grains (Steet and Tong, 1996, Cheng et al., 2004). However, within many green-pea genotypes there is also a susceptibility toward degradation of chlorophyll content in unprocessed grains resulting in the loss of green color. This discoloration is known as bleaching and can occur pre-harvest due to adverse environmental conditions or post-harvest due to storage conditions (Gubbels and Ali-Khan, 1990). It is generally understood to be a cosmetic defect affecting marketability rather than functionality (Phelps, 2015), however bleaching has been linked to loss of seed vigor and increased seed coat (hull) permeability for sugars, amino acids and organic acids (Maguire et al., 1973, Browning and George, 1981). Chlorophyll degradation during bleaching has been attributed mainly to chlorophyllase activity, however the activity of this enzyme was not found

to be significantly different between bleaching-resistant and bleaching-susceptible green-pea genotypes (Cheng et al., 2004).

Phenolic compounds within the hulls of pulse grains are also closely linked to the expressed color (Williams and Singh, 1988). These compounds are understood to form a protective layer over the cotyledon due to their antioxidant and antimicrobial properties which can act to inhibit oxidative enzyme activity, effectively slowing the degradation of chlorophylls (Dueñas et al., 2004, Zhang et al., 2015, Amarowicz et al., 2010, Yamauchi et al., 2004). Dry field pea classes with darker colored hulls, such as dun-type peas, generally have much higher concentrations of phenolic compounds compared with the opaque hulls which are characteristic of most green pea genotypes (Maharjan et al., 2019, Williams and Singh, 1988, Magalhães et al., 2017).

Despite the comparatively low concentration of phenolic compounds in the hulls of green pea compared with other field pea types, some green pea genotypes exhibit a level of resistance to bleaching. It has been suggested that the ratio of phenolic compounds to chlorophyll content may be related to genotypic resistance since significant differences in this ratio were observed between a resistant and susceptible genotype (Ubayasena et al., 2013).

Understanding the relation between genotypic resistance to bleaching and grain composition would be a valuable tool within field pea breeding programs in developing new cultivars with improved color stability and market acceptance. Therefore, the aim of the present study was to observe changes in chlorophyll and phenolic acid content of green peas during post-harvest bleaching and determine whether a relationship exists between the presence of these compounds and the known resistance to bleaching of these genotypes. Five genotypes were included in the study and the resistance of each to bleaching was assessed by the range of whole-grain colors observed. Color scores, chlorophyll content and phenolic acid content were analyzed separately for hull and cotyledon to account for the role of each component.

4.2 Materials and Methods

4.2.1 Samples

Green pea samples were sourced from a field trial grown at Rupanyup in western Victoria, Australia, and stored in dark conditions immediately after harvest. There were 15 green pea samples, consisting of five genotypes (Aragorn, Excell, OZB1308, OZB1309 and OZB1316) replicated three times within the field trial. From previous studies Excell was known to be

susceptible to bleaching and OZB1308 was known to exhibit some resistance (Brand, 2016, McDonald et al., 2019). In the following sections, the methods for producing bleached grains, assessing color and quantifying composition constituents (chlorophyll and phenolic acids) are outlined.

4.2.2 Bleaching green peas

The pea samples were first sieved to obtain uniform grain size and to remove any dust or contaminants. There was no visible sign of mold or microbial activity. Samples were then sorted into visibly uniform grain color within each genotype-replicate to obtain a homogeneous sample of 150 to 200 grains. Each color-sorted sample was divided evenly between two petri dishes and stored according to the method outlined in McDonald et al. (2019); one petri dish was wrapped in aluminum foil to block out light (and avoid bleaching) and the other petri dish was left unwrapped (to stimulate bleaching). All petri dish samples were stored at room temperature (22^{o}C and 40% RH) and exposed to light intensity of 9000 lux.

Bleaching occurred over a storage period of 24 weeks and subsampling (15 grains) was undertaken at 6-week intervals from the beginning of the storage period to capture grain exhibiting various degrees of bleaching. The sampled grain was placed in an airtight bag then wrapped in foil and stored at -18^{o}C until the completion of the 24 weeks.

4.2.3 Image Capture

Following the 24-week storage period all subsampled grain was imaged on a matte-white background using a Nikon D7200 camera fixed to a copy stand (macro lens, f8 aperture, 1/200s shutter speed and Low 1.0 ISO) and the images were stored in Nikon raw format (NEF). A flat-field reference image (REF_{flat}) was captured of the white background with no sample and a dark reference image (REF_{dark}) was captured with the lens cap on. Following the capture of whole-grain images (Fig 4.1a), each sample was dehulled and imaged again under the same conditions with the hull and cotyledon separated (Fig 4.1b).

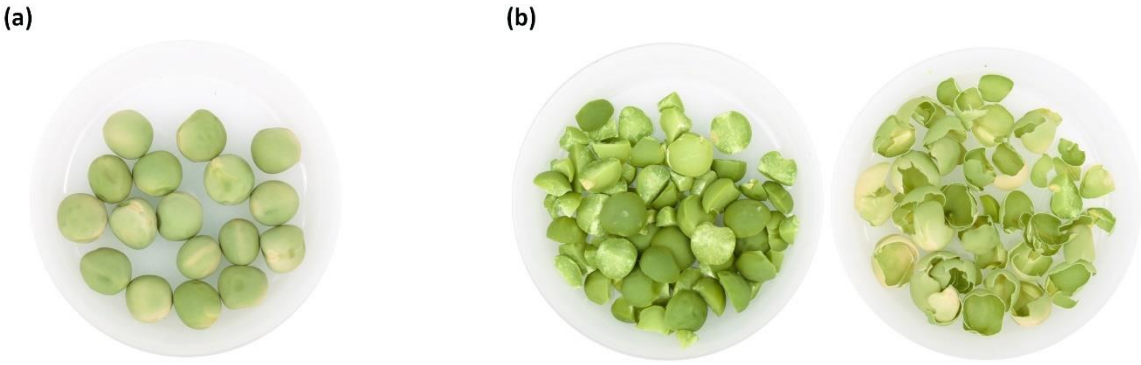

Figure 4.1. Illustration of the grain-sample presentation for images captured of **(a)** whole grain and **(b)** dehulled grain separated into cotyledon (left) and hull (right).

4.2.4 Image processing and color analysis

Images were processed and analyzed within the Matlab R2019a programming environment with the image processing toolbox (The MathWorks). A Gaussian smoothing kernel (σ=3) was applied to all reference and sample images prior to further processing. Pixel intensities of each sample image (I_n) were compared to those of the flat field image through the following pixel-wise calculation: $I_{ratio} = (I_n - REF_{dark})/ (REF_{flat} - REF_{dark})$. Pixel color-intensity values for each channel (red, green and blue) in a sample image were first translated by the REF_{dark} values ($I_n - REF_{dark}$) then divided by a correction factor. Each correction factor was determined by the location of the maximum peak in the pixel-intensity histogram of the relevant color channel in I_{ratio} (to match intensities in the common background pixels).

Color-standardized images were segmented to isolate the grains. Images were then transformed into the XYZ color space through the inbuilt Matlab function rgb2xyz. Mean pixel values were collected from each color channel in the grain regions of the XYZ images. These mean pixel values were used as the independent variables in a linear regression model with interactions to determine a bleaching color score for each sample. The color scores (dependent variable) were based on the scale presented by McDonald et al. (2019). Development of the regression model was based on spectrophotometric color assessment (Konica Minolta CM5) and image analysis of an independent dataset of whole grain samples (n=1800).

4.2.5 Analysis of chlorophyll content

The method for chlorophyll determination was adapted from Mazza and Oomah (1994) and US EPA SOP # 2030 (Environment Response Team, 1994). Briefly, ground samples were weighed (500 mg for cotyledon and 100 mg for hull) into a 24-well titer plate (SPEX® SamplePrep,

Metuchen, NJ, USA). Stainless steel grinding balls (4mm) and 4 mL of 80% acetone with 0.005% ammonium hydroxide were added to the sample. The plates were subsequently sealed with rubber-sealing cap-mats and locked into a 2010 Geno/Grinder® (SPEX® SamplePrep, USA). Chlorophylls were extracted into the solvent by homogenisation for 3 min at 1000 strokes/min. The homogenate was centrifuged at 4000 rpm for 5 min. The supernatant was transferred into a labelled tube and the remnant chlorophyll was extracted again with a fresh 4 ml of extraction buffer. The absorbance of pooled supernatant from the two extractions measured at 626 nm, 645 nm, 663 nm and 700 nm were recorded in quartz cuvettes (1 cm path length) using UV-1800 spectrophotometer (Shimadzu Corporation, Kyoto, Japan). The chlorophyll concentrations in the supernatant were calculated using the following equations and converted to mg/100g for reporting results:

Chlorophyll A (nMoles/mL) = ($14.18 \times Abs_{663} \times 2.91 \times Abs_{645}$) – $0.22 \times Abs_{626}$

Chlorophyll B (nMoles/mL) = $26.01 \times Abs_{645} - 4.66 \times Abs_{663} - 0.36 \times Abs_{626}$

Where:

Abs_{626} = absorbance at 626 nm – absorbance at 700 nm

Abs_{645} = absorbance at 645 nm – absorbance at 700 nm

Abs_{663} = absorbance at 663 nm – absorbance at 700 nm

4.2.6 Analysis of phenolic profiles

The method for determining phenolic acid profiles was adapted from Mirali et al. (2016). The cotyledon and hull samples were ground to a fine powder using a Laboratory Mill 3303 (Perten Instruments, Hägersten, Sweden) and weighed into 2 mL Eppendorf tubes (100 mg for hulls and 250 mg for cotyledons). Acetone (1 mL of 70%) was added to the samples and then vortexed followed by sonication for 5 min. The extraction step was continued on the Thermo-Shaker PCMT (Grant Instruments Ltd, Shepreth, Cambridgeshire, UK) at 1200 rpm at 25°C for 60 min. The extract was centrifuged at 12000 rcf for 5 mins. The supernatant was collected in a new tube and the extraction process repeated. The pooled supernatant was vortexed and an aliquot (1mL) of the supernatant was dried at 40◦C under a nitrogen blanket. The residue was re-dissolved in 1 mL of 10% Methanol and filtered through a 0.22 µm syringe filter. The polyphenol contents in the extract were determined using Waters UPLC system (Waters Corporation, Milford, MA, USA), as described by Maharjan et al. (2019), and then identified using the UV spectrum and the molecular mass. Briefly, the UPLC system comprised UPLC Binary Solvent Manager (BSM) (H10UPB941A), UPLC Sample Manager (G10UPA77M) and UPLC Photodiode Array Detector (PDA) (D10UPD 707A) and ACQUITY QDa Mass Detector. The column used for polyphenol

analysis was an ACQUITY BEH C18 column (2.1 × 50 mm, 1.8 µm) (Waters Corporation, USA). Column temperature was 45°C, sample temperature was 25°C and the A1 and B1 mobile phases were Acetonitrile with 0.1% acetic acid and reverse osmosis MilliQ water with 0.1% acetic acid respectively. Empower 3 Software (Waters Corporation, USA) was used for collection and analysis of chromatographic data. Phenolic compound concentrations are reported in mg/kg.

4.2.7 Moisture Analysis

The moisture content of each hull and cotyledon sample was determined by the Karl Fischer method using the automated Metrohm Karl Fischer system (Metrohm AG, Herisau, Switzerland). Ground samples (50mg) were placed in sealed vials and incubated within the Metrohm oven at 180°C with and air flow of 40 mL/min. The resulting gas was collected within the reaction vessel containing Hydranal Methanol Rapid (Honeywell Fluka, North Carolina, USA) and titrated using Hydranal Composite 5 (Honeywell Fluka). The composition of chlorophyll and phenolic acids were reported on a dry matter basis (DB).

4.3 Results and discussion

4.3.1 Grain color

Color scores for whole grain, cotyledon and hull samples were derived through image processing and multiple linear regression (MLR). Low scores corresponded to dark green samples and higher scores to lighter green. Table 4.1 summarizes the sample color scores measured across the five genotypes. Since the model for assessing color was developed on whole grain samples, some negative values were computed for cotyledon color (Fig 4.2b), as the cotyledons were significantly darker than the whole grains. In the context of this study, only whole grain color scores were used for quantifying the extent of, and resistance to bleaching, but the cotyledon color values were still considered appropriate for observing trends and differences. The distribution of whole-grain, cotyledon and hull color scores observed within each genotype is depicted in Fig 4.2.

Table 4.1. Descriptive statistics of color scores for whole grain, cotyledon and hull.

	Genotype	*N*	*Color score mean*	*95% CI Mean*	*Variance*	*Range* (max - min)*
Whole Grain	Aragorn	*30*	44.6	(43.4, 45.9)	10.7	14.4
	Excell	*30*	46.1	(44.9, 47.4)	13.0	15.1
	OZB1308	*30*	41.6	(40.3, 42.8)	7.7	9.9
	OZB1309	*28*	25.0	(23.7, 26.3)	23.2	18.7
	OZB1316	*30*	44.2	(43.0, 45.5)	5.9	10.4
Cotyledon	Aragorn	*30*	3.0	(1.8, 4.2)	9.0	12.0
	Excell	*30*	9.7	(8.5, 10.9)	22.8	17.9
	OZB1308	*30*	8.5	(7.4, 9.7)	7.2	10.1
	OZB1309	*30*	8.5	(7.3, 9.7)	7.7	9.3
	OZB1316	*30*	5.5	(4.4, 6.7)	7.0	10.9
Hull	Aragorn	*30*	65.4	(63.5, 67.3)	12.8	14.0
	Excell	*30*	64.7	(62.8, 66.6)	23.3	19.4
	OZB1308	*30*	56.8	(54.9, 58.7)	32.7	18.3
	OZB1309	*30*	20.5	(18.6, 22.4)	54.8	24.0
	OZB1316	*30*	60.2	(58.3, 62.1)	14.0	14.1

* The whole-grain color score range for each genotype was used as the relative measure of bleaching-resistance. Smaller range values indicated greater bleaching-resistance

Color scores varied between genotypes independent of any bleaching, as some genotypes are naturally darker than others. However, greater variability in color scores within a genotype indicated a greater extent of bleaching and therefore, the range of color scores (measured on whole grain samples) within each genotype was taken as a relative score for susceptibility to bleaching. In order of increasing susceptibility (i.e. decreasing resistance), the genotypes in this study were ranked as follows: OZB1308, OZB1316, Aragorn, Excell and OZB1309 (Table 4.1). These results support previous reports wherein Excell and OZB1308 were observed to be relatively susceptible and resistant respectively (Brand, 2016, McDonald et al., 2019).

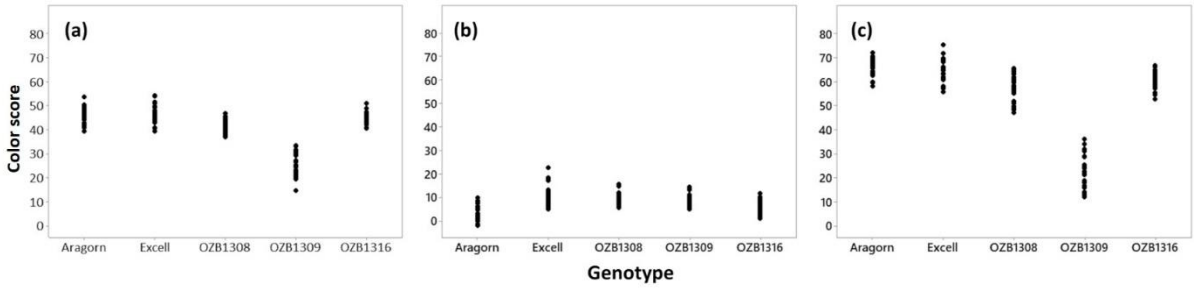

Figure 4.2. Individual value plots. Depiction of the range and distribution of color scores within each genotype for (a) Whole grain, (b) Cotyledon and (c) Hull samples.

Resistance to bleaching was not strongly related to the mean color of the whole-grain, hull or cotyledon samples (Table 4.1). The least resistant genotype (i.e. the genotype with the greatest range of whole grain color scores) had the darkest mean whole-grain color and was also significantly darker than all other genotypes in the mean hull-color (Fig 4.3). However, there was no relation overall between the grain color and resistance to bleaching. For cotyledon-color scores, the least resistant (OZB1309) was statistically indifferent from the most resistant genotype (OZB1308) but significantly lighter than Aragorn, which ranked third in resistance (Table 4.1, Fig 4.3).

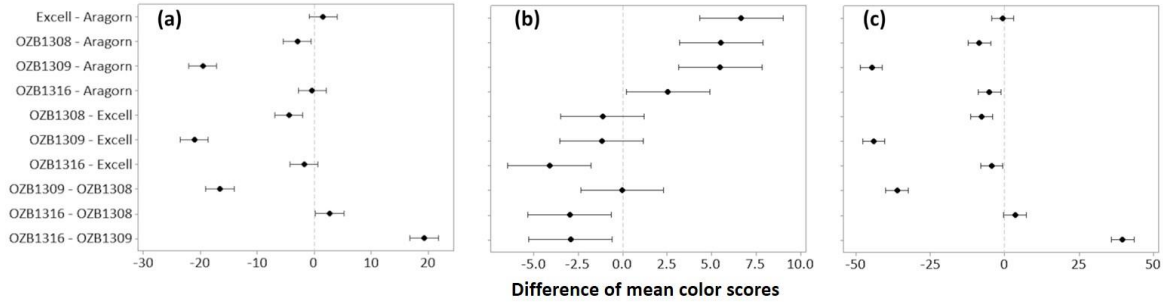

Figure 4.3. Tukey simultaneous 95% confidence intervals. Differences in mean color scores between genotypes for (a) whole grain, (b) cotyledon and (c) hull.

Although grain was sampled at regular intervals the rate of bleaching over the storage period was not calculated. This is because bleaching does not occur uniformly within green pea genotypes (McDonald et al., 2019), and therefore the subsamples would be too small to make an assumption of uniformity for that purpose. Measured concentrations of phenolic acids and chlorophyll were related to grain color (i.e. extent of bleaching) rather than to the time spent in storage.

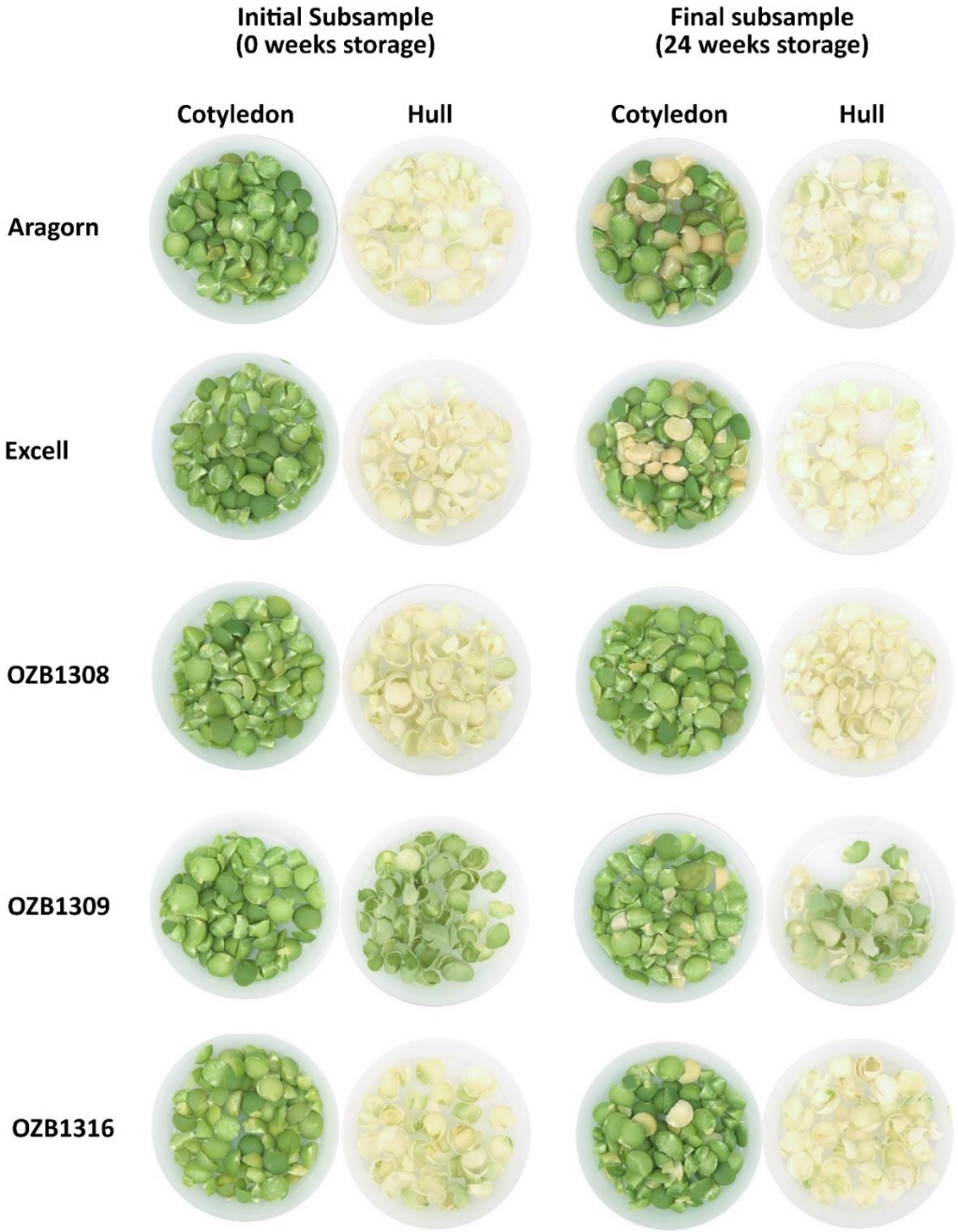

Figure 4.4. Bleaching color extremities observed within each genotype**.** Images of cotyledon and hull for each of the five green pea genotypes from an initial subsample prior to storage (left) and a final subsample after 24-weeks of storage under light conditions (right).

4.3.2 Chlorophyll content

Typically, the whole-grain color of green field pea is attributed to the chlorophyll content in the cotyledon since concentrations of chlorophyll in the hull are very low and often below the levels of detection (Table 4.2). Only one of the five genotypes, OZB1309, had colored hulls (Fig 4.4)

and contained detectable concentrations of chlorophyll in the hull (Table 4.2). The chlorophyll content within the hull of OZB1309 was predominantly composed of chlorophyll B and was much lower in concentration than in the cotyledon.

Total chlorophyll concentration measured in the cotyledon samples ranged from 3.1 to 23.8 mg/100g and was predominantly composed of chlorophyll A (Table 4.2).The concentration of total chlorophyll (cotyledon) was significantly higher ($p<0.05$) for Aragorn than any other genotype and the lowest chlorophyll concentrations were observed in Excell and OZB1308.

In agreement with the results of Cheng et al. (2004), total chlorophyll concentration (cotyledon) was correlated ($r=-0.73$, $p<0.001$) with the cotyledon color (Fig 4.5a). However, the chlorophyll concentration was not highly correlated ($r=-0.21$, $p=0.01$) with the whole-grain color (Fig 4.5b) and therefore, could not account fully for the differences in green color between genotypes or for bleaching within a genotype. Cheng et al. (2004) reported significant differences between a susceptible and resistant green pea cultivar in both the chlorophyll content and chlorophyll A/B ratio. While the results of the present study do show that there are significant differences in both chlorophyll content and the chlorophyll A/B ratio between genotypes, there was no correlation of these values to resistance of the genotype (Table 4.3, Fig 4.6c and d). The chlorophyll A/B ratio for Excell, which is susceptible to bleaching, was not significantly different from that of the most resistant genotype (Fig 4.5c).

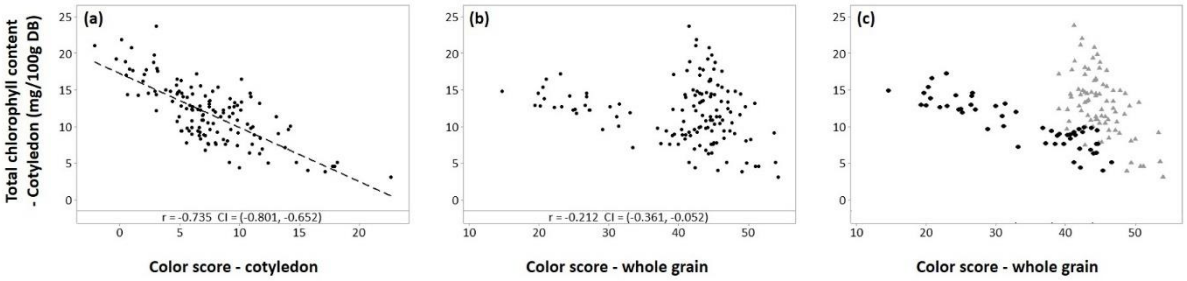

Figure 4.5. Relationship between cotyledon chlorophyll content and (a) cotyledon color score, (b) whole grain color score and (c) whole grain color score grouped by genotypes with higher mean phenolic acid content, i.e. >100 mg/kg, (black dots) and with lower mean hull phenolic content, i.e. <100 mg/kg, (grey triangles).

Table 4.2. Descriptive statistics for the concentration (mg/100g DB) of chlorophyll in green pea cotyledon and hull samples.

	Genotype	N	*Chlorophyll A mean ± SE*	*Chlorophyll B mean ± SE*	*Total Chlorophyll mean ± SE*	*Total Chlorophyll Range (Max – Min)*	Ratio A/B *mean ± SE*
Cotyledon	Aragorn	*29*	11.1 ± 0.5	5.5 ± 0.1	16.6 ± 0.7	15.5	2.0 ± 0.1 [d]
	Excell	*30*	5.3 ± 0.4	3.7 ± 0.2	9.0 ± 0.5	11.4	1.4 ± 0.1 [e]
	OZB1308	*30*	4.7 ± 0.2	3.3 ± 0.1	7.9 ± 0.3	5.9	1.4 ± 0.0 [e]
	OZB1309	*30*	8.5 ± 0.3	4.6 ± 0.1	13.1 ± 0.4	10.0	1.9 ± 0.0 [d]
	OZB1316	*30*	9.0 ± 0.3	4.5 ± 0.1	13.5 ± 0.4	8.5	2.0 ± 0.1 [d]
Hull	Aragorn	*29*	n.d.	n.d.	n.d.	n.d.	--
	Excell	*30*	n.d.	n.d.	n.d.	n.d.	--
	OZB1308	*30*	n.d.	n.d.	n.d.	n.d.	--
	OZB1309	*30*	n.d.	1.0 ± 0.1	1.0 ± 0.1	1.3	--
	OZB1316	*28*	n.d.	n.d.	n.d.	n.d.	--

Significant differences of means calculated by using the Tukey method and 95% confidence. Groups are labelled in descending order of mean value.

n.d. = not detected

Table 4.3. Concentration (mg/kg DB) of the main phenolic acids detected in the green pea cotyledon and hull samples.

	Genotype	*N*	*o-coumaroyl malic acid mean ± SE*	*p-coumaroyl malic acid mean ± SE*	*feruloyl malic acid † mean ± SE*	*Sum of main phenolic acids mean ± SE*
Cotyledon	Aragorn	*29*	0.6 ± 0.1	3.4 ± 0.3	2.7 ± 0.2	6.7 ± 0.5^{c}
	Excell	*30*	2.7 ± 0.4	3.7 ± 0.4	2.5 ± 0.4	8.9 ± 1.1^{b,c}
	OZB1308	*30*	7.9 ± 0.5	10.4 ± 0.5	6.5 ± 0.5	24.8 ± 1.6^{a}
	OZB1309	*30*	2.5 ± 0.3	6.2 ± 0.6	2.3 ± 0.2	11 ± 1.1^{b}
	OZB1316	*30*	0.7 ± 0.1	0.5 ± 0.1	0.3 ± 0.1	1.4 ± 0.2^{d}
Hull	Aragorn	*29*	4.5 ± 0.9	15.4 ± 2.9	19 ± 3.1	38.9 ± 6.4^{g}
	Excell	*30*	9.2 ± 1.9	15.1 ± 2.3	8.6 ± 1.6	33 ± 5.4^{g,h}
	OZB1308	*30*	49 ± 2.9	67.6 ± 3.9	44.1 ± 3	160.8 ± 8.6^{f}
	OZB1309	*30*	69.6 ± 2.7	101.9 ± 5.3	64.3 ± 5.3	235.8 ± 12.4^{e}
	OZB1316	*28*	2.8 ± 0.9	1.7 ± 0.5	1.9 ± 0.2	6.4 ± 1.5^{i}

Significant differences of means calculated using the Tukey method and 95% confidence. Groups are labelled in order of descending mean value.

† Feruloyl malic acid is reported as the sum of the cis and trans isomers

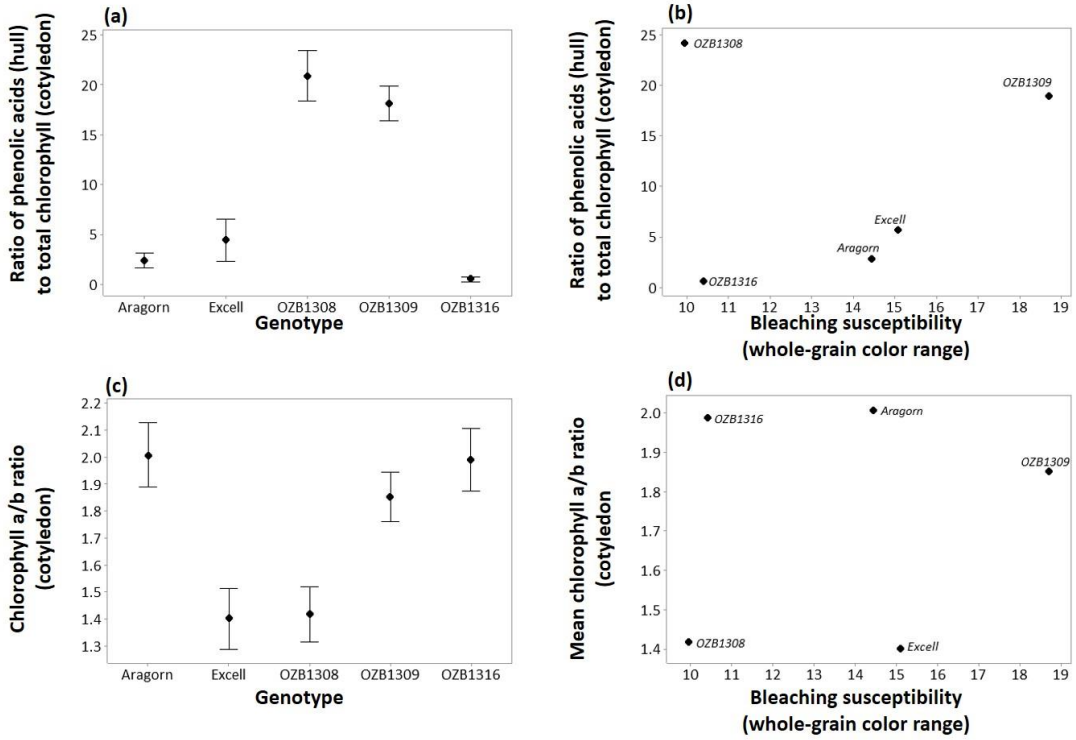

Figure 4.6. Genotypic differences in the ratio of phenolic content in pea hulls to the chlorophyll content of pea cotyledon; (a) Interval plot of phenolic acid to chlorophyll ratio values grouped by genotype, (b) Relation between phenolic acid to chlorophyll ratio values and the genotypic bleaching susceptibility, (c) Interval plot of cotyledon chlorophyll A/B ratio grouped by genotype, (d) Relation between cotyledon chlorophyll A/B ratio and the genotypic bleaching susceptibility.

4.3.3 Phenolic acid content

The three phenolic acid compounds detected in the highest concentrations were o-coumaroyl malic acid, p-coumaroyl malic acid and feruloyl malic acid, where feruloyl malic acid is reported as the sum of its cis and trans isomers (Table 4.3). The sum of three main phenolic acids was assumed to be representative of the total phenolic acid content since they accounted for a large proportion of phenolic acids present (Fig 4.7). These compounds were also observed within a previous study as the phenolic acids occurring in the greatest concentrations in white pea, which have similar opaque hulls to green pea (Maharjan et al., 2019).

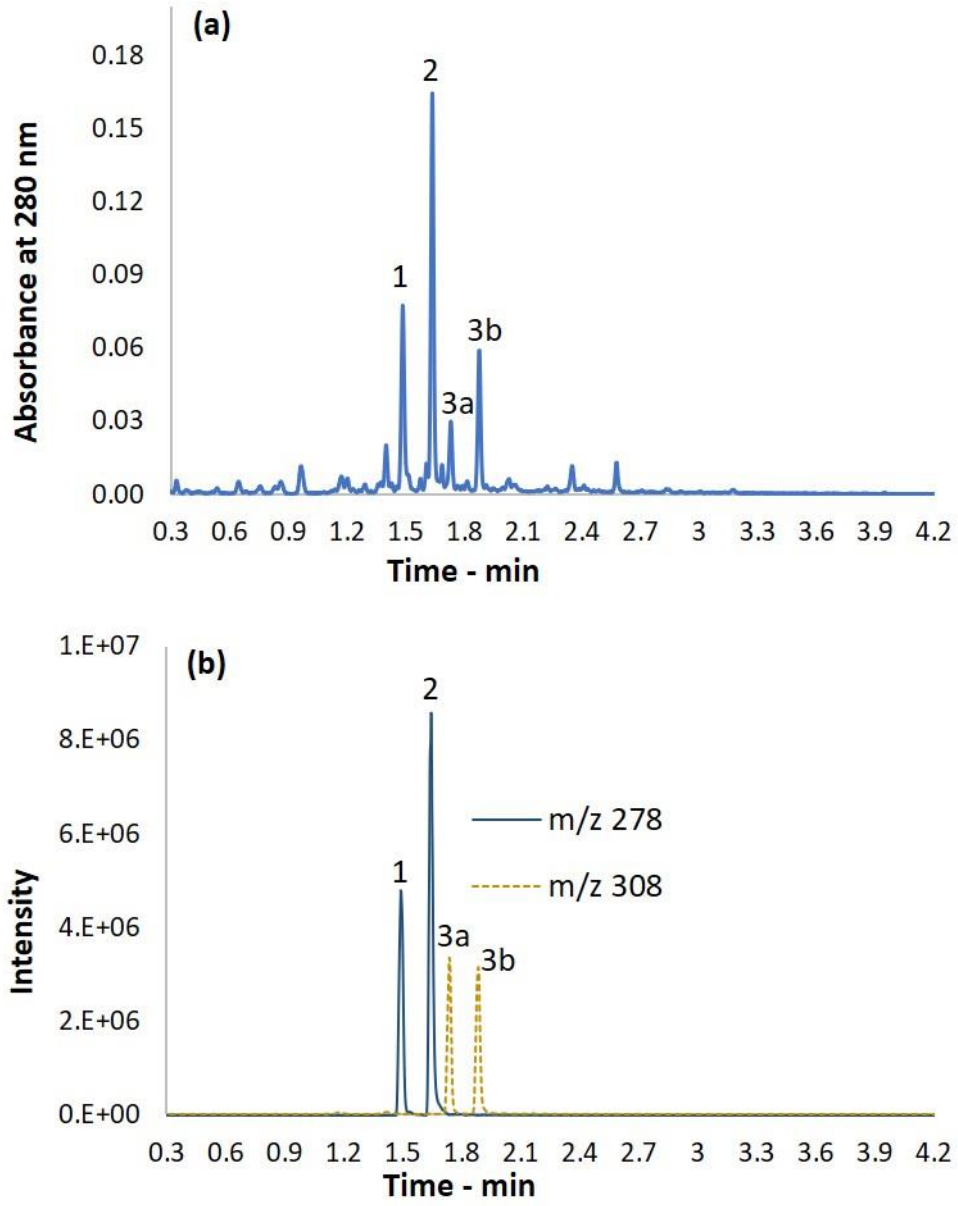

Figure 4.7. Chromatogram of phenolic extracts from hulls of OZB1309 (storage time = 0 weeks). (a) PDA chromatogram at 280 nm (b) QDa chromatogram at m/z of 278 and 308. Peak identity: 1 = o-coumaroyl malic acid; 2 = p-coumaroyl malic acid; 3a and 3b = cis trans and isomers of feruloyl malic acid.

Phenolic acids in the field pea hulls were typically in higher concentrations than those observed in the cotyledons. The p-coumaroyl malic acid content varied widely between genotypes but was the most prevalent phenolic compound overall, measured at concentrations between 0.1 and 17.4 mg/kg for cotyledon and 0.0 to 144.4 mg/kg for hull. The concentrations of phenolic acids observed in the hulls of all green pea genotypes was comparable to other studies, although there is a large variation in the concentration of phenolic compounds in field peas

reported within the literature, due largely to differences between market classes (e.g. dun pea compared with white pea) (Marles et al., 2013, Magalhães et al., 2017, Padhi et al., 2017, Singh et al., 2017, Parikh and Patel, 2018, Maharjan et al., 2019, Dueñas et al., 2004).

The concentration of phenolic acids in the hulls was significantly higher ($p<0.05$) for OZB1308 and OZB1309 (Fig 4.8b), however in the same two genotypes, there was also the greatest depletion of phenolic acids within the hull as the whole grain color score increased, i.e. the phenolic content of the hull decreased as the grain bleached (Fig 4.8d). Phenolic acid content in the cotyledon showed no significant correlation, within each genotype, to the whole grain color (Fig 4.8c) and was significantly higher ($p<0.05$) for OZB1308 than all other genotypes in both mean value and range (Table 4.3, Fig 4.8a). OZB1316 contained the lowest concentration of phenolic acid content in both hull and cotyledon. The total mean phenolic acid concentrations in OZB1316 were only of the order of 2.7 to 21.4% of the concentrations observed in the other genotypes.

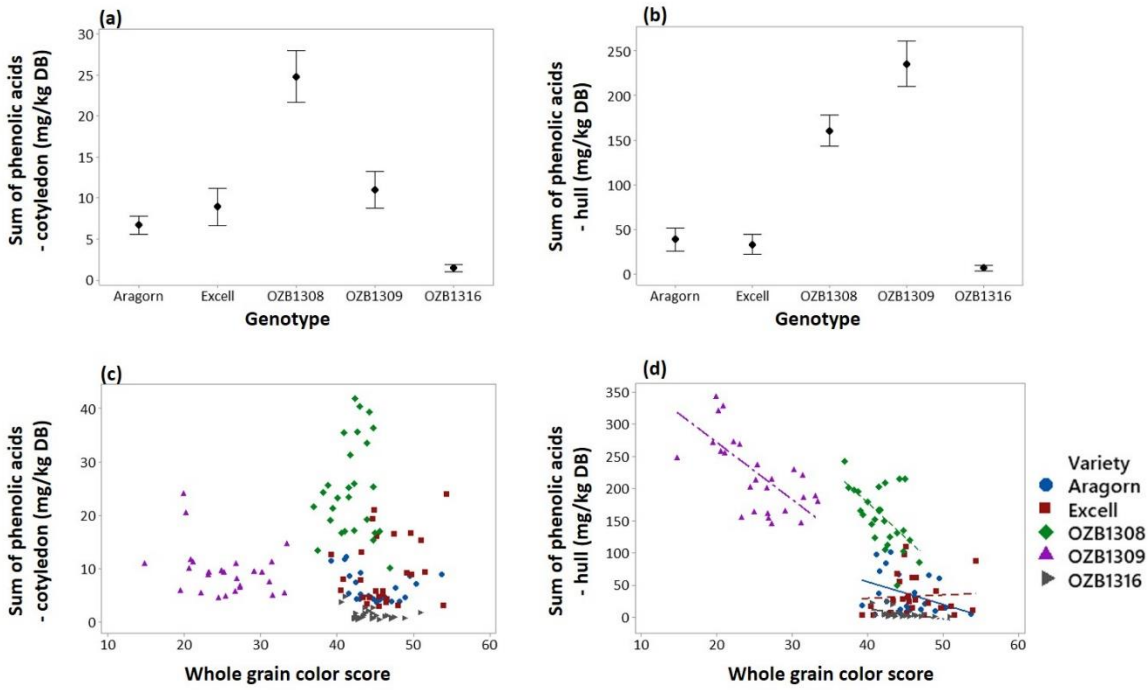

Figure 4.8. Genotypic differences in phenolic acid content. Interval plots, grouped by genotype, for phenolic acid content of (a) cotyledon and (b) hull samples. Changes in phenolic acid concentration in (c) cotyledon and (d) hull for each genotype as whole grain color scores (i.e. bleaching scores) increased.

Ubayasena et al. (2013) reported ratio of phenolic compounds in the hull to chlorophyll content in the cotyledon may be related to bleaching-resistance within green field pea genotypes since the antioxidant activity of carotenoids and phenolic compounds in the hull may result in retarding the depletion of chlorophyll in the cotyledon. In the present study there were significant differences between genotypes in the phenolic acid/chlorophyll ratio (Fig 4.6a) however, there was no clear trend observed between the phenolic acid/chlorophyll ratio and bleaching-resistance of each genotype (Fig 4.6b). However, the genotypes which had a higher total concentration of phenolic compounds in the hull (>100 mg/kg) tended to also have a slower degradation of chlorophyll content in the cotyledon as bleaching color scores increased (Fig 4.5c). Nevertheless, the color of the whole grains still bleached even with the reduced degradation of chlorophyll, which supports the earlier finding that color changes in the whole-grain may also be attributed to more than chlorophyll degradation in the cotyledon. Although OZB1309 had the greatest phenolic acid content (hulls), it was also the least resistant to bleaching and while bleaching in this genotype is due partially to the depletion of chlorophyll in the cotyledon and hull, but it is likely that other compounds in the hull also contribute to the grain color and degradation thereof.

4.4 Conclusions

Green field pea genotypes can vary widely in color, composition and resistant to bleaching. This study has shown that, within genotypes, there is an association between the extent of bleaching (whole-grain color) and the concentration of phenolic acids and chlorophylls in the hull and cotyledon. The concentrations of total chlorophyll and phenolic acids decreased as bleaching increased. However, degradation of total chlorophyll in the cotyledon did not account fully for the observed changes in whole-grain color.

The concentrations of chlorophylls and total phenolic acids as well as ratios between these constituents could not account fully for anecdotal observations of resistance to bleaching of green pea genotypes. Therefore, is it possible that there are genotypic differences in the concentration of minor phenolic acids or other compounds which regulate color stability in green peas. Furthermore, it is not understood whether structural properties of the grain, such as hull adherence to cotyledon, could impact the bleaching response or whether preharvest conditions can impact the resistance of grain to post-harvest bleaching. Therefore, further examination of several green pea genotypes harvested across differing environments would be a valuable contribution to the study of bleaching resistance.

4.5 Acknowledgments

The authors gratefully acknowledge Agriculture Victoria Research (AVR) and the Grains Research and Development Corporation (GRDC) for funding this research, as well as Dr. Jason Brand for providing grain samples and Nathan Good for technical support.

4.6 References

AMAROWICZ, R., ESTRELLA, I., HERNÁNDEZ, T., ROBREDO, S., TROSZYŃSKA, A., KOSIŃSKA, A. & PEGG, R. B. 2010. Free radical-scavenging capacity, antioxidant activity, and phenolic composition of green lentil (Lens culinaris). *Food Chemistry,* 121**,** 705-711.

BRAND, J. 2016. Expanding the use of pulses in the southern region: 2015 Results Summary. Available: https://grdc.com.au/research/reports/report?id=6752.

BROWNING, T. H. & GEORGE, R. A. T. 1981. The effects of mother plant nitrogen and phosphorus nutrition on hollow heart and bleaching of pea (Pisum sativum L.) seed. *Journal of Experimental Botany,* 32**,** 1085-1090.

CANADIAN GRAIN COMMISSION 2018. Official Grain Grading Guide Winnipeg: Canadian Grain Commission.

CHENG, M., MCPHEE, K. E. & BAIK, B. K. 2004. Bleaching of Green Peas and Changes in Enzyme Activities of Seeds under Simulated Climatic Conditions. *Journal of Food Science,* 69**,** 511-518.

DAHL, W. J., FOSTER, L. M. & TYLER, R. T. 2012. Review of the health benefits of peas (Pisum sativum L.). *British Journal of Nutrition,* 108**,** S3-S10.

DUEÑAS, M., ESTRELLA, I. & HERNÁNDEZ, T. 2004. Occurrence of phenolic compounds in the seed coat and the cotyledon of peas (Pisum sativum L.). *European Food Research and Technology = Zeitschrift für Lebensmittel-Untersuchung und -Forschung. A,* 219**,** 116-123.

ENVIRONMENT RESPONSE TEAM 1994. Chlorophyll Determination SOP#: 2030. *In:* AGENCY, U. S. E. P. (ed.).

GRAIN TRADE AUSTRALIA. 2018. *Australian Pulse Standards 2018* [Online]. Available: http://www.graintrade.org.au/commodity_standards [Accessed].

GUBBELS, G. H. & ALI-KHAN, S. T. 1990. Screening green field pea genotypes for resistance to color loss. *Canadian Journal of Plant Science,* 70**,** 45-49.

KHAN, T. N. & CROSER, J. S. 2004. PEA | Overview. *In:* WRIGLEY, C. (ed.) *Encyclopedia of Grain Science.* Oxford: Elsevier.

MAGALHÃES, S. C. Q., TAVEIRA, M., CABRITA, A. R. J., FONSECA, A. J. M., VALENTÃO, P. & ANDRADE, P. B. 2017. European marketable grain legume seeds: Further insight into phenolic compounds profiles. *Food Chemistry,* 215**,** 177-184.

MAGUIRE, J., KROPF, J. & STEEN, K. 1973. Pea seed viability in relation to bleaching. *Proceedings of the Association of Official Seed Analysts,* 63**,** 51-58.

MAHARJAN, P., PENNY, J., PARTINGTON, D. L. & PANOZZO, J. F. 2019. Genotype and environment effects on the chemical composition and rheological properties of field peas. *Journal of the Science of Food and Agriculture,* 99**,** 5409-5416.

MARLES, M. S., WARKENTIN, T. D. & BETT, K. E. 2013. Genotypic abundance of carotenoids and polyphenolics in the hull of field pea (Pisum sativum L.). *Journal of the Science of Food and Agriculture,* 93**,** 463-470.

MAZZA, G. & OOMAH, B. D. 1994. Color evaluation and chlorophyll content in dry green peas. *Journal of Food Quality,* 17**,** 381-392.

MCCALLUM, J., TIMMERMAN-VAUGHAN, G., FREW, T. & RUSSELL, A. 1997. Biochemical and Genetic Linkage Analysis of Green Seed Color in Field Pea. *Journal of the American Society for Horticultural Science,* 122**,** 218-225.

MCDONALD, L., PANOZZO, J., SALISBURY, P. & FORD, R. 2016. Discriminant Analysis of Defective and Non-Defective Field Pea (Pisum sativum.) into Broad Market Grades Based on Digital Image Features. PLoS ONE, 11, e0155523.

MCDONALD, L. S., SALISBURY, P. A., FORD, R. & PANOZZO, J. F. 2019. Quantifying the colour loss of green field pea (Pisum sativum L.) due to bleaching. *PLOS ONE,* 14**,** e0221523.

MIRALI, M., PURVES, R. W. & VANDENBERG, A. 2016. Phenolic profiling of green lentil (Lens culinaris Medic.) seeds subjected to long-term storage. *European Food Research and Technology,* 242**,** 2161-2170.

PADHI, E. M. T., LIU, R., HERNANDEZ, M., TSAO, R. & RAMDATH, D. D. 2017. Total polyphenol content, carotenoid, tocopherol and fatty acid composition of commonly consumed Canadian pulses and their contribution to antioxidant activity. *Journal of Functional Foods,* 38**,** 602-611.

PARIKH, B. & PATEL, V. H. 2018. Total phenolic content and total antioxidant capacity of common Indian pulses and split pulses. *Journal of Food Science and Technology,* 55**,** 1499-1507.

PHELPS, S. 2015. *Bleaching in Green Pea* [Online]. Available: https://saskpulse.com/files/general/151027_Bleaching_in_Green_Pea.pdf [Accessed].

SINGH, B., SINGH, J. P., SHEVKANI, K., SINGH, N. & KAUR, A. 2017. Bioactive constituents in pulses and their health benefits. *Journal of Food Science and Technology,* 54**,** 858-870.

SINGH, N. & PRATAP, A. 2016. Food Legumes for Nutritional Security and Health Benefits. *In:* SINGH, U., PRAHARAJ, C. S., SINGH, S. S. & SINGH, N. P. (eds.) *Biofortification of Food Crops.* New Delhi: Springer India.

STEET, J. A. & TONG, C. H. 1996. Degradation Kinetics of Green Color and Chlorophylls in Peas by Colorimetry and HPLC. *Journal of Food Science,* 61**,** 924-928.

UBAYASENA, L., VIJAYAN, P., BETT, K. E., GRAY, G. R., KÜSTER, H. & WARKENTIN, T. D. 2013. Gene expression profiles of seed coats and biochemical properties of seed coats and

cotyledons of two field pea (Pisum sativum) cultivars contrasting in green cotyledon bleaching resistance. *Euphytica,* 193**,** 49-65.

WILLIAMS, P. C. & SINGH, U. 1988. Quality screening and evaluation in pulse breeding. *In:* SUMMERFIELD, R. J. (ed.) *World crops: Cool season food legumes: A global perspective of the problems and prospects for crop improvement in pea, lentil, faba bean and chickpea.* Dordrecht: Springer Netherlands.

YAMAUCHI, N., FUNAMOTO, Y. & SHIGYO, M. 2004. Peroxidase-mediated chlorophyll degradation in horticultural crops. *Phytochemistry Reviews,* 3**,** 221-228.

ZHANG, B., DENG, Z., RAMDATH, D. D., TANG, Y., CHEN, P. X., LIU, R., LIU, Q. & TSAO, R. 2015. Phenolic profiles of 20 Canadian lentil cultivars and their contribution to antioxidant activity and inhibitory effects on α-glucosidase and pancreatic lipase. *Food Chemistry,* 172**,** 862-872.

CHAPTER 5

Images, features, or feature distributions? A comparison of inputs for training convolutional neural networks to classify lentil and field pea milling fractions

Abstract

Lentil and field pea are commonly marketed and consumed as split and dehulled products. Split-yield is a targeted trait within genetic improvement programs. However, traditional assessment of split-yield requires milled grain to be manually sorted into split and dehulled fractions, which is time-consuming and impacts the number of germplasm lines that can be evaluated.

A machine vision approach, based on artificial neural networks, was proposed to classify split and dehulled fractions of lentil and field pea from multispectral images of single grains. Three neural networks were trained on different inputs derived from the multispectral images. The networks were: (1) A convolutional network trained on the full multispectral images, (2) a convolutional network trained on image-feature distributions, and (3) a fully connected network trained on means and standard deviations of image-features. The accuracy and training times were compared to determine the trade-offs between training networks with smaller inputs (image-features and feature-distributions) for computational efficiency and full-image inputs for accuracy.

The convolutional network based on the automatic selection from the given image-feature distributions achieved a validation accuracy of 88.1%. On average, this was 1.6% greater than the image-based convolutional network and 4.6% greater than the image-feature based, fully connected network. The networks with reduced input-data dimensionality (image-features and feature-distributions) were more computationally efficient, completing network training and predictions in half the time taken by the image-based network. Reduction of multispectral images to simple (mean and standard deviation) image-features lead to a reduction in generality of the fully connected network by comparison with the image-based, convolutional

network. However, feature-distributions extracted from the multispectral images captured the diversity of image data required to differentiate milling categories, leading to gains in computational efficiency over the image-based network without loss of network generality. Feature-distribution based networks could be equally be applied in classification tasks for grading other agricultural products.

5.1 Introduction

Lentil and field pea are typically sold as a bulk commodity and their market value is based on the visual appearance of the product. Each market has defined quality-trait specifications based on how these pulses are traditionally consumed which determines how they are processed. In most cases pulses undergo secondary processing consisting of dehulling and splitting (Pratap, Mehandi, Pandey, Malviya, & Katiyar, 2016; Sozer, Holopainen-Mantila, & Poutanen, 2017). Consumer preference dictates that the split product, referred to as dahl, contain no unevenly split cotyledon and that the cotyledon not have attached hulls. A high split-yield is an important economic outcome for the processing industry as other milling fractions typically have a lower value.

Within plant-breeding programs, variability in dehulling and splitting efficiency has been observed between genotypes and in relation to seed size (Erskine, Williams, & Nakkoul, 1991a, 1991b), so genetic improvement for these traits can be achieved through rigorous evaluation of the germplasm. Within the laboratory, small-scale evaluation of germplasm for dehulling and splitting efficiency involves passing the grain through rotating carborundum discs with an optimised gap based on the grain-size. The milled product consisting of five fractions (split with hull attached, dehulled split, whole grain with hull attached, dehulled whole grain and broken grain) is manually sorted and each fraction weighed. The manual sorting process is an expensive labour component, is time-consuming and impacts on the number of germplasm lines that can be evaluated.

To overcome the subjective and time-consuming nature of human inspection, machine learning approaches based on image analysis have been a topic of research interest in the agricultural sciences (Brosnan & Sun, 2002, 2004; Churchill, Bilsland, & Cooper, 1992). To date there has been no reported machine vision methods for classifying lentil and field pea split and dehulled fractions. However, machine vision approaches have been applied to the assessment of grain quality traits relating to size, shape and market class (Amaral, Rocha, Gonçalves,

Ferreira, & Ferreira, 2009; Costa et al., 2011; Fıratlıgil-Durmuş, Šárka, Bubník, Schejbal, & Kadlec, 2010; Kumar, Bora, & Lin, 2013; LeMasurier, Panozzo, & Walker, 2014; McDonald, Panozzo, Salisbury, & Ford, 2016) as well as colour and defect classifications (Mahajan, Das, & Sardana, 2015; McDonald, Salisbury, Ford, & Panozzo, 2019; Mendoza, Dejmek, & Aguilera, 2006; M.A. Shahin & Symons, 2001; M. A. Shahin & Symons, 2002) and processing quality (Muhammad A. Shahin, Symons, & Wang, 2012; Yadav & Jindal, 2001).

Artificial neural networks (ANN) are a subset of machine learning methods which have become increasingly popular over the last two decades (Kakani, Nguyen, Kumar, Kim, & Pasupuleti, 2020). More recently ANNs have been utilised in assessment of some agricultural products, such as classifying cereal grain varieties (Kozłowski, Górecki, & Szczypiński, 2019; Zapotoczny, 2011) and identifying the presence of defects in crops and fruit (Lu, Yi, Zeng, Liu, & Zhang, 2017; Zeng & Li, 2020; Zhang, Jiang, Li, & Yang, 2020). The recent interest in, and viability of ANN applications can be attributed to the combination of technological advances in big data acquisition and processing capacities as well as ongoing optimisations of ANN architectures and learning algorithms (Fan, Ma, & Zhong, 2019; Fukushima, 1980, 2008, 2010; Y. LeCun, Bengio, & Hinton, 2015; Y. LeCun et al., 1989; Y LeCun, Haffner, Bottou, & Bengio, 1999).

Fully Connected Networks (FCN) are the simplest of the deep ANN architectures; each node in one layer is connected to each node in the next layer. For machine vision applications the first layer of an FCN is typically composed of either the input image pixels (reshaped to a one-dimensional array) or a collection of image features. Convolutional Neural Networks (CNNs) were first proposed for image recognition tasks in the 1980s (Fukushima, 1980; Y. LeCun et al., 1989) and are now the preferred class of ANNs in machine vision systems. The machine learning potential of CNNs was demonstrated in the ImageNet Large Scale Visual Recognition Challenge (ILSVRC) of 2010 and 2012, where the winning model (a deep CNN) achieved nearly 11% lower test error rate (top-five) than the second-placed model (Krizhevsky, Sutskever, & Hinton, 2012). The architecture of CNNs differs from Fully Connected Networks (FCN) in the use of multi-dimensional convolution kernels to learn patterns and features within localised pixel neighbourhoods (Krizhevsky et al., 2012; Yann LeCun & Bengio, 1998; Sengupta et al., 2020). In effect this reduces the number of learnable network parameters compared with FCNs and therefore improves the computational efficiency of network training.

CNNs are generally trained on two- or three-dimensional images to either predict values/classes directly from the input images or to extract image-features which are subsequently used as the inputs for other machine learning methods such as support vector machines (Wang & Cheng, 2015) or random forests (Hall, McCool, Dayoub, Sunderhauf, & Upcroft, 2015). However, CNNs can also be applied to learning-tasks based on one-dimensional inputs such as time series (Yann LeCun & Bengio, 1998) where the input data has strong correlations within local neighbourhoods. Smaller input arrays enable greater computational efficiency in network training and application, which is an important consideration in applying neural networks to agricultural product grading.

Extraction of image-features is a common method for reduction of image-data size, but this can adversely impact the generality and accuracy of models by reducing the diversity of features within the input data. Moreover, image-features are often computed as a collection of summary statistic values (e.g. mean or standard deviation) which are largely uncorrelated and are therefore unsuited as CNN inputs. However, the extraction of image-features as distributions rather than summary statistics, would enable application of CNNs on data containing local correlations and with reduced dimensionality compared to the original images. Minimal image pre-processing is typically preferred in the development of CNNs to maximise generality of the network. But generality and performance would not be hindered if the feature distributions captured the critical information for the learning-task.

The success of CNN architectures for image recognition and classification tasks makes this class of ANNs particularly attractive for use in automated product grading systems. With consideration given to the accuracy and computational efficiency of such models, there is potential to greatly improve on labour and time expenses of traditional manual assessments. This study presents a comparison of the accuracy and computational cost (network-training and prediction time) of three neural network architectures for classification of lentil and field pea milling classes through image analysis. The first model is a CNN trained on multispectral images, the second is a CNN trained on image-feature distributions, and the third is an FCN trained on image-feature mean and standard deviation values. While pulse milling classifications are specifically addressed in this study, the methods presented herein are equally applicable across many product-grading applications.

5.2 Materials and methods

5.2.1 Grain samples and reference data acquisition

Grain was sourced from 158 red-lentil and 216 field pea samples. Each sample was separated into grain-size fractions through stacked round-hole sieves (LeMasurier et al., 2014) and 100g of the most abundant size fraction was retained. Grain samples were dehulled and split and aspirated to remove the hulls. The dehulled and split fractions were then manually sorted into the categories outlined in Table 5.1. Each fraction was imaged according to the image acquisition method outlined in Section 2.2

Table 5.1. Description of milling classes for lentil and field pea. Milled lentil and field pea samples were manually sorted to the five classes.

Milling fraction categories	*Description*
SPLTD	Split and de-hulled grain
SPLTH	Split grain with hull attached
WHOLD	Whole grain, de-hulled
WHOLH	Whole grain with hull attached
BROKN	Broken fragments

5.2.2 Image acquisition and processing

Multispectral images (with colour channels at 405, 470, 530, 590, 660 and 850nm) were acquired of each grain sample through an EyeFoss^{TM} (FOSS Analytical, Hoganas, Sweden). Through this system, grain was poured into a sample hopper and mechanically dispersed onto a conveyor belt such that the grains were generally non-touching. The conveyor carried the grain in a single layer into a camera unit where it was imaged by a fixed-resolution, line-scan camera and concurrently scanned, by laser, for object surface height (given in reflectance units) at each pixel location. Through the EyeFoss^{TM} system images were automatically cropped such that there was a single object within each. In total there were 34095 lentil and 9192 field pea labelled images. The distribution of these images across the five milling classes is given in Table 5.2. Lentil images were selected such that there were approximately equal class sizes. However, since each 100g field pea sample contained fewer grains than 100g of lentil, there were insufficient field pea images to create evenly distributed classes.

Table 5.2. Total number of lentil and field pea images within each of the milling classes

	BROKN	*SPLTD*	*SPLTH*	*WHOLD*	*WHOLH*	*Total*
Lentil images	6806	6816	6839	6779	6855	**34095**
Field pea images	23	1679	3072	1387	3031	**9192**

Images were processed in the Matlab programming environment with the Image Processing and Deep Learning toolboxes. All images were segmented (i.e background-pixel values were set to zero), then padded with zeros equally on all sides and stored as 8-bit unsigned integer arrays of size 150 x 150 x 7. The seven channels correspond to the six colour bands and the surface height image. All analyses and network training were performed on a Dell Precision 7520 laptop with Intel(R) Core(TM) i7-7920HQ CPU.

5.2.3 Neural network models

Three neural network architectures were developed for classification of milling fractions (Figs 5.1 and 5.2); two convolutional networks (named ImgCNN and DistCNN), and one fully connected network (SmpFCN). The two CNN model architectures were developed as a series of three convolutional layers followed by two fully connected layers (Table 5.3). The ImgCNN model was trained on the segmented multispectral images and the DistCNN model was trained on Feature-Distribution Vectors (FDV) derived from the multispectral images as described below. The third model, SmpFCN, was a fully connected network with three hidden layers (Fig 5.2c). This model was trained on the mean and standard deviation of 12 image-features based on grain colour and size.

Table 5.3. Architecture of the two CNN models; ImgCNN (trained on multispectral image inputs) and DistCNN (trained on FDVs)

Network Layer	***ImgCNN***	***DistCNN***
Input	Multispectral image 150 x 150 x 7	Image feature-vector 1 x 360 x 1
Conv1	8 convolutions (8x8x7) with stride [2,2] and same padding. Batch normalisation ReLu activation	8 convolutions (1x16x1) with stride [1, 4] and same padding. Batch normalisation ReLu activation
MP1	2 x 2 maxpooling with stride [2,2]	1 x 2 maxpooling with stride [2,2]
Conv2	16 convolutions (4x4x8) with stride [2, 2] and same padding. Batch normalisation ReLu activation	16 convolutions (1x8x8) with stride [1, 2] and same padding. Batch normalisation ReLu activation
MP2	2 x 2 maxpooling with stride [2,2]	1 x 2 maxpooling with stride [2,2]
Conv3	32 convolutions (3x3x16) with stride [2, 2] and same padding. Batch normalisation ReLu activation	32 convolutions (1x4x16) with stride [1, 2] and same padding. Batch normalisation ReLu activation
FC1	Fully connected 1x1x16	Fully connected 1x1x16
FC2	Fully Connected 1x1x10 Softmax	Fully Connected 1x1x10 Softmax

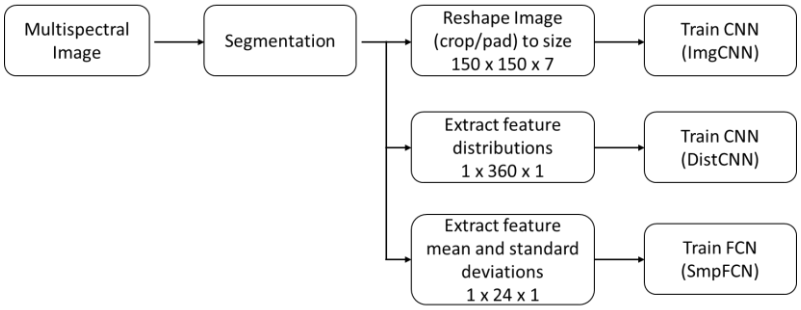

Figure 5.1. Image pre-processing stages prior to training the three neural networks: ImgCNN, DistCNN and SmpFCN.

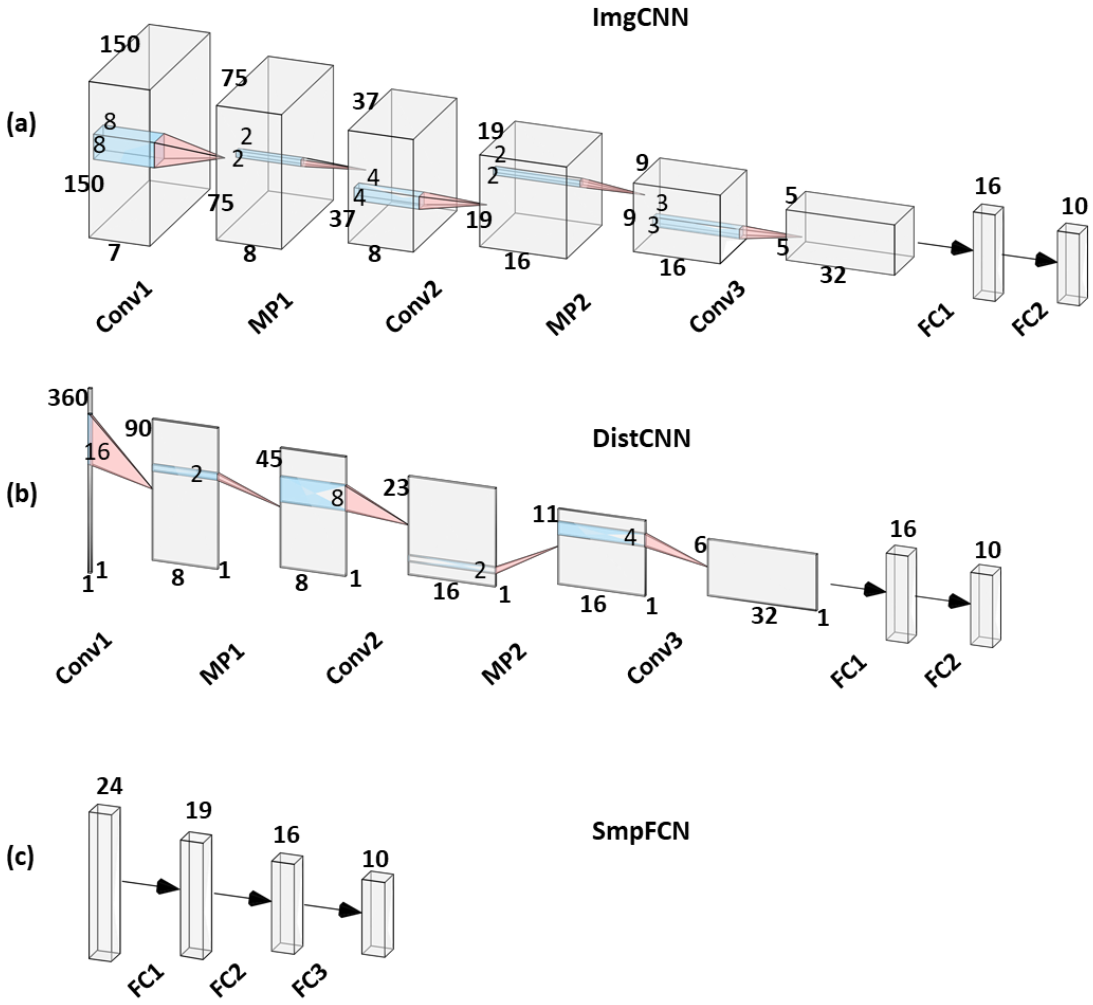

Figure 5.2. Neural network architectures for classification of lentil and field pea milling fractions. **(a)** ImgCNN: a convolutional network with multispectral image inputs of size 150x150x7. **(b)** DistCNN: a convolutional network with image-feature distributions (size 1x360x1) as the inputs. **(c)** SmpFCN: a fully connected network with image-feature vectors of size 1x24x1 as the inputs. The network diagrams displayed in this image were images were created with open source software developed by LeNail (2019).

FDVs comprised the concatenation of 12 image-feature distributions (Fig 5.3). Feature distributions were captured to give a broad representation of grain colour, shape and size characteristics and enable the DistCNN model to learn patterns and features within the locally correlated distributions. Descriptions and calculations for the 12 feature-distributions are outlined in Table 5.4. The SmpFCN model was trained on the mean and standard deviation of the same 12 image-features.

Table 5.4. Description of the features computed from multispectral images

Feature	***Description***	***Computation***
C405	405nm colour distribution	Proportion of pixel-intensity histogram counts (30 equidistant bins from 0 to 255) within the grain region of the first colour band in the multispectral-image.
C470	470nm colour distribution	As above for the second multispectral colour band
C530	530nm colour distribution	As above for the third multispectral colour band
C590	590nm colour distribution	As above for the fourth multispectral colour band
C660	660nm colour distribution	As above for the fifth multispectral colour band
C850	850nm colour distribution	As above for the sixth multispectral colour band
H	H colour distribution (HSV image)	Proportion of pixel-intensity histogram counts (30 equidistant bins from 0 to 255) within the grain region of the first colour band in the HSV image*.
S	S colour distribution (HSV image)	As above for the second HSV colour band
V	V colour distribution (HSV image)	As above for the third HSV colour band
HtD	Grain height distribution	Proportion of pixel-intensity histogram counts (30 equidistant bins from 0 to 255) within the grain region of the first colour band in the laser-generated image.
HtP	Grain height profile	30 equidistant, linearly interpolated, intensity values computed across the grain diameter (through the centre of mass and perpendicular to the maximum diameter). Values were scaled by 1/255 to standardise
RdD	Grain radius distribution	Grain radius (pixel distance from the centre of mass to boundary point) computed at 30 points around the grain perimeter (12^{o} spacing between points). Values were scaled by 1/50 to standardise

*HSV image was computed from the red, green and blue (660, 530 and 470nm) multi-spectral colour bands through the inbuilt Matlab^{TM} function *rgb2hsv*.

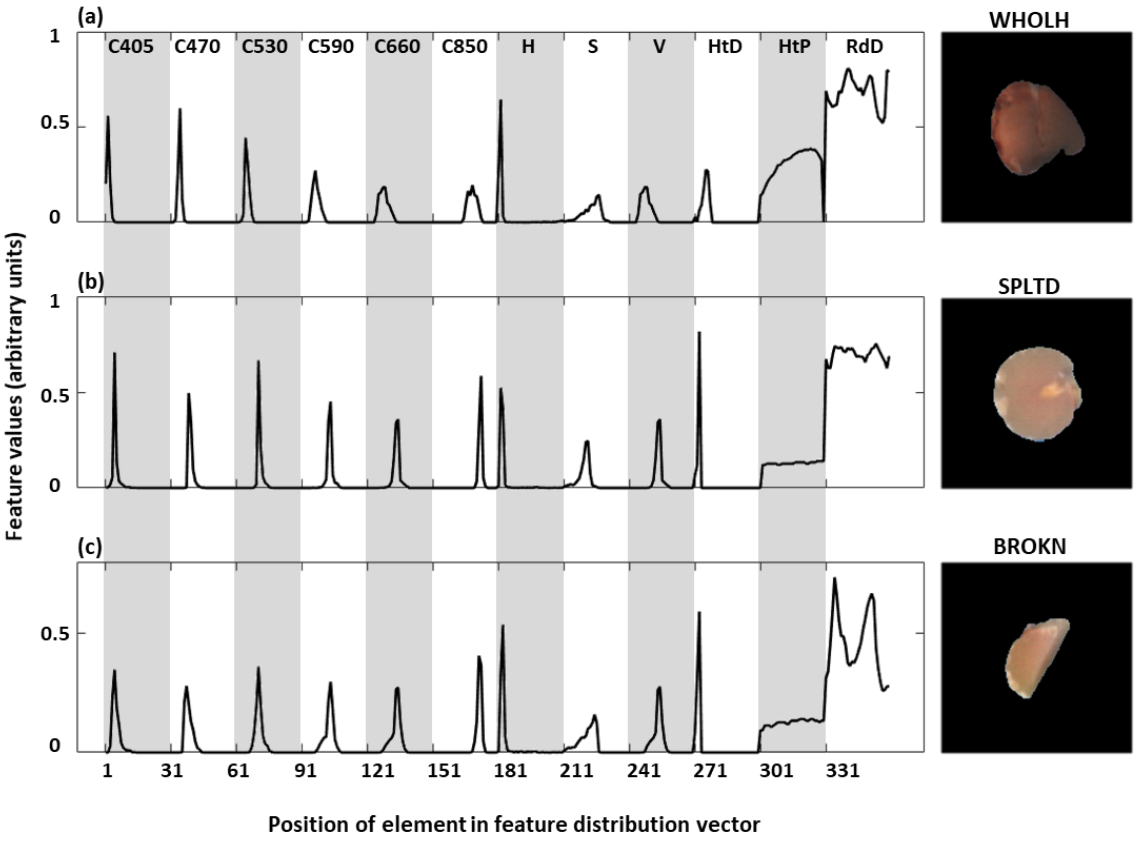

Figure 5.3. Example feature vectors of (a) a lentil wholegrain with hull, (b) a dehulled lentil-split and (c) a broken fragment of lentil. Alternating shaded regions correspond to the feature distributions described in Table 5.4.

5.3 Results and discussion

The practicality of applying CNNs to classification of lentil and field pea milling fractions is largely dependant on the accuracy of predictions, and the time taken to process, train, and make predictions (i.e., inference) with a model. Typically, CNNs learn directly from image inputs to maximise the network generality, however larger input data arrays require the network to optimise more learnable parameters which increases the computational cost of both training and prediction through the network. Conversely, reducing the input array-size can improve computational cost, but can adversely affect the network accuracy if critical features of the original images are lost in the process. A comparison in the performance (accuracy and computational expense) of three network architectures, which were trained on the multispectral image, FDV and image feature inputs, is presented in Section 3.1. Since field pea images were not evenly distributed over the five milling-categories, class precision (Eq. 1) and recall (Eq. 2) values were calculated in addition to overall validation accuracy. Section 5.3.2 discusses the impact of the number of the training images on performance of each of the CNNs.

$$\text{Class Precision} = \frac{\text{True Positive}}{\text{True Positive+False Positive}} \quad \text{... Equation (1)}$$

$$\text{Class Recall} = \frac{\text{True Positive}}{\text{True Positive+False Negative}} \quad \text{... Equation (2)}$$

All three networks were trained using the SGDM (Stochastic Gradient Descent with Momentum) solver with momentum held constant at 0.9. The learning rate was initially set to 0.001 and reduced by a factor of 0.1 every 10 epochs. The training duration for each model was 50 epochs and three training replicates were performed. Minibatches of size 16, 32, 64, 128 and 256 were trialled on the three network architectures to select the optimum size for each based on training time and validation accuracy. Similarly, dropout levels of 0, 5, 10, 15 and 20% were also tested on the CNN architectures. The ImgCNN model was subsequently trained with minibatches of size 128 and 5% dropout after the first maxpool layer. The DistCNN and SmpFCN networks were both trained without dropout and with minibatches of size of 16.

Model training datasets comprised 9192 lentil images (randomly selected within each milling category and approximately evenly distributed across the five categories) in addition to all field pea images (9192). The dataset was partitioned into 80% training and 20% validation images. Network training was replicated three times, re-randomising the training and validation image sets for each replicate.

5.3.1 Network performance: Comparison of architecture and inputs

All models performed well, achieving validation accuracies up to 88.1% (Table 5.5, Fig 5.4). Performance of DistCNN was not significantly different from ImgCNN in overall class precision ($p = 0.85$) and recall ($p = 0.209$). The two convolutional networks outperformed the fully connected network (SmpFCN) in overall validation accuracy and in the precision and recall of each milling fraction (Fig 5.5). Network generality was reduced by using the fully connected architecture and condensing input images to a set of simple (mean and standard deviation) image-features. However, the DistCNN architecture was trained on distributions of the same image features and achieved the highest validation accuracy, which was on average 4.6% ($p=0.01$) higher than for SmpFCN and 1.6% ($p=0.09$) higher than for ImgCNN. Therefore, distributions of the image-features as network inputs achieved superior classification results, despite the reduced input array-size. Extraction of features as distributions coupled with the implementation of a convolutional network architecture, enabled learning of the patterns critical in differentiating milling categories. For example, the profiles of grain height (HtP) and

radius (RdD), depicted in Fig 5.3, describe aspects of grain shape (e.g. roundness) which distinguish broken fragments from whole or split portions of grain. In simplifying the height and radius profiles to mean and standard deviation values, representation of grain shape was largely lost while size information was retained. The impact of this was noticeable in predictions of the broken field pea class (PBROKN) training and validation images in. SmpFCN classified a greater proportion of the PBROKN class into split lentil classes than the DistCNN model.

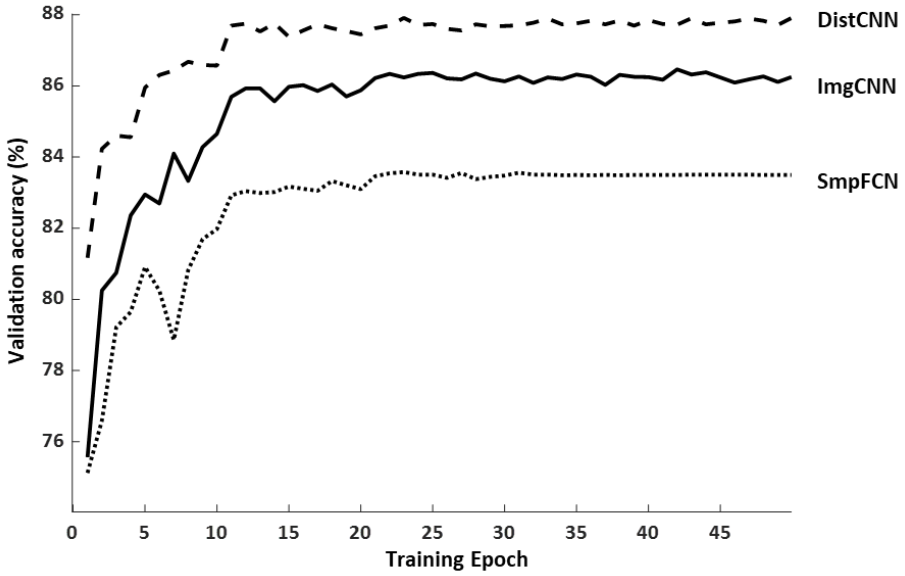

Figure 5.4. Validation accuracy over 50 training epochs for the ImgCNN (solid line), DistCNN (dashed line) and SmpFCN (dotted line) network architectures. Plot traces display the average of three training replicates for each model.

Overall, the lentil images were predicted with better precision and recall than the field pea images (Fig 5.5). Dehulled classes were typically predicted with greater precision and recall than grain with hull. The PBROKN class had the lowest precision and recall across all models but was also the class with the fewest images for network training. There was very little misclassification across grain types, i.e. only 0.2% of lentil images were misclassified into field pea classes and 3.2% of field pea images classified as lentil.

Table 5.5. Neural network performance. Accuracy and computational cost of three network architectures trained on multispectral image (ImgCNN), FDV (DistCNN) and image-feature (SmpFCN) inputs.

Model	*Validation accuracy (%)*	*Training time (s/epoch)*	*Prediction time (s/1000 Images)*	*Learnable parameters (nearest 100)*
ImgCNN	86.5 ± 0.5	75.3 ± 0.4	2.0 ± 0.0	19800
DistCNN	88.1 ± 0.4	32.7 ± 1.3	1.0 ± 0.0	6600
SmpFCN	83.5 ± 0.5	25.2 ± 0.9	1.0 ± 0.0	900

Table entries are the mean (± s.e.) of three network-training replicates.

Reported network accuracies were affected by the following sources of reference-data error: (1) Human error - grain that was manually misclassified, (2) Camera view – e.g. hull attached to the underside of a split or whole grain was not always captured within the camera view and (3) Motion of the imaging apparatus – movement of grain in the sample hopper caused some hull to become detached and some cracked wholegrains to split after they had been manually classified.

The most common misclassification across all three models was split-with-hull grain classified as split-dehulled, for both lentil and field pea images. Due to the two-dimensional view of the camera, some hull sections were not captured within the images, and the movement of grain during the image acquisition process, caused some hull sections to detach from cotyledon. This is supported by the low precision relative to recall values of the split-dehulled classes, and conversely the low recall relative to precision of the split with hull classes. Of all images which were misclassified, there were a total of 1448 which were misclassified in every training-replicate of each model. A large proportion of these misclassified images, which accounted for 3.3% of all images, would be false negative classifications due to the three causes of reference-data error.

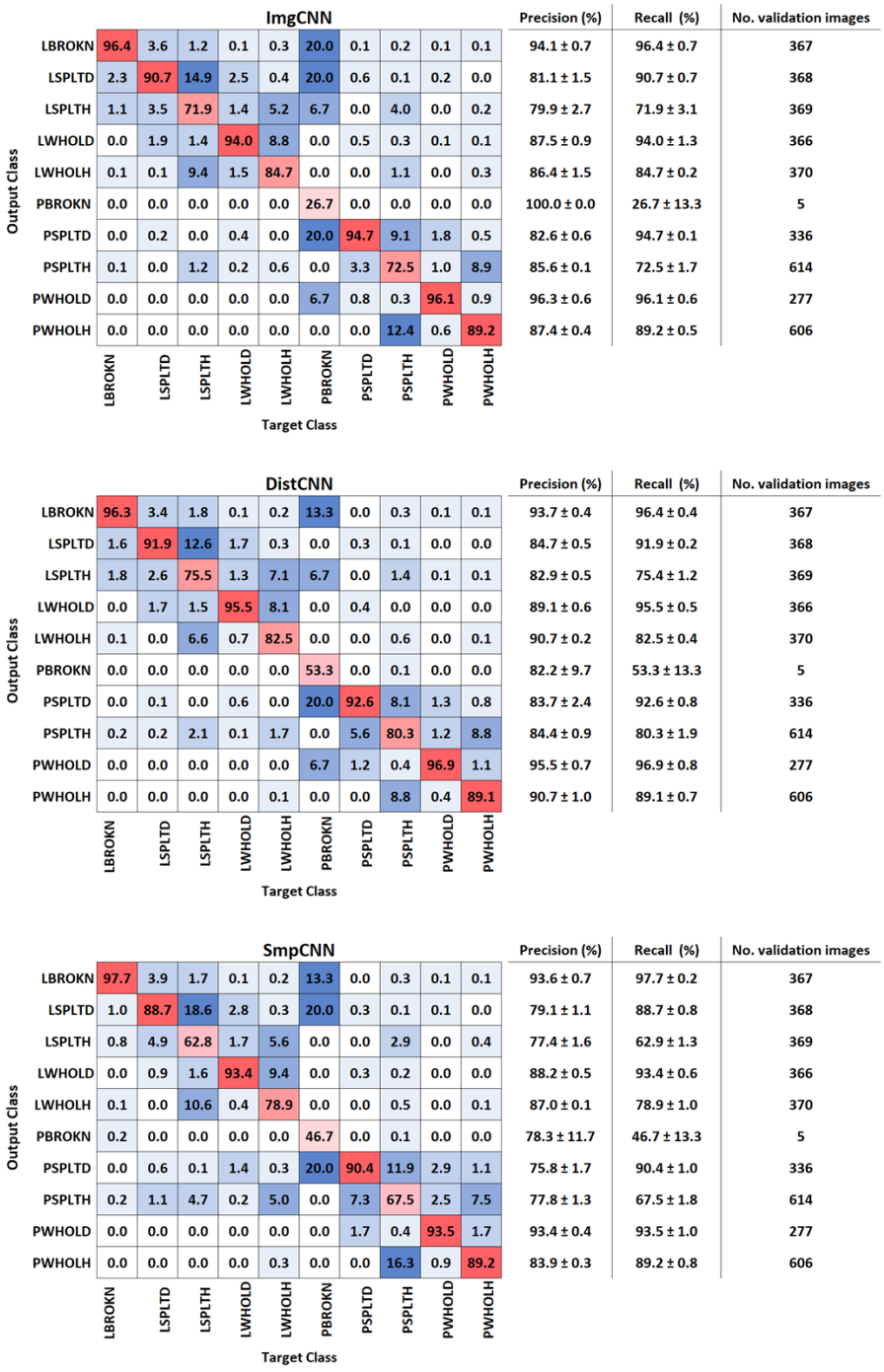

Figure 5.5. Validation precision and recall of the ImgCNN, DistCNN and SmpFCN architectures. (Left) Confusion matrices given as a percentage of the number of validation images in each class. Elements along each matrix diagonal are equivalent to the class recall values. Red tones indicate correctly classified images, blue tones indicate misclassified images and darker colours correspond to higher values. (Right) Tables of mean (± s.e.) of class precision and recall values. All depicted values are the average of three training replicates. Class names beginning with "L" and "P" are lentil and field pea classes respectively.

Network training times are important for efficient model development, particularly for models which undergo continuous learning as new images are analysed and added to the training set. However, application of CNNs to classify lentil and field pea splits would be dependent more on the model prediction times rather than training times. The training and prediction times of the ImgCNN was approximately double that of the image-feature and FDV based networks due to the size of the input data arrays which impacts the number of learnable network parameters (Table 5.5). However, these times do not account for the computational cost of extracting features or FDVs for the SmpFCN and DistCNN models. So, optimisation of feature and FDV extraction would be required to maintain the training and prediction time advantage of the faster networks. In this study, the images used in the ImgCNN architecture were 150 x 150 x 7 in size. In applications using images with larger dimensions (e.g. higher resolution or larger objects for classification), there would likely be a greater difference in prediction times between image-based and FDV-based models.

5.3.2 Training dataset size

The acquisition of large, labelled datasets is one of the greatest challenges in developing machine vision systems for agricultural product grading. Training deep neural networks on small datasets can lead to prediction inaccuracies and model overfitting. The two best performing networks presented in this study, ImgCNN and DistCNN, were trained (non-replicated) on 80, 60, 40 and 20% of the image dataset to observe the impact of reduced training data on model performance. Model training time, validation accuracy, precision and recall decreased for both models as the number of training images were reduced (Figs 5.6a and b). Even at half of the original training set size (i.e. with a 40%:60% training to validation ratio compared with 80%:20%), both CNN models achieved the same or greater validation accuracy than the fully connected network which was trained on 80% and validated on 20%. The FDV-based model maintained better class precision, class recall and accuracy than ImgCNN under the constraints on the size of the training dataset (Figs 5.6c and d). Moreover, ImgCNN displayed a tendency toward overfitting, with validation accuracy diverging from training accuracy, as the input dataset reduced in size.

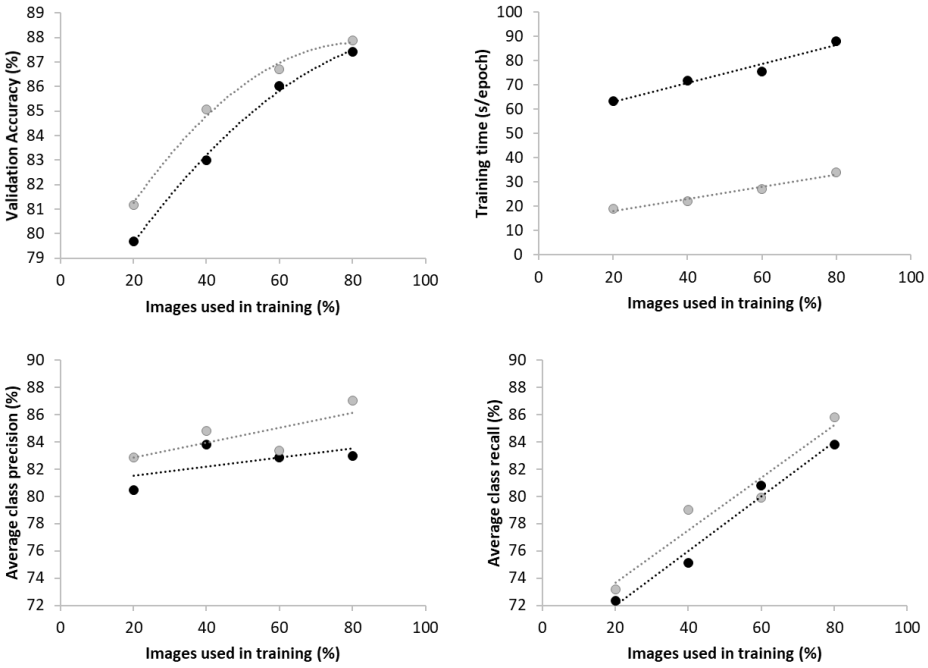

Figure 5.6. Comparison of **(a)** Validation accuracy, **(b)** network training time, **(c)** average class precision and **(d)** average class recall between the ImgCNN model (black) and DistCNN model (grey) with varying input dataset sizes.

5.4 Conclusion

In this study three neural network models were developed for classifying milling fractions post dehulling and splitting of lentil and field pea. The models were: (1) ImgCNN - trained on multispectral images of size 150 x 150 x 7, (2) DistCNN - trained on image-feature distributions (360 elements) and (3) SmpFCN - trained on the means and standard deviations of the same image-features (24 elements). The best performing model, DistCNN, achieved an overall validation accuracy of 88.1% which was on average 4.6% greater than SmpFCN and 1.6% greater than ImgCNN. Network training and prediction times for the feature-based models, SmpFCN and DistCNN, were approximately half that of ImgCNN. The gains in computational efficiency were due to the reduction in input array size from full multispectral images to either a vector of simple image features, for training SmpFCN, or an FDV for training DistCNN. Simple feature inputs, based on mean and standard deviation of grain colour and size traits, caused a reduction in network generality for SmpFCN compared with ImgCNN, which was trained on the full multispectral images. However, distributions of the same grain traits captured the diversity of size and colour information as well as shape, which was critical to differentiating the split and dehulled classes. As a result, DistCNN was trained more efficiently on a reduced

input data size and without loss of generality by comparison with ImgCNN. Moreover, with a diminished training dataset size, DistCNN was less impacted than ImgCNN in classification precision, making it more suitable for applications with limited datasets. The DistCNN classification of lentil and field pea fractions provides an efficient and accurate method for assessment of milling efficiency compared with the traditional hand-sorting of milled product. Classification tasks, based on visual traits, are common for grading many agricultural products. Therefore, with the appropriate choice of image-features to extract as distributions, FDV-based CNNs would be applicable across many product-grading applications.

5.5 Acknowledgements

The authors are grateful to Agriculture Victoria Research (AVR) and the Grains Research and Development Corporation (GRDC) for funding this study and to members of the AVR Seed Phenomics and Quality Traits team for providing technical support.

5.6 References

AMARAL, A. L., ROCHA, O., GONÇALVES, C., FERREIRA, A. A. & FERREIRA, E. C. 2009. Application of image analysis to the prediction of EBC barley kernel weight distribution. Industrial Crops and Products, 30, 366-371.

BROSNAN, T. & SUN, D.-W. 2002. Inspection and grading of agricultural and food products by computer vision systems--a review. Computers and Electronics in Agriculture, 36, 193-213.

BROSNAN, T. & SUN, D.-W. 2004. Improving quality inspection of food products by computer vision--a review. Journal of Food Engineering, 61, 3-16.

CHURCHILL, D. B., BILSLAND, D. M. & COOPER, T. M. 1992. Comparison of Machine Vision With Human Measurement of Seed Dimensions. Transactions of the ASAE, 35, 61-64.

COSTA, C., ANTONUCCI, F., PALLOTTINO, F., AGUZZI, J., SUN, D. W. & MENESATTI, P. 2011. Shape Analysis of Agricultural Products: A Review of Recent Research Advances and Potential Application to Computer Vision. Food and Bioprocess Technology, 4, 673-692.

ERSKINE, W., WILLIAMS, P. C. & NAKKOUL, H. 1991a. Splitting and dehulling lentil (Lens culinaris): Effects of genotype and location. Journal of the Science of Food and Agriculture, 57, 85-92.

ERSKINE, W., WILLIAMS, P. C. & NAKKOUL, H. 1991b. Splitting and dehulling lentil (Lens culinaris): Effects of seed size and different pretreatments. Journal of the Science of Food and Agriculture, 57, 77-84.

FAN, J., MA, C. & ZHONG, Y. 2019. A Selective Overview of Deep Learning. Ithaca: Cornell University Library, arXiv.org.

FıRATLıGIL-DURMUŞ, E., ŠÁRKA, E., BUBNÍK, Z., SCHEJBAL, M. & KADLEC, P. 2010. Size properties of legume seeds of different varieties using image analysis. Journal of Food Engineering, 99, 445-451.

FUKUSHIMA, K. 1980. Neocognitron: A self-organizing neural network model for a mechanism of pattern recognition unaffected by shift in position. Biological Cybernetics, 36, 193-202.

FUKUSHIMA, K. Recent Advances in the Neocognitron. In: ISHIKAWA, M., DOYA, K., MIYAMOTO, H. & YAMAKAWA, T., eds. Neural Information Processing, 2008// 2008 Berlin, Heidelberg. Springer Berlin Heidelberg, 1041-1050.

FUKUSHIMA, K. Increased Robustness against Background Noise: Pattern Recognition by a Neocognitron. In: WONG, K. W., MENDIS, B. S. U. & BOUZERDOUM, A., eds. Neural Information Processing. Models and Applications, 2010// 2010 Berlin, Heidelberg. Springer Berlin Heidelberg, 574-581.

HALL, D., MCCOOL, C., DAYOUB, F., SUNDERHAUF, N. & UPCROFT, B. Evaluation of Features for Leaf Classification in Challenging Conditions. 2015 IEEE Winter Conference on Applications of Computer Vision, 5-9 Jan. 2015 2015. 797-804.

KAKANI, V., NGUYEN, V. H., KUMAR, B. P., KIM, H. & PASUPULETI, V. R. 2020. A critical review on computer vision and artificial intelligence in food industry. Journal of Agriculture and Food Research, 2, 100033.

KOZŁOWSKI, M., GÓRECKI, P. & SZCZYPIŃSKI, P. M. 2019. Varietal classification of barley by convolutional neural networks. Biosystems Engineering, 184, 155-165.

KRIZHEVSKY, A., SUTSKEVER, I. & HINTON, G. E. 2012. ImageNet Classification with Deep Convolutional Neural Networks. 1097-1105.

KUMAR, M., BORA, G. & LIN, D. 2013. Image processing technique to estimate geometric parameters and volume of selected dry beans. Journal of Food Measurement and Characterization, 7, 81-89.

LECUN, Y. & BENGIO, Y. 1998. Convolutional networks for images, speech, and time series. The handbook of brain theory and neural networks. MIT Press.

LECUN, Y., BENGIO, Y. & HINTON, G. 2015. Deep learning. Nature, 521, 436-444.

LECUN, Y., BOSER, B., DENKER, J. S., HENDERSON, D., HOWARD, R. E., HUBBARD, W. & JACKEL, L. D. 1989. Backpropagation Applied to Handwritten Zip Code Recognition. Neural Computation, 1, 541-551.

LECUN, Y., HAFFNER, P., BOTTOU, L. & BENGIO, Y. 1999. Object Recognition with Gradient-Based Learning. Shape, Contour and Grouping in Computer Vision. Berlin, Heidelberg: Springer Berlin Heidelberg.

LEMASURIER, L. S., PANOZZO, J. F. & WALKER, C. K. 2014. A digital image analysis method for assessment of lentil size traits. Journal of Food Engineering, 128, 72-78.

LENAIL, A. 2019. NN-SVG: Publication-Ready Neural Network Architecture Schematics. Journal of Open Source Software, 4, 474.

LU, Y., YI, S., ZENG, N., LIU, Y. & ZHANG, Y. 2017. Identification of rice diseases using deep convolutional neural networks. Neurocomputing, 267, 378-384.

MAHAJAN, S., DAS, A. & SARDANA, H. K. 2015. Image acquisition techniques for assessment of legume quality. Trends in Food Science & Technology, 42, 116-133.

MCDONALD, L., PANOZZO, J., SALISBURY, P. & FORD, R. 2016. Discriminant Analysis of Defective and Non-Defective Field Pea (Pisum sativum.) into Broad Market Grades Based on Digital Image Features. PLoS ONE, 11, e0155523.

MCDONALD, L., SALISBURY, P., FORD, R. & PANOZZO, J. 2019. Quantifying the colour loss of green field pea (Pisum sativum L.) due to bleaching. PLOS ONE, 14, e0221523.

MENDOZA, F., DEJMEK, P. & AGUILERA, J. M. 2006. Calibrated color measurements of agricultural foods using image analysis. Postharvest Biology and Technology, 41, 285-295.

PRATAP, A., MEHANDI, S., PANDEY, V. R., MALVIYA, N. & KATIYAR, P. K. 2016. Pre- and Post-harvest Management of Physical and Nutritional Quality of Pulses. In: SINGH, U., PRAHARAJ, C. S., SINGH, S. S. & SINGH, N. P. (eds.) Biofortification of Food Crops. New Delhi: Springer India.

SENGUPTA, S., BASAK, S., SAIKIA, P., PAUL, S., TSALAVOUTIS, V., ATIAH, F., RAVI, V. & PETERS, A. 2020. A review of deep learning with special emphasis on architectures, applications and recent trends. Knowledge-Based Systems, 105596.

SHAHIN, M. A. & SYMONS, S. J. 2001. A machine vision system for grading lentils. Canadian Biosystems Engineering / Le Genie des biosystems au Canada, 43, 7.9-7.14.

SHAHIN, M. A. & SYMONS, S. J. Instrumental Colour and Size Grading of Pulse Grains. Proceedings of the World Congress of Computers in Agriculture and Natural Resources (13-15, March 2002, Iguacu Falls, Brazil), 2002 St. Joseph, MI. ASABE, 107-113.

SHAHIN, M. A., SYMONS, S. J. & WANG, N. 2012. Predicting dehulling efficiency of lentils based on seed size and shape characteristics measured with image analysis. Quality Assurance and Safety of Crops & Foods, 4, 9-16.

SOZER, N., HOLOPAINEN-MANTILA, U. & POUTANEN, K. 2017. Traditional and New Food Uses of Pulses. Cereal Chemistry, 94, 66-73.

WANG, X. & CHENG, C. Weed seeds classification based on PCANet deep learning baseline. APSIPA Annual Summit and Conference, 2015 Hong Kong. 408-415.

YADAV, B. K. & JINDAL, V. K. 2001. Monitoring milling quality of rice by image analysis. Computers and Electronics in Agriculture, 33, 19-33.

ZAPOTOCZNY, P. 2011. Discrimination of wheat grain varieties using image analysis and neural networks. Part I. Single kernel texture. Journal of Cereal Science, 54, 60-68.

ZENG, W. & LI, M. 2020. Crop leaf disease recognition based on Self-Attention convolutional neural network. Computers and Electronics in Agriculture, 172, 105341.

ZHANG, M., JIANG, Y., LI, C. & YANG, F. 2020. Fully convolutional networks for blueberry bruising and calyx segmentation using hyperspectral transmittance imaging. Biosystems Engineering, 192, 159-175.

CHAPTER 6

Conclusions

The plant breeding cycle for pulse crops is a 10 to 12-year process with the overall objective of producing new cultivars with advantageous characteristics; a combination of adaptive traits for abiotic and biotic effects during plant growth along with improved phenotypic traits for plant architecture and grain quality. The breeding process begins with the first inter-cross in the glasshouse and is followed by extensive field-based testing involving thousands from the derived progeny. Timely and accurate evaluation of grain harvested in each generation of the breeding cycle is critical to the success of a breeding program. The aim at the end of the cycle is to identify an ideal cultivar for commercial release, which combines agronomic and quality traits for the grower to remain profitable in a constantly changing environment.

The adoption of innovation at each stage of the value-chain by the plant breeder, grain-testing laboratory, grower, grains industry and end-user, is paramount for the viability of the grains industry. This requires scientists to adopt innovative tools such gene-editing, computational science and high-throughput phenomics testing, and ultimately for downstream users to adopt sensor-based technologies to more accurately quantify grain-traits associated with end-use quality. Innovated technologies, particularly where automation is practicable or where multiple measurements can be derived, are of most value within plant breeding programs and the grains industry. Emerging spectral technologies integrated into machine vision systems offer the greatest opportunities for efficiency and accuracy gains within the breeding cycle and the wider industry.

Benefits of spectral technologies have been realised within the wheat value-chain through the adoption of NIR-screening methods for several grain and flour traits. For the grains industry, these methods facilitate rapid assessment of traits, such as moisture and protein content, which impact on subsequent grain processing. Within breeding programs these rapid screening methods have reduced the breeding cycle timeline and enabled high-throughput screening for timely and informed genetic-selections. To attain the same benefits within the lentil and field pea industries and breeding programs, similar technological advances and adoption are

required. Therefore, this study was an investigation of opportunities to adopt machine vision applications to improve efficiency and consistency of quality assessments of lentil and field pea germplasm.

The first stage in quantifying grain quality of lentil or field pea is classification of the grain into broad market categories. Market classes determine the end-use of the grain and whether it will be traded as whole grain, in which case visual characteristics of cleanliness, colour, shape and uniformity are important, or whether it will be split and dehulled, in which case the processing quality and visual appeal of the split product is important. Since quality definitions of lentil and field pea are heavily dependent on visual characteristics of the grain, machine vision systems are a fitting choice for rapid, objective and consistent assessments.

Well-constructed machine vision systems, with an appropriately chosen image acquisition environment and suitable image analysis algorithms, offer objective and rapid alternatives to manual grain-assessment methods. Choice of imaging apparatus determines the subsequent grain-traits which can be analysed (e.g. visual traits from RGB images or compositional traits from NIR-hyperspectral images) and the requirements for image pre-processing, such as segmentation to identify pixel-regions of interest and standardisation of pixel intensity values for consistent colour assessment. The grain-traits which were analysed in this study were all visual and physical properties of lentil and field pea and therefore multispectral images, with six colour bands at 405, 470, 530, 590, 660 and 850nm as well as a laser-derived height intensity band, were used for model development. Image analysis methods were developed for classification of field pea market classes, quantitation of bleaching discoloration in green field pea and classification of lentil and field pea milling fractions.

6.1 Field pea market-grade classification

Broad market classes are defined in part by characteristics of the plant (e.g. colour of blossoms), but more so by appearance of the grain. Therefore, the model to predict field pea market classes was based on colour, shape and size features extracted from the grain-region of the multispectral images. The eight classes (Yellow, Green, Kaspa-Type, Kaspa-Dun, Green-Dun, Mottled-Dun, Marrowfat and Yellow-forage) were completely linearly separable when described by four colour features provided that the grain was sound (i.e. no visible defects). Sound grain was classified with 100% accuracy into the correct classes through Linear Discriminant Analysis (LDA). Grain defects impacted on the colour of the grain, such as through

darkened disease spots and exposed cotyledon, and therefore caused overlap between the market-grade clusters which were based solely on colour features. Choice of image features is therefore important for model generality. A more robust LDA model was based on size and shape features of the grain as well as colour features.

While the LDA model was developed to identify the overall market-class of each sample, it could equally be applied seed by seed to germplasm from breeding programs, to identify proportions of genetic segregation or as a quality control measure to determine levels of admixture due to mechanical malfunction during harvest. Further improvements to the model, for example to identify foreign matter within a sample, could include a threshold on the Mahalanobis distance of the samples to each cluster (market-class) mean. In this way, grain or objects that do not reasonably fit a predetermined class profile would be classified as “other” rather than being forced into the nearest class.

There are two broad lentil market classes, red and green, determined by the colour of the cotyledon. Red lentil is subsequently classified by size since small and plump red lentil are typically traded as dehulled grain and larger red lentil are split and dehulled. Green lentil varieties are much more diverse in appearance; however, this diversity is not captured within market class definitions as these are not processed and traded in the same quantities as red lentil. There is a greater number of field pea market classes and therefore the image-analysis method was developed to classify these, but the same methodology and image-features, particularly colour and size, could be applied to lentil classification.

6.2 Quantitation of bleaching-discoloration in green pea

Discoloration of pulse grains has major implications for the perception and assessment of quality. Bleaching is one such discoloration which is prominent within the green pea market class and occurs as a result of chlorophyll depletion. During bleaching the colour of field pea fades from green to cream/yellow in appearance and this effect is typically non-uniform within grain samples. Bleaching can occur pre-harvest due to environmental conditions (e.g. rain events) or post-harvest due to processing or storage conditions (e.g. exposure to light or high humidity).

In the absence of a standard measure to quantify bleaching, scoring is typically achieved by a visual estimate of the proportion of seed affected within a sample. At times this involves

painstakingly peeling seed hull to reveal bleached cotyledon then estimating the ratio of yellow to green surface area. Standard assessments of grain colour, more generally, are achieved with a colorimeter or spectrophotometer and reported as the three coordinates in CIE L*a*b* space. While these measures for colour are accurate and objective, they do not capture variation within samples. Moreover, hue and chromaticity of bleached grain varies widely between green pea genotypes and so it is difficult to capture the extent of bleaching through the CIE L*a*b* colour space. Therefore, a new colour scale was proposed in this study to quantify the extent of bleaching based on visible reflectance spectra. An image analysis method was developed to predict bleaching extent by the same colour scale and applied at a single-seed level to objectively determine colour uniformity.

Colour-band intensity values from the multispectral images were highly correlated (R^2 = 0.99) and closely matched (Lin's concordance statistic of 0.99) with reflectance values from the colour spectrophotometer. Therefore, grain colour assessments by multispectral image analysis could be accurately standardised, through Multiple Linear Regression (MLR), to the reference spectrophotometer output. With careful calibration of pixel intensity values, image analysis methods offer greater flexibility than a colorimeter or spectrophotometer for accurate colour assessment. Through image analysis the spatial distribution of colour can be determined as well as the overall mean colour. Consequently, it was demonstrated in this study that uniformity of bleaching colour scores within each green pea sample could only be assessed through the image analysis method. Furthermore, samples which have too few grains for assessment by spectrophotometer can still be assessed for colour through image processing.

While image-derived bleaching scores can be applied directly to quality assessment of breeding trials they also enable further quantitative research; for example, to study the genotypic susceptibility to abiotic factors during seed development which is often expressed through the colour of the seed coat. An application of this was to investigate a grains-industry issue of bleaching in 'green field peas' where the loss of colour impacts on the marketable quality. The study investigated the relationships between grain composition (chlorophyll and phenolic acid content) and genotypic susceptibility to bleaching and demonstrated the potential of adopting image-based characterisations of grain.

Grain discoloration can be caused by many factors including disease, weather damage, storage conditions and aging of the grain among others. The expressed colour changes can also take many forms including bleaching, darkening and browning. The concept of the bleaching-model could equally be applied to quantify other forms of discoloration. This would have application within breeding programs and the wider pulse industry to quantitatively define acceptable grain colour and variation.

6.3 Milling efficiency

The assessment of milling efficiency is one of the most time-consuming processes undertaken for evaluation of lentil and field pea germplasm. The standard laboratory method involves hand-sorting the milled product into five fractions: Split-dehulled, split with hull attached, whole-dehulled, whole with hull attached and broken grain. As a result of the time expense in this process, the number of breeding lines which can reasonably be assessed for splitting and dehulling efficiency is greatly restricted. Therefore, an image analysis method was developed in this study to rapidly classify milled fractions of lentil and field pea.

Manual sorting of split and dehulled fractions is based on human recognition of visual characteristics (size, shape and colour) of the milled product. For example, broken or split grain can be visually differentiated from whole grain through the recognition of geometric characteristics and, similarly, colour perception can distinguish regions of seed coat from cotyledon. However, milling fractions were not distinctly separable based on simple image-derived representations of the size, shape and colour of the grains. Therefore, Artificial Neural Network (ANN) models were developed for classifying milling fractions based on three input types.

The first model utilised the strength of ANNs to self-learn features from input data. This model was a Convolutional Neural Network (CNN) trained directly on multispectral images; no prior knowledge of class descriptions was assumed. The second model was a CNN trained on distributions of colour, size and shape features extracted from the multispectral images. The features were deliberately chosen to encompass traits that would directly influence manual class selections. This model utilised the capacity of CNNs to identify local patterns within each of the feature-distributions while requiring lower dimensional input data for more computationally efficient training and application. The third model was a Fully Connected Network (FCN) trained on the mean and standard deviations of the same image features. These

were similar features to those used for classifying market classes. The FCN model had the lowest dimensional input data and therefore also the fewest learnable parameters within the network, so it was the most computationally efficient network.

Applied knowledge of the grain features, which differentiate milling classes, was beneficial for optimising the accuracy and efficiency of the ANN models. The use of image-feature distributions for model training enabled significant gains in computational efficiency through the reduction of input-data dimensionality. Redundancies in the multispectral image data were effectively reduced for a more directed computation which also lead to improved model accuracy. The image-feature distributions captured the diversity of information required to distinguish split and dehulled categories without loss of generality. By contrast the mean and standard deviation values of the same image-features resulted in a loss of model generality and accuracy.

Applied to the evaluation of germplasm, this image analysis approach to classification of split and dehulled fractions would result in significant time savings, particularly if implemented into a machine vision system with sorting capability. Considering the time required for splitting, aspirating and then capturing and processing images of the split product, the overall gain in efficiency compared with the current standard method is estimated to be at least 10-fold. There is capacity to improve this further through optimised computational infrastructure.

The high-throughput assessment of milling fractions would not only enable increased sample numbers for evaluation but would facilitate the development of models to identify the grain traits, such as shape or uniformity, that are directly linked to milling performance. With this understanding, plants breeders could make more targeted selections sooner in the breeding cycle to meet market specifications.

6.4 Concluding remarks

This study demonstrates the efficacy of image analysis applied to assessment of lentil and field pea quality traits, particularly the traits which are determined by visual properties. Generality of the image analysis models is dependent on diversity within the training data. Therefore, machine vision systems developed in collaboration with plant breeding programs benefit from access to a wider diversity of germplasm. Adoption of these algorithms within breeding programs could reduce the length of the breeding cycle and enable targeted, objective and intuitive measures of grain quality at all stages of breeding, including early generation

germplasm when seed quantity is limited. The high-throughput nature of image analysis offers breeding programs greater testing capacity than the current standard methods.

Machine vision systems have potential benefits throughout the pulse value chain. Pre-breeding, image-based techniques could be applied to the rapid screening of crop wild relatives to identify potential breeding candidates with desirable traits. Within the grains industry, the applications developed within this study using machine vision methods offer consistent and accurate assessments and the potential to give quantitative definitions of acceptable quality.